Respiratory carbon loss in plant tissues under environmental stress

Clare Woods

Pembroke College

Thesis submitted for the degree of Doctor of Philosophy

University of Oxford

Department of Plant Sciences

Michaelmas term 2014

Abstract

Crop productivity is a balance between carbon gain by photosynthetic assimilation of CO_2 and the release of fixed carbon as CO_2 via respiration. Respiration is the process by which carbohydrates are oxidised to produce ATP to fuel biochemical reactions, whilst simultaneously releasing CO_2 as a by-product; therefore, increased demand for ATP or decreased efficiency of ATP production by uncoupling of the mitochondrial electron transport chain results in greater CO_2 production. ATP produced by respiration is either used to support processes involved in growth or to power cell maintenance processes, such as macromolecule turnover or maintenance of membrane ion gradients. Respiration increases when plants are exposed to high temperatures; a factor that will become increasingly important as we try to maximise food production as the global climate changes. However, it is unknown if increased respiration at high temperature is necessary to provide energy to support growth, is a consequence of increased ATP consumption for maintenance processes or is due to increased mitochondrial uncoupling at high temperature.

Flux measurements showed that CO_2 production by excised *Arabidopsis thaliana* roots increases with temperature up to 37°C. Although growth also increased up to 37°C resulting in increased respiration associated with growth processes, the majority of overall CO_2 production at high temperatures could be accounted for by non-growth respiration. An analysis of ATP-consuming processes demonstrated that protein turnover and maintenance of ion gradients collectively account for the majority of maintenance respiration, but that ATP consumption for the maintenance of ion gradients is quantitatively more important than protein turnover at high temperature. Furthermore, a decrease in *in vivo* P/O ratio at high temperature was demonstrated; the results presented suggest that this is most likely due to increased basal proton leak across the inner mitochondrial membrane. It can be concluded that increased CO_2 production at high temperature results from a combination of increased ATP consumption for the maintenance of ion gradients and a decrease in coupling of the mitochondrial electron transport chain through a common mechanism of increased membrane fluidity and ion leak.

Table of contents

Abstract 2

Table of contents 3

Abbreviations 9

Acknowledgements 11

1. Introduction 12

The effect of temperature on respiration 13

Factors that may lead to increased respiration at high temperatures 14

Growth 14

Maintenance respiration 15

Mitochondrial uncoupling 22

Thesis aims 26

2. Materials and Methods 27

Materials 27

Plant materials and growth conditions 27

Radiolabelling 28

Feeding 28

Extraction of soluble biomass components 28

Fractionation of methanol-soluble cell extract 28

Fractionation of methanol-insoluble cell residue 29

Determination of radioactivity 30

Experiments using isolated mitochondria 30
Purification of mitochondria from arabidopsis seedlings 30
Measurements of oxygen consumption 31
Respiratory coupling assay 31
Outer membrane integrity 32
Assays for uncoupling mechanisms in the mtETC 32
Western blots 32
SDS-PAGE 32
SDS-PAGE 32
Protein transfer 33
Immunodetection of proteins 33
Pulse-chase experiment with D_2O 34
Feeding 34
Extraction and hydrolysis of total protein 34
Sample preparation and GC-MS analysis 34
ATPase assay 35
Membrane extraction 35
Assays 36
Ion conductance assay 36
Determination of *in vivo* P/O ratio 37
Feeding with $H_2{}^{18}O$ 37
Metabolite extraction 37

HPLC 38

Glycerokinase reaction 39

LC-MS 39

3. The effect of short-term temperature increase on respiration rate and carbon use efficiency . 40

Introduction 40

Carbon conversion efficiency 40

Growth and maintenance coefficients 43

Chapter aims 44

Results 45

Establishing an experimental system for the determination of CCE 45

The short-term temperature response of growth, respiration and CCE 48

Estimation of non-growth respiration using a flux-balance model 49

Determination of the source of non-growth CO_2 production 54

Discussion 56

CCE decreases with temperature with a two-phase response 56

Non-growth respiration increases with temperature up to 37°C 58

Summary 61

4. Identifying ATP-consuming processes that contribute to increased ATP consumption 62

Introduction 62

Major ATP-consuming processes 62

Methods for studying protein turnover 63

Methods to assess ATP cost for maintaining ion gradients 65

Chapter aims 66

Results 66

Calculation of the protein turnover rate at 23°C and 33°C 66

Estimation of the cost of maintaining ion gradients 71

Construction of an ATP budget 72

Discussion 85

There was no difference in the rate of protein turnover at 23°C and 33°C 85

Increased ion leakage leads to greater ATP consumption for ATPase activity in arabidopsis roots at high temperature 87

Protein turnover, ion gradient homeostasis and growth are sufficient to explain the majority of ATP consumption at 23°C and 33°C 89

Summary 91

5. Is increased non-growth respiration at elevated temperature caused by a reduction in mitochondrial coupling? 92

Introduction 92

Assessing uncoupling by studying the activity of uncoupling mechanisms 92

Chapter aims 98

Results 99

Experiments using isolated mitochondria 99

Establishing a method for determination of the *in vivo* P/O ratio 103

Discussion 108

There is no evidence for changes in the capacity of AOP, alternative NAD(P)H dehydrogenases or mitochondrial pulsing consistent with decreased mitochondrial coupling at elevated temperature 108

Proton leakage is increased at 33°C compared with 23°C 110

There is a decrease in *in vivo* P/O ratio at elevated temperature 111

Summary 113

6. Acclimation of non-growth respiration to temperature 114

Introduction 114

The extent of respiratory acclimation 114

The biochemical causes of respiratory acclimation 115

Membrane fluidity and *FAD* genes 117

Aims 118

Results 118

Non-growth respiration in roots of 23°C and 30°C grown arabidopsis seedlings 118

ATPase activities and ion leak of 23°C and 30°C grown arabidopsis roots 120

Protein turnover in arabidopsis roots grown at 23°C and 30°C 122

Non-growth respiration in response to short-term elevated temperature treatment in *fad2.2* mutants 124

Discussion 124

Non-growth respiration acclimates to temperature 124

Acclimation of non-growth respiration is accompanied by acclimation of ion leakage and ATPase activity 127

Alterations in membrane fluidity in the *fad2.2* mutant does not lead to reduced non-growth respiration at elevated temperature 129

Summary 130

7. Discussion 132

Summary of results 132

Key findings 132

Non-growth respiration is an important component of total respiration 133

Non-growth respiration can be attributed to changes in ATP consumption for the maintenance of ion gradients and P/O ratio 134

Changes in membrane fluidity play a key role in increasing non-growth respiration at high temperature, as well as acclimation to high temperature 135

Implications for engineering heat tolerance in plants 135

Remaining questions 137

What is the effect of non-growth respiration on the growth rate of whole plants? 137

Are the conclusions from this study applicable to other plant systems? 138

What is the effect of abiotic stress combinations on non-growth respiration? 139

Summary 140

Appendix 141

References 143

Abbreviations

ADP	adenosine diphosphate
AOX	alternative oxidase
ATP	adenosine triphosphate
BSA	bovine serum albumin
CCCP	carbonyl cyanide *m*-chlorophenyl hydrazone
CCE	carbon conversion efficiency
CHI	cycloheximide
CoA	coenzyme A
ConcA	concanamycin A
COX	cytochrome oxidase
CUE	carbon use efficiency
DNA	deoxyribonucleic acid
DTT	dithiothreitol
ECL	enhanced chemiluminescence
EDTA	ethylenediaminetetraacetic acid
ETC	electron transport chain
GABA	gamma-aminobutyric acid
GC-MS	gas chromatography - mass spectrometry
HEPES	4-(2-hydroxyethyl)-1-piperazineethanesulfonic acid
HPLC	high performance liquid chromatography
K_D	dissociation constant
LC-MS	liquid chromatography - mass spectrometry
MES	2-(*N*-morpholino)ethanesulfonic acid
mtETC	mitochondrial electron transport chain
MOPS	3-(*N*-morpholino)propanesulfonic acid
mRNA	messenger ribonucleic acid
NAD^+	nicotinamide adenine dinucleotide, oxidised
$NADP^+$	nicotinamide adenine dinucleotide phosphate, oxidised
OPPP	oxidative pentose phosphate pathway
PAGE	polyacrylamide gel electrophoresis

Pi	inorganic phosphate
PPi	inorganic pyrophosphate
PVP	polyvinylpyrrolidone
REC	relative electrical conductivity
RNA	ribonucleic acid
ROS	reactive oxygen species
SDS	sodium dodecyl sulphate
SEM	standard error of the mean
tBDMS	tert-butyldimethylsilyl ether
TBS	Tris buffered saline
TBST	TBS-tween
TCA	tricarboxylic acid
UCP	uncoupling protein

Acknowledgements

I wish to thank my supervisors Lee Sweetlove and Nick Kruger for their continued support and enthusiasm throughout my DPhil. Thank you to the entire Sweetlove lab for their help and input, and to Kate, Andy, Annette, Gemma and Costa for taking me to the pub.

I'd like to thank my parents for the food and wine, even when I didn't deserve it. And to Chris – I probably couldn't have finished this without you.

I acknowledge funding from BBSRC.

1. Introduction

Green plants are the primary carbon fixers of terrestrial ecosystems and ultimately all our food is derived, either directly or indirectly, from this fixed carbon. Furthermore, given the need to feed a growing world population, there is pressure to produce more food on less land, including land that is affected by unfavourable conditions for crop growth.

Plant productivity is dependent on the balance between photosynthetic assimilation of atmospheric CO_2 and its conversion into bulk biomass components, such as cell wall, lipid, starch and protein. This, in turn, is largely dependent on the rate and efficiency of photosynthesis and respiration. Respiration is the process by which the oxidation of primarily carbohydrates is coupled to ATP production, releasing CO_2 as a by-product. Plant respiration releases 30–80% of carbon gained by photosynthesis back into the atmosphere (Atkin & Tjoelker, 2003). On a global scale, plant and soil respiration releases vastly more carbon into the atmosphere than human activities; 107 gigatonnes of carbon is released as CO_2 each year from respiration, compared with the CO_2 release from fossil fuels of 7.8 gigatonnes per year (IPCC, 2013). Changes in this flux, therefore, have the potential to greatly alter total CO_2 in the atmosphere, a critical aspect of climate change.

Plant respiration is highly plastic and alters depending on the environmental conditions faced by the plant and is sensitive to abiotic stresses; in particular, changes in temperature can have a large impact on respiratory rate. A solid understanding of how plant respiration changes with temperature is necessary to predict how climate change will affect biomass assimilation and therefore food production, as well as CO_2 release back into the atmosphere.

The effect of temperature on respiration

It is well established that respiration is sensitive to short-term changes in temperature, such as those experienced by plants on a daily basis. Respiration increases as temperature rises with a Q_{10} of between 1.1 and 2.9 depending on the species, tissue and temperature range studied (Atkin & Tjoelker, 2003). However, it is unclear what the driving forces behind temperature-dependent changes in respiration are. Respiration rate can be affected by a number of factors including enzyme kinetics, adenylate restriction due to limiting ADP and substrate supply, and these different factors appear to be important at different temperature ranges. At low temperatures, the main factor limiting respiration is enzyme capacity: between 5°C and 15°C in Plantago roots it was shown that additional of exogenous glucose or CCCP, a mitochondrial uncoupling agent, did not significantly stimulate respiratory rate. Thus supply of substrate or ADP was not limiting the rate of respiration. However, at moderate temperatures (15–30°C), respiration was stimulated by supplying CCCP, indicating that respiration was limited by adenylate control. Furthermore, respiration was stimulated by addition of glucose to a lesser extent, indicating that adenylate control was the dominant force controlling respiratory rate at moderate temperatures (Covey-Crump et al., 2007). Additionally, Wiskich and Dry (1985) found that the respiration rate of isolated mitochondria exceeded measured rates of intact tissues, highlighting that TCA cycle enzyme capacity does not limit respiratory rate at moderate temperatures *in vivo*.

With longer term exposure to changes in temperature, respiration can acclimate to the new temperature (Atkin et al., 2000). Respiratory acclimation results in plants exposed to an elevated temperature displaying a reduced rate of respiration over time. It has been suggested that acclimation of roots to low temperature (i.e. increased respiration after exposure to low temperatures) may be due to alleviation of adenylate control, as well as increased capacity of the respiratory system; there is evidence that ATP-consuming processes involved in growth and maintenance acclimate after prolonged exposure to the cold thus increasing ATP turnover (Atkin

et al., 2000). Although the exact mechanism behind respiratory acclimation to elevated temperature has not been studied, given the effect of adenylate control on respiration in response to short-term high-temperature treatments, it seems likely that adenylate control might play a role in respiratory acclimation at elevated temperatures.

Factors that may lead to increased respiration at high temperatures

If adenylate control restricts respiration at moderate temperatures, then increased respiration with short-term increases in temperature must occur as a result of changes in processes involved in the consumption or production of ATP. Plant respiration provides ATP, as well as carbon skeletons and reductant (NAD(P)H) required for processes associated with plant growth and maintenance. Consequently, changes in the rate of these processes to support changes in growth rate or to adapt to different environmental conditions will affect the rate of respiratory carbon loss. In this section, I will review potential factors that may act to increase respiration during high temperature treatment.

Growth

Reductant and ATP generated by the TCA cycle and through oxidative phosphorylation are energy inputs for the biosynthetic reactions that produce plant biomass. Major biomass components such as fatty acids, protein, cell wall components and starch have different ATP and reductant requirements for their synthesis. For example, fatty acid synthesis requires one mole of ATP per mole of acetyl-CoA incorporated, whereas protein synthesis requires 4.3 moles of ATP per amino acid incorporated, additional to energy requirements for the synthesis of amino acids and protein translocation across membranes (Alonso et al., 2007; Schwender et al., 2006). The effect that alterations in biomass composition can have on respiratory metabolism was demonstrated by

examining *wri1-1* mutants of *Arabidopsis thaliana* (arabidopsis). *WRI1* encodes a transcription factor involved in regulating oil synthesis and in *wri1-1* plants, seed oil content is reduced by 74% compared with wild type, accompanied by an increase in protein content. Examination of metabolic fluxes in these mutants revealed an increase in cyclic TCA fluxes, most likely to meet the increased ATP demand for protein synthesis. This was accompanied by a substantial increase in CO_2 release from pyruvate dehydrogenase and the TCA cycle (Lonien and Schwender, 2009).

Additionally, the biosynthetic pathways of several biomass components lead directly to CO_2 release. Whilst not originating from respiratory metabolism, this loss of CO_2 is important in terms of carbon availability for growth. Fatty acids, for instance, are synthesised by the joining of multiple two-carbon acetyl-CoA units. These are in turn generated by the pyruvate dehydrogenase catalysed reaction in which pyruvate, the three-carbon product of glycolysis, is decarboxylated to form acetyl-CoA. This reaction results in the loss of one carbon as CO_2, so for each two-carbon moiety added to a fatty acid chain, one carbon is released as CO_2. A striking example of how differences in biomass composition can affect carbon loss as CO_2 is seen in maize kernels; in the embryo, fatty acids are produced as the main storage product, resulting in a carbon use efficiency (CUE) of 57-71% (Alonso et al., 2010). In the endosperm, a higher proportion of starch is produced, giving a higher CUE of 76-92% (Alonso et al., 2011).

Maintenance respiration

Despite the effect that changes in growth rate and biomass composition can have on growth-associated respiration, a large proportion of ATP generated by plant cells is predicted to fuel processes not associated with growth, although estimates of the importance of this are varied; Masakapalli et al. (2010) predicted that just 15% of total ATP consumption supports growth whereas Cheung et al. 2013 predicted that 84% of ATP consumption could be attributed to growth processes. The remainder of ATP and reductant generated by respiration is used to fuel

cell maintenance processes, including turnover of macromolecules and maintenance of ion gradients across cellular membranes.

Changes in energy consumption by maintenance processes can have a large effect on plant respiration and growth. In ryegrass, genotypes with fast and slow rates of dark respiration in mature leaves were shown to have different maintenance costs. Measuring the respiration of mature leaves gives an indication of maintenance respiration as growth is not occurring and thus respiration is primarily fuelling maintenance processes (see Chapter 3 for a discussion of different approaches to measure maintenance respiration). At harvest, it was found that slowly respiring genotypes had a faster CO_2 net assimilation rate and greater plant dry weight than the genotypes that respired at a faster rate, suggesting that reduced costs for maintenance allow greater provision of substrate for growth (Wilson & Jones, 1982; Wilson, 1982).

Macromolecule turnover

Macromolecules such as proteins, lipid and nucleic acids are constantly turning over to adapt to changing environmental conditions and to replace macromolecules that have become damaged. This is particularly important under abiotic stress conditions, when overproduction of reactive oxygen species can cause damage to proteins, lipids, DNA and carbohydrates (Gill and Tuteja, 2010).

Protein turnover

Protein turnover is defined as the cycle of protein degradation and resynthesis (Quigg and Beardall, 2003). Protein turnover has previously been shown to be a major ATP cost; it has been estimated that protein turnover accounts for 7–60% of total maintenance ATP expenditure (Quigg & Beardall, 2003). This is unsurprising given the large number of ATP-consuming processes that

contribute to protein turnover including protein breakdown, amino acid activation, polypeptide elongation, RNA editing, post translational modification, mRNA turnover and transport across membranes (Zerihun et al., 1998). Small changes in protein turnover, therefore, have the potential to translate into large changes in maintenance cost. Moreover, given the role that protein turnover plays in adapting to changing environmental conditions as well as the potential for damage by ROS (Møller et al., 2007), it is reasonable to expect that the rate of protein turnover might increase under abiotic stress. Evidence for this partly comes from studies looking at gene expression under stress conditions; expression of genes associated with the ubiquitin pathway of protein degradation was shown to be increased under heat shock in arabidopsis (Sun and Callis, 1997), tobacco and maize (Christensen 1992; Genschik 1992). Additionally, during salinity stress, transcripts involved in protein synthesis and degradation were upregulated in rice (Kawasaki et al., 2001). Direct measurements of protein turnover in plants under high temperature treatment have previously been made in wheat and petunia and it has been shown that the protein half-life is lower under high temperature than control conditions (Ferguson et al., 1990; Hachiya et al., 2007).

Turnover of other macromolecules

While turnover of proteins is the most dominant in term of ATP cost, degradation and resynthesis of other cellular components may also be important. Firstly, the rate of mRNA turnover is thought to be significant and related to the rate of protein turnover. The energy cost of mRNA turnover has been estimated to be 0.22–0.26 g glucose/ g protein (Penning de Vries, 1975). Membrane turnover has been shown to occur rapidly; estimates of membrane turnover range from ten minutes to three hours, depending on the cell type being studied (Steer, 1988). However, there are no reliable estimates of the ATP cost for membrane turnover and it is not clear whether membrane lipids are degraded and resynthesised during membrane turnover (Amthor, 2000),

which would have a large effect on the ATP cost and CO_2 production for membrane turnover. Membrane turnover under stress conditions is likely to involve fatty acid resynthesis as ROS generated during abiotic stress conditions are able to oxidise fatty acids (Møller, 2001), however, there are no data available to confirm this. Additionally, the turnover of other macromolecules such as DNA and carbohydrates was estimated to be unimportant with respect to maintenance respiration (Penning de Vries, 1975).

Maintenance of ion gradients

Transport of ions and other small molecules across the plasma membrane and tonoplast is essential for plant function; nutrients must be transported into roots from the soil, ions and metabolites are moved into the vacuole for storage and sugars are transported into phloem for transport to other parts of the plant. While a proportion of transport costs can be attributed to the provision of substrates for growth, a certain proportion can be considered a maintenance cost: leakage of ions back through membranes requires that more ATP is consumed to maintain ion gradients than would be necessary to support growth in the absence of ion leak. Active movement of solutes across biological membranes requires an input of energy in the form of ATP, and is powered by membrane proton pumps that use ATP hydrolysis to generate a proton gradient across a membrane. This proton gradient is then used to power secondary transport of solutes through various symporters and antiporters. Proton gradients across cellular membranes must be maintained to allow continuous transport of solutes. Maintaining proton gradients uses a large amount of ATP and consequently a large proportion of respiration can be attributed to membrane ATPase activity; ion uptake has been estimated to consume 70% of available respiratory energy in roots (Poorter et al., 1991), although no estimates are available for how much of this respiratory cost can be attributed to the maintenance role and how much to the growth role of ion transport. There are two membrane-bound ATPases that contribute to the ATP-

dependent maintenance of ion gradients: V-ATPase in the tonoplast and P-ATPase in the plasma membrane.

Transport across the tonoplast

The vacuole acts as a storage organelle for many solutes and contains the majority of sugar, organic acids and ions such as K^+ and Ca^{2+} found in the plant cell (Martinoia et al., 1981). This storage function requires active transport of these solutes, which in turn requires uphill transport of H^+. The V-ATPase enzyme is composed of multiple domains that form a cytoplasmic ATP hydrolysis motor (V_1) and a membrane integral domain consisting of a ring of subunits (V_0) which are connected by a central stalk. ATP hydrolysis by subunits of V_1 causes rotation of the central stalk, which in turn translates into rotation of the V_0 subunit ring. Protons are driven across the membrane by rotation of the ring against the proton channel (Stevens and Forgac, 1997). Changes in the expression of V-ATPase subunits is likely to play a role in regulating V-ATPase activity under certain stress conditions. V-ATPase expression increases under salt stress in maize (Zörb et al., 2004), cucumber (Du et al., 2010) and wheat (Wang et al., 2008). This makes sense as plants adapt to high salt stress by sequestering NaCl in the vacuole. Whether V-ATPase protein levels are affected by other stresses is unclear, but protein levels of V-ATPase were unchanged in response to osmotic stress (Tsiantis et al., 1996) and cold stress treatment (Zhang et al., 2006). However, it is also possible that more rapid changes in activity to respond to rapid changes in environmental conditions occur through post-translational regulation of the enzyme. It has been suggested that dissociation and reassembly of the V_1 subcomplex may occur to regulate V-ATPase activity; in yeast in glucose-depleted medium, 70% of yeast V_1 was found to be dissociated from the membrane. Providing glucose stimulated V_1 subunits to reassemble with the rest of the enzyme (Kane, 1995). Additionally, changes in the proton coupling ratio, the ratio of proton-pumping to proton-pumpingATP hydrolysis, may act to regulate V-ATPase *in vivo*. In red beet, it was found

that the coupling ratio decreased when the pH gradient increased from 2.8 to 4.7 pH units (Davies et al., 1994). Similarly, the coupling ratio of V-ATPase in vesicles isolated from lemon fruit decreased as ΔpH across the tonoplast increased (Müller and Taiz, 2002). There is evidence that this mechanism regulates V-ATPase activity in response to salt stress in carrot (Low et al., 1996), however, it is unclear whether post-translational regulation modulates V-ATPase activity *in vivo* in response to other stresses.

Alongside V-ATPase, the tonoplast PPase also acts to generate a proton gradient across the membrane by coupling PPi hydrolysis to proton translocation. The V-PPase is a major contributor to the proton gradient formed across the tonoplast membrane, but the activity of the two pumps are non-additive as they are both kinetically controlled by the H^+ gradient (Rea et al., 1992). A possible explanation for the existence of the V-PPase is as a backup to the V-ATPase: PPi is generated as a by-product of biosynthetic reactions, such as during acylation of coenzyme A during fatty acid synthesis. Unlike ATP, levels of PPi remain very stable despite changes in environmental conditions and the V-PPase might act to ensure constant acidification of the vacuole. Whilst PPase activity does not actively consume ATP and does not have a direct effect on respiration, activity may alter the ATP consumption of the V-ATPase and so it is important to consider here.

Transport across the plasma membrane

The H^+-ATPase located in the plasma membrane is responsible for pumping protons out of the cell to acidify the area surrounding the cell. As with transport across the tonoplast, this proton gradient drives secondary transport of solutes and is essential for nutrient uptake into the cell. The plasma membrane H^+-ATPase belongs the P-ATPases; a family of ATPases that also includes Ca^{2+}-ATPases as well as ATP-dependent heavy metal pumps, although the plasma membrane H^+-ATPase is the predominant ATPase in this group (Portillo, 2000). P-ATPases differ in structure from

the V-ATPase, being composed of a single polypeptide chain rather than a multi-subunit assembly, and this difference in structure underlies differences in post-translational regulation of the two ATPases *in vivo*. Activity of the plasma membrane H^+-ATPase is modulated by its own C-terminal tail interacting with the active site of the enzyme; deletion of the C-terminal tail by trypsin (Palmgren et al., 1990) or genetic modification (Regenberg et al., 1995) lead to constitutive activation of the plasma membrane ATPase. Activation of the plasma membrane H^+-ATPase may occur by binding of a 14-3-3 protein directly to the C-terminal tail after phosphorylation; there is evidence that plasma membrane H^+-ATPase activation under salt stress may occur via this mechanism but it is unclear whether the plasma membrane H^+-ATPase is activated by other stresses via this mechanism. The plasma membrane H^+-ATPase may also be subject to regulation by gene expression and protein levels; during chilling stress in cucumber, the protein level of plasma membrane H^+-ATPase increased in isolated membrane vesicles, and this corresponded to increased proton transport (Ahn et al., 2000).

The effect of temperature on ATPase activity

Although only limited data have been published on the effect of temperature on ATPase activities, it is well established that increased temperature directly increases membrane fluidity (Los and Murata, 2004). Increases in membrane fluidity may facilitate the passage of ions back down their concentration gradients, therefore necessitating greater ATP expenditure to maintain ion gradients. Membrane fluidity is also dependent on the saturation of membrane lipids; unsaturated lipids are unable to pack together as closely as saturated lipids and therefore lipid desaturation results in decreased membrane viscosity. With changes in environmental conditions, particularly changes in ambient temperature, plants are able to adjust the fluidity of their membranes. In arabidopsis it was shown that lipids become more unsaturated in colder conditions compared with warm conditions (Falcone et al., 2004) and increased fluidity in warm

temperatures is compensated for by increases in membrane lipid saturation (Martinière et al., 2011). Additionally there is evidence that activity of fatty acid desaturases is inhibited at elevated temperature (Burgos et al., 2011; O'Quin et al., 2010). This suggests that ATP consumption is likely to increase to counteract ion leak due to greater membrane fluidity in the short-term, but over the longer term, acclimation to high temperature can be achieved.

Mitochondrial uncoupling

An additional factor affecting the respiration rate in plant tissues is the degree to which electron transfer is coupled to ATP synthesis by the mitochondrial electron transport chain (mtETC). The TCA cycle is linked to ATP production by the mtETC located in the inner mitochondrial membrane, which contains protein complexes that pump protons into the intermembrane space upon electron flow. This generates a proton gradient used to drive ATP synthesis by the F_1F_0 ATP synthase (Figure 1.1). In addition to these proton-pumping complexes, plant mitochondria possess mechanisms that uncouple NADH oxidation from ATP synthesis, such as the alternative oxidase (AOX), alternative NAD(P)H dehydrogenases and uncoupling protein (UCP) (Møller & Lin, 1986; Vanlerberghe & Mcintosh, 1992; Vercesi et al., 2006) . These mechanisms reduce the efficiency of ATP synthesis with respect to carbon consumption as greater TCA cycle flux is required to synthesise an equivalent amount of ATP.

As previously discussed, abiotic stresses are accompanied by the accumulation of ROS, which leads to damage of cellular components and ultimately to cell death (Apel and Hirt, 2004). The ETC of mitochondria are a major source of ROS in heterotrophic plant cells (Møller, 2001); over-reduction of the mtETC leads to the transfer of single electrons to oxygen, forming superoxide. Levels of ROS production are lower in systems in which the mtETC is chemically uncoupled (Purvis, 2001) highlighting that mtETC reduction level affects ROS production. Similarly, the energy-dissipating mechanisms of the plant mtETC might play a role in ameliorating mtETC over-

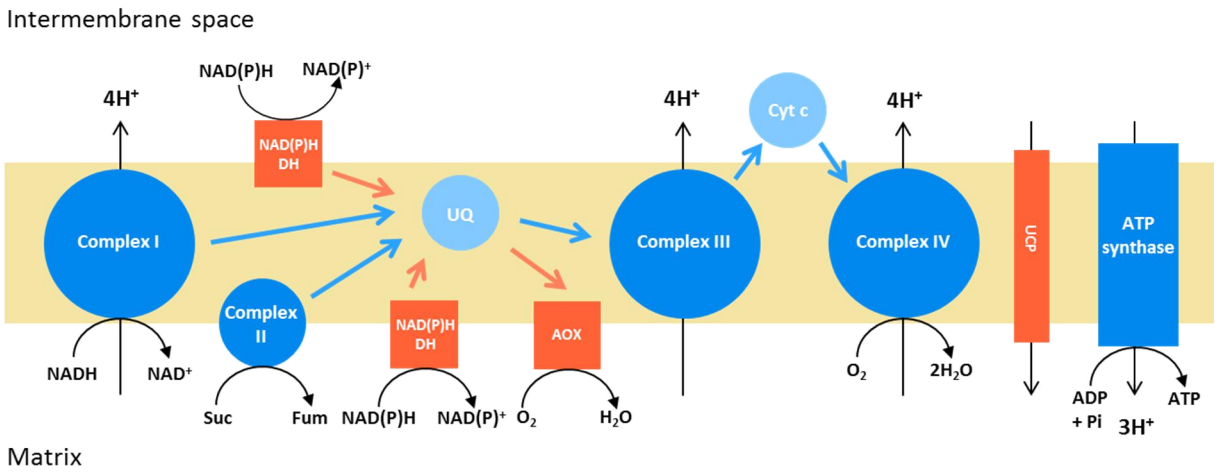


Figure 1.1 The plant mitochondrial electron transport chain. The blue arrows represent electron flow through fully coupled to ATP synthesis: complex I oxidises matrix NADH from the TCA cycle, reducing ubiquinone. Electrons are transferred to complex III, which reduces cytochrome c. Complex IV then oxidises cytochrome c, mediating the transfer of four electrons to oxygen to produce water. Electrons can also enter via complex II which oxidises succinate to fumarate, using ubiquinone as an electron acceptor. Upon electron flow, complexes I, III and IV pump protons into the intermembrane space, generating a proton gradient across the inner membrane. Protons diffuse back into the mitochondrial matrix via the F_1F_0 ATP synthase, and the free energy released drives ATP synthesis. Red figures represent mtETC uncoupling mechanisms AOX, alternative NAD(P)H dehydrogenases and UCP.

reduction and reducing ROS production under stress conditions by uncoupling NAD(P)H oxidation from ATP synthesis.

Alternative oxidase

AOX is a terminal oxidase that uses ubiquinol as an electron donor for the reduction of oxygen. Electron flow through AOX bypasses protein pumping complexes III and IV and consequently AOX reduces the efficiency of ATP production. An impact of mtETC uncoupling by AOX on growth has been demonstrated: tobacco cells with suppressed *AOX* expression showed an enhanced growth rate under stress conditions. Furthermore, whereas wild type cells displayed a reduction in CUE in response to P and N depletion, cells with reduced AOX maintained a constant CUE (Sieger et al., 2005). Despite this detrimental effect on growth, AOX appears to be important in stress tolerance.

Decreased *AOX* expression has been shown to increase ROS production under stress conditions in arabidopsis (Umbach et al., 2005) and tobacco (Amirsadeghi et al., 2006; Maxwell et al., 1999; Pasqualini et al., 2007). Furthermore, it was demonstrated that arabidopsis lacking AOX had a more acute stress response to light and drought compared with wild type (Giraud et al., 2008). The response of partitioning between the cytochrome and alternative pathways to short-term temperature changes has been characterised in mung bean and arabidopsis and it was observed that electron partitioning remained stable at temperatures above 19–20°C, however, electron flow through AOX declined substantially at temperatures below this (Armstrong et al., 2008; Gonzalez-Meler et al., 1999).

Alternative NAD(P)H dehydrogenases

Alternative NAD(P)H dehydrogenases are present both on the external and internal sides of the inner mitochondrial membrane and oxidise the cytosolic and matrix pools of NAD(P)H, respectively. They pass electrons directly to ubiquinone, bypassing complex I (Koeppe & Miller, 1972; Wilson & Hanson, 1969). In arabidopsis, alternative dehydrogenases are encoded by a gene family composed of seven members; NDA1, NDA2 and NDC1 proteins are internally-facing, whereas NDB1-4 proteins are externally-facing (Elhafez et al., 2006; Michalecka et al., 2003). The oxidation of cytosolic and matrix NAD(P)H by alternative dehydrogenases lowers the reduction state in these compartments, thus reducing ROS formation. The role of the alternative dehydrogenases in stress response is highlighted by the dependency of external alternative NAD(P)H dehydrogenase activity on Ca^{2+} (Geisler et al., 2007; Michalecka et al., 2003; Møller et al., 1981) the intracellular concentration of which increases in response to stress (Geisler *et al.*, 2007). Expression of genes encoding alternative NAD(P)H dehydrogenases increase in response to phosphate stress in arabidopsis (Vijayraghavan and Soole, 2010) and cold storage of beetroot (Fredlund et al., 1991) and there is evidence that their expression is coordinated with *AOX* (Clifton

et al., 2006); however, the effect of temperature on alternative dehydrogenase activity has yet to be characterised.

Proton leak

Mitochondrial uncoupling proteins (UCPs) 1-3 (Palmieri et al., 2008) are inner mitochondrial membrane localised anion channels that allow the free fatty acid-mediated passage of protons from the intermembrane space into the matrix (Vercesi et al., 2006). They therefore dissipate energy by reducing the proton gradient generated by proton-pumping complexes I, III and IV. To maintain this gradient for ATP production, more reductant must be oxidised by the ETC for proton-pumping to occur, and this comes from increased oxidation of carbohydrates, resulting in greater respiratory CO_2 release. UCP has also been assigned the role of acting in response to stress in which ROS are formed in the mitochondria. There is ample evidence suggesting that ROS cause a nucleotide-sensitive activation of UCP (Considine et al., 2003; Echtay et al., 2001). This creates a feedback cycle in which ROS levels increase due to stress, leading to UCP activation and the dissipation of membrane potential, mitigating further ROS production (Vercesi *et al.*, 2006). A number of studies have demonstrated cold-induced expression of AtUCP1 (Maia *et al.*, 1998) and its homologues in potato (Laloi et al., 1997). Consistent with this, it was recently demonstrated that the promoter of AtUCP1 contains regulatory elements occurring in cold-responsive genes and a low-temperature responsive element (Nogueira et al., 2011). Whereas genes encoding AOX and alternative NAD(P)H dehydrogenases show upregulation of expression in response to a variety of stresses, an analysis of global transcript profiling datasets for *AtUCP* gene expression under stress, demonstrated expression to be almost unchanging for stress conditions other than cold (Nogueira *et al.*, 2011).

Alongside protein-mediated proton leak, a basal proton leak is also present in mitochondria. The basal proton leak is thought to contribute significantly to the mtETC activity; in animal systems it

accounted for 20–50% of resting metabolic rate (Brand 1999; Rolfe 1996). Although basal proton leak is not regulated, it is thought to be affected by the abundance of the adenine nucleotide transporter (ANT), leading to the hypothesis that proton leak occurs at the protein-fatty acid interface (Brand et al., 2005). Basal proton conductance was studied in mitochondria from mice and *Drosophila melanogaster* that had been genetically modified to contain variable amounts of ANT and a correlation between basal proton leak and ANT content was found, leading to the conclusion that two-thirds of the basal proton leak occurred via the ANT route in these systems (Brand et al., 2005). Although the effect of temperature on basal proton leak has not been studied, the inner mitochondrial membrane is subject to the same changes in membrane fluidity as discussed previously for the plasma membrane and tonoplast and it is therefore possible that basal proton leak will increase at elevated temperature.

Thesis aims

While both the short- and long-term effects of temperature changes on respiration are well characterised, the underlying biochemical basis of increased respiration at high temperature has not been established. Understanding the biochemical basis behind temperature-mediated changes in respiration will allow us to determine whether it is possible to use genetic engineering to modify plants to prevent increased respiratory carbon loss at high temperatures. Similarly, we do not know what mechanisms act in the process of respiratory acclimation to long-term changes in temperature. With this in mind, the aims of my thesis are as follows:

1. Characterise the effect that elevated temperature has on respiratory rate of excised arabidopsis roots, and identify the underlying biochemical processes responsible.

2. Explore whether respiratory acclimation occurs with long-term exposure to elevated temperatures and to determine if this is due to acclimation of ATP-consuming processes.

2. Materials and Methods

Materials

Unless otherwise stated, general chemicals were purchased from Sigma-Aldrich (St. Louis, MO, USA) or Fisher Scientific (Loughborough, UK). ^{14}C-labelled glucose was purchased from PerkinElmer (Waltham, MA, USA), D_2O and $H_2{}^{18}O$ were purchased from Sigma-Aldrich. Enzymes were purchased from Roche (Basel, Switzerland) or Sigma-Aldrich.

Plant materials and growth conditions

The Columbia (Col-0) accession of *arabidopsis thaliana* was used for all wild-type experiments. Seeds of homozygous *fad2.2* mutants in a Col-0 background (described in Miquel et al., 1993) were provided by John Browse, Washington State University, WA, USA. Seeds were surface sterilised with 5% (v/v) sodium hypochlorite containing 0.1% (v/v) TWEEN-20 for 15 minutes before washing with sterile dH_2O three times. Seeds were transferred to conical flasks (approximately 30 per 100 ml flask) containing 30 ml 0.22% (w/v) Murashige and Skoog medium (Duchefa Biochimie, Haarlem, Netherlands), 2.56 mM MES-KOH (pH 5.7) and 170 mM glucose. Seeds were kept in the dark at 4°C for 2 days before transfer to a growth facility with a 16-hour photoperiod at a constant temperature of 23°C, shaking at 40 rpm. For seedlings grown at 30°C, flasks were transferred to a growth cabinet with a 16-hour photoperiod at a constant temperature of 30°C after 4 days at 23°C.

Short-term high-temperature treatment was carried out at a constant temperature of 30°C, 33°C, 37°C, 38°C or 39°C, as described for individual experiments.

Radiolabelling

Feeding

Roots (approximately 100 mg fresh weight) from 14-day-old seedlings were removed with scissors at the base of the root and transferred to a 100 ml flask containing 5 ml 30 ml 0.22% (w/v) Murashige and Skoog medium, 2.56 mM MES-KOH (pH 5.7) and 170 mM glucose, feeding was initiated by the addition of 74 kBq [U-^{14}C]glucose per flask. Roots were incubated with [U-^{14}C]glucose in the dark at a continuous temperature of 23°C, 30°C, 33°C, 37°C, 38°C or 39°C with shaking at 40 rpm. Roots were harvested by vacuum filtration, washed with 3 x 5 ml dH_2O and snap-frozen in liquid nitrogen. CO_2 production was determined in separate flasks, in which feeding was stopped by the injection of 1 ml 12 M formic acid into the medium to stop metabolism and release dissolved CO_2 (Harrison and Kruger, 2008). CO_2 was collected in 1 ml 10% (w/v) KOH in a vial suspended within each flask.

Extraction of soluble biomass components

To disrupt cells, 4 ml 100% methanol at –20°C was added to the frozen roots, followed by snap freezing in liquid nitrogen. Roots were then thawed on ice for 2 hours. The sample was centrifuged at 1,500 *g* for 15 minutes at 4°C and the supernatant removed and stored on ice. The roots were resuspended in 4 ml of cold methanol and centrifuged as before. The roots were then further extracted with 4 ml methanol for 10 minutes at 70°C and the supernatant combined with that of the cold extractions. The insoluble cell residue was stored at –80°C.

Fractionation of methanol-soluble cell extract

Chloroform and dH_2O were added to the methanolic fraction to generate a mixture of chloroform: methanol: water at a ratio of 4:4:2 (v/v). The mixture was centrifuged at 1,500 *g* for 20 minutes at

room temperature to aid phase separation. The aqueous methanol phase was removed and retained and the chloroform-soluble phase washed with dH_2O and methanol before measurement of total radioactivity. Pooled aqueous methanol fractions were dried by rotary evaporation at 40°C and resuspended in 5 ml dH_2O. Total radioactivity of an aliquot was determined by liquid scintillation counting of a 1ml aliquot, before separation of the remainder into basic (amino acid), acidic (organic acid) and neutral (sugar) fractions by solid-phase extraction on Dowex ion-exchange columns. Basic and acidic fractions were freeze dried, resuspended in 1 ml dH_2O and total radioactivity measured. Neutral fractions were freeze-dried and resuspended in 2 ml dH_2O. Total radioactivity of an aliquot was measured and the remainder was separated into sucrose, glucose and fructose by thin-layer chromatography. Neutral fractions were lyophilised and redissolved in 50 µl 50% ethanol. 25 µl was spotted onto a TLC plate (20 cm x 20 cm, Polygram® CEL 300, Layer 0.1 mm cellulose, Macherey-Nagel, Germany). Sugars were separated three times by a solvent mixture containing formic acid: butanone: tert-butanol: water (1.5: 3: 4: 1.5, v/v) until the solvent front reached 2 cm from the top of the plate. Dried plates were exposed to phosphor imaging screens (Fuji, Tokyo, Japan) for 24 hours. Phosphor screens were imaged using Molecular Imager FX (Biorad, Hercules, CA, USA). Intensities of bands representing glucose, fructose and sucrose were measured using Quantity One (Biorad, version 4.4.1) software. Relative abundances of sugars determined from the imaged phosphor screens were used to calculate the corresponding radioactive counts of each sugar.

Fractionation of methanol-insoluble cell residue

Insoluble residue was ground using a pestle and mortar, autoclaved at 121°C, 104 kPa for 3 hours and resuspended in dH_2O to a final volume of 2 ml. Total radioactivity was determined by incubating a 100 µl aliquot of insoluble residue with 400 µl of Soluene-350 tissue solubiliser (PerkinElmer) at 60°C for 16 hours. Fractionation was achieved by a two-step enzymatic digestion

to obtain the starch, cell wall and protein components: Remaining insoluble material was incubated with 400 µl sodium acetate containing 20 U α-amylase and 10 U amyloglucosidase for 16 hours at 37°C, followed by addition of 400 µl of 400 mM Tris-HCl (pH 7.8) containing 10 U protease, type XIV and incubation for a further 16 hours at 37°C. The digest was centrifuged at 13,000 *g* for 5 minutes and the supernatant was separated into basic, acidic and neutral fractions by ion exchange chromatography, as before. Radioactivity in the remaining undigested material, cell wall, was determined after solubilisation with tissue solubiliser.

Determination of radioactivity

Radioactivity was determined by counting disintegrations per minute using a Beckman LS 6500 scintillation counter. An aliquot of each fraction (<1 ml) was mixed with 4 volumes of Optiphase HiSafe scintillation fluid (PerkinElmer). Each sample was counted for 5 minutes.

Experiments using isolated mitochondria

Purification of mitochondria from arabidopsis seedlings

Mitochondria were isolated using a method adapted from Sweetlove et al. (2007). All steps were carried out at 4°C using detergent-free equipment. Seedlings (approximately 20 g fresh weight) were removed from liquid culture and excess media removed using dH_2O. Tissue was ground using a pestle and mortar in 600 ml extraction buffer (0.25 M sucrose, 1.5 mM EDTA, 15 mM MOPS-KOH [pH 7.4], 100 mM ascorbic acid, 0.4% [w/v] BSA, 0.6% PVP-40, 10 mM DTT) at 4°C and the extract was filtered through one layer of Miracloth and two layers of muslin. Filtered tissue was then re-ground in extraction medium with sand, and filtered as above. The pooled extract was centrifuged for 5 minutes at 1,100 g. The supernatant was retained and centrifuged at 18,000 g for 20 minutes at 4°C after which the pellet was resuspended in residual supernatant gently

using a fine wet brush. 100 ml wash buffer (0.3 M sucrose, 10 mM TES-KOH [pH 7.5], 0.1% [w/v] BSA) was added to the resuspended pellet and the solution was centrifuged for 5 minutes at 1,100 *g*. The supernatant was retained and re-centrifuged at 18,000 *g* for 20 minutes at 4°C as before, and the pellet resuspended in residual supernatant. The resuspended pellet was layered over a 0–4.4% (w/v) PVP-40 gradient and centrifuged for 40 minutes at 40,000 *g* at 4°C, with the brake off. Mitochondria formed a white band near the bottom of the tube. Mitochondria were collected in a fresh tube and approximately 50 ml resuspension buffer (0.3 M sucrose and 10 mM TES-KOH [pH 7.5]) was added. The suspension was centrifuged for 15 minutes at 23,700 *g* for 5 minutes to pellet mitochondria. Mitochondria were suspended in 500 µl resuspension buffer.

Measurements of oxygen consumption

Oxygen consumption measurements on isolated mitochondria were performed with a Clark type oxygen electrode (Hansatech Instruments, Kings Lynn, UK) and the rate of oxygen consumption was measured using Oxygraph software (Hansatech Instruments). For calibration, oxygen was removed from the water by addition of sodium bisulphite. For all assays, mitochondria were suspended in the electrode chamber at 23°C or 33°C in 1 ml buffer containing 5 mM $MgCl_2$, 0.2 M mannitol, 0.1 M MOPS-KOH (pH 7.2), 0.1% (w/v) BSA, 20 mM KH_2PO_4.

Respiratory coupling assay

Isolated mitochondria were provided with 10 mM pyruvate, 10 mM malate, 0.1 mM TPP and 0.3 mM NAD^+. Oxygen uptake of isolated mitochondria was measured during state III and state IV respiration after addition of 0.1 mM ADP. The respiratory control coefficient was calculated as the ratio of oxygen consumption during state III and state IV respiration.

Outer membrane integrity

Oxygen uptake of isolated mitochondria was measured after each addition of 10 mM ascorbate, 0.05 mM cytochrome c, 0.05% (v/v) Triton-X and 0.05 mM KCN. To calculate the latency of complex IV to exogenous cytochrome c, the rate of oxygen consumption before addition of Triton-X was expressed a percentage of the rate after Triton-X addition.

Assays for uncoupling mechanisms in the mtETC

Mitochondria were incubated with 10 mM succinate and 0.25 mM ATP to stimulate state II respiration followed by addition of 0.1 mM ADP to initiate state III respiration. To measure AOX capacity, oxygen uptake via the COX pathway was inhibited by 0.5 mM KCN during state III, followed by inhibition of AOX with 0.05mM propyl-gallate. AOX capacity was calculated as total state III oxygen uptake after inhibition with KCN. To determine oxygen consumption as a consequence of mitochondrial pulsing, calcium channels were inhibited during state 3 by addition of 2 mM $LaCl_2$ (Schwarzländer et al., 2012). Proton leak was determined by measuring the rate of oxygen consumption before and after addition of ADP, and expressing state II respiration as a percentage of state III.

Western blots

SDS-PAGE

SDS-PAGE

Protein samples were boiled for 10 minutes in SDS-PAGE buffer (2% [w/v] SDS, 62.5 mM Tris-HCl [pH 6.8], 10% [v/v] mercaptoethanol, 0.002% [w/v] bromophenol blue). 10 µg of mitochondrial protein was loaded per well. SDS-PAGE gels consisted of 10% (w/v) polyacrylamide separation gel containing 0.1% (w/v) SDS and a 5% (w/v) polyacrylamide stacking gel. Electrophoresis was conducted in running buffer (25 mM Tris, 192 mM glycine, 1% [w/v] SDS) at 8–10 V/cm gel until

the sample reached the separation gel, followed by 12–15 V/cm until the marker dye reached the end of the gel.

Protein transfer

Proteins were transferred onto nitrocellulose membranes by semi-dry transfer. Gels were rinsed with dH_2O, and equilibrated for 5 minutes in transfer buffer (25 mM Tris, 192 mM glycine, 20% [v/v] methanol) along with gel-sized pieces of blotting paper (Whatman). Soaked blotting paper was placed on the anode followed by the gel and a further pieces of blotting paper. Transfer was achieved using a constant current of 0.8–1 mA/cm2 for 25–40 minutes. Transferred proteins were visualised using Ponceau-S staining to ensure even transfer of proteins; the membrane was incubated with Ponceau dye (0.1% [w/v] Ponceau S, 5% [w/v] acetic acid) for 5 minutes and the blot rinsed. Ponceau dye was removed by repeated washes with dH_2O.

Immunodetection of proteins

The membrane was blocked for 1 hour at 4°C with blocking solution (5% dried milk [Marvel] 140 mM NaCl, 2.7 mM KCl, 25 mM Tris-HCl [pH 7.4]). Blots were probed for 1 hour with primary antibodies in blocking solution at the following concentrations: anti-NDA and anti-NDB 1:1500 (Rasmusson and Agius, 2001), anti-UCP 1:500, anti-COX subunits 1 and 2 1:100. Blots were washed with blocking solutions four times followed by addition of ECL peroxidase labelled anti-rabbit antibody (GE Healthcare Life Sciences) at 1:10,000. Secondary antibody was removed by 4 washes after 1 hour with TBST (140 mM NaCl, 2.7 mM KCl, 25 mM Tris-HCl [pH 7.4], 0.1% TWEEN-20). Bands were visualised using SuperSignal West Pico Chemiluminescent substrate (Thermo Scientific, Waltham, MA, USA) and photographic film (Kodak, Watford, UK).

Pulse-chase experiment with D_2O

Feeding

Arabidopsis seedlings were grown in liquid media, as described previously, however, media was supplemented with 20% (v/v) D_2O. On Day 11, seedlings were switched to D_2O-free media, and roots were excised at the times specified in Chapter 4.

Extraction and hydrolysis of total protein

Root tissue was ground under liquid nitrogen using a pestle and mortar and the ground tissue was added to 5 ml ice cold methanol. Samples were allowed to thaw on ice before centrifugation at 4500 *g* for 10 minutes at 4°C. The supernatant was freeze dried and retained for analysis of free amino acids. The pellet was combined with 1 ml 50 mM HEPES-KOH (pH 8.0) and centrifuged as before, the supernatant (containing proteins and membranes) was retained. Protein precipitation was carried out by tri-chloro acetic acid extraction: 250 µl 100% (w/v) ice-cold trichloroacetic acid was added to the samples, followed by incubation at 4°C for 2 hours. Samples were then centrifuged at 10,000 rpm for 10 minutes and the protein pellet washed twice with 200 µl ice-cold acetone. Pellets were dried at 95°C for 5 min and protein hydrolysis was carried out by adding 500 µl 6 M hydrochloric acid and treating at 100°C for at least 16 hours. Samples were dried under vacuum and then dissolved in 0.5 ml in dH_2O. Samples were adjusted to pH 4–6 with potassium hydroxide and dried again.

Sample preparation and GC-MS analysis

To derivatise, completely dry samples were incubated with 25 µl pyridine at 37°C, with shaking at 900 rpm for 30 minutes. 35 µl tert-butyldimethylsilylester (tBDMS) reagent (Sigma-Aldrich) was added and the samples incubated at 65°C, with shaking at 900 rpm for a further 30 minutes.

Samples were moved to glass vials and sealed with a septum cap. GC-MS analysis was performed using an Agilent 79890 GC/5975, quadrupole MS detector (70 eV) with a Varian VF5-ms column (30 m, 10 m guard column , 0.25 mm inner diameter). The mass spectrometer was calibrated before each run using the Agilent autotune method. For each run, 1 µl sample was injected. The oven was heated to 70°C for 5 minutes, then temperature increased at a rate of 5°C per minute until a temperature of 280°C. This temperature was held for 3 minutes before decreasing to 70°C at a rate of 120°C per minute. Helium gas flow rate was 0.6 ml per minute, and a solvent delay of 10 minutes was included.

GC peaks and ion abundances were obtained using Chemstation software (Agilent Technologies, Wokingham, UK). Mass ions were corrected for naturally occurring heavy isotopes and proportional abundance of heavy isotopes determined using MSCorr software (Wahl et al., 2004).

ATPase assay

Membrane extraction

Roots were excised from 14-day-old arabidopsis seedlings and were snap frozen in liquid nitrogen before grinding in a pre-cooled pestle and mortar under liquid nitrogen. Per gram of root powder, 3 ml of extraction buffer (350 mM sucrose, 70 mM Tris-HCl [pH 8] 10% glycerol, 3 mM Na_2EDTA, 0.15% BSA, 1.5% PVP-40, 4 mM DTT, containing proteinase inhibitor cocktail [Sigma-Aldrich]) was added and incubated on ice for 10 minutes. The suspension was centrifuged twice for 5 minutes at 2,000 *g* at 4°C. The supernatant was then centrifuged for 1 hour at 100,000 *g* at 4°C. The supernatant was discarded and the pellet (containing organelles and membrane fragments) was washed in 2 ml extraction buffer followed by centrifugation at 100,000 *g* for 1 hour. The pelleted membrane fraction was then used for assays of ATPase activity.

Assays

ATPase activities were determined by spectrophotometrically measuring production of Pi from ATP hydrolysis (Chifflet et al., 1988). V-ATPase and P-ATPase activity was assessed by measuring the reduction in ATP hydrolysis after inhibition with 50 mM KNO_3^- or 500 µM sodium orthovanadate, respectively. PPase activity was assessed by measuring the increase in PPi hydrolysis after PPase activation by addition of 50 mM KCl. Each reaction was prepared in an Eppendorf tube with 130 µl ATPase reaction medium (50 mM KCl, 3 mM $MgSO_4$, 0.1 mM EDTA, 1 mM molybdate, 50 mM Tricine [pH 7.0 with BTP] and 0.015 $mg.ml^{-1}$ Brij-58), 2.5 µg of membrane protein, and 20 µl of the appropriate inhibitor, made up to a final volume of 175 µl. The reaction was started by adding 3 mM ATP. Samples were incubated for 45 minutes at 20°C, after which the reaction was stopped by the addition of 200 µl 12% SDS. After 10 minutes, 300 µl of phosphate reaction medium (1:1 mixture of 6% [w/v] ascorbic acid in 1 M HCl and 1% [w/v] NH_4 -molybdate) was added, and after a further 5 minutes, 300 µl of citrate reaction medium (2% trisodium citrate, 2% sodium metaarsenite, 2% acetic acid) was added to stop Pi measurement. Solutions were transferred to cuvettes and absorbance measured at 850 nm. Phosphate concentration was determined by reference to a standard curve.

Ion conductance assay

For short-term temperature experiments, roots were excised from 23°C-grown arabidopsis plants and transferred to 10 ml media containing 170 mM glucose and 2.56 mM MES-KOH (pH 5.7). Roots were treated at 23°C or 33°C, with shaking (60 rpm). Media was replaced at 0.5, 1, 2 and 4 hours and removed media transferred to a 50 ml Falcon tube. Conductivity of the media after removal from the roots was measured; the conductivity meter was zeroed using fresh media. For each time point, a cumulative value of conductivity was calculated that included conductivity readings measured at all previous time points. For long-term temperature treatments, plants were grown at 30°C or 23°C, roots excised and treated in the at either 23°C or 30°C. Conductivity

over time was determined as before. Results were expressed as the relative electrical conductivity (REC) = conductivity / total conductivity. Total conductivity was determined by autoclaving the samples at 121°C, 1.04 Pa to release electrolytes from the cells and measuring conductivity.

Determination of *in vivo* P/O ratio

In vivo P/O ratio was investigated using a method adapted from Nemutlu et al. (2012) that uses a $^{18}H_2O$ labelling strategy. The work flow for the determination of ATP turnover is shown in Figure 2.1.

Feeding with $H_2{}^{18}O$

Roots were excised from 14-day-old seedlings grown in liquid culture. Roots from each flask were then incubated in 2 ml 0.22% (w/v) Murashige & Skoog, 170 mM glucose, 2.56 mM MES (pH 5.7), supplemented with 20% $H_2{}^{18}O$ for time intervals ranging from 1–60 minutes. After incubation, tissue was snap frozen in liquid nitrogen, and stored at –80°C.

Metabolite extraction

Metabolites were extracted by TCA precipitation; frozen root tissue was ground under liquid nitrogen using a pestle and mortar and transferred to Eppendorf tubes containing 1 ml ice-cold 12% TCA (w/v), 5 mM EDTA. Samples were thawed on ice for 2 hours before centrifugation at 4,000 *g* for 10 minutes. The supernatant was retained and 1 ml dH_2O saturated diethyl ether added to remove TCA from the aqueous phase. Samples were vortexed, centrifuged at 4,000 *g* for 2 minutes and the ether removed. TCA was extracted with 1 ml diethyl ether a total of four times. 10 µl 5 M KOH was added to the sample to neutralise.

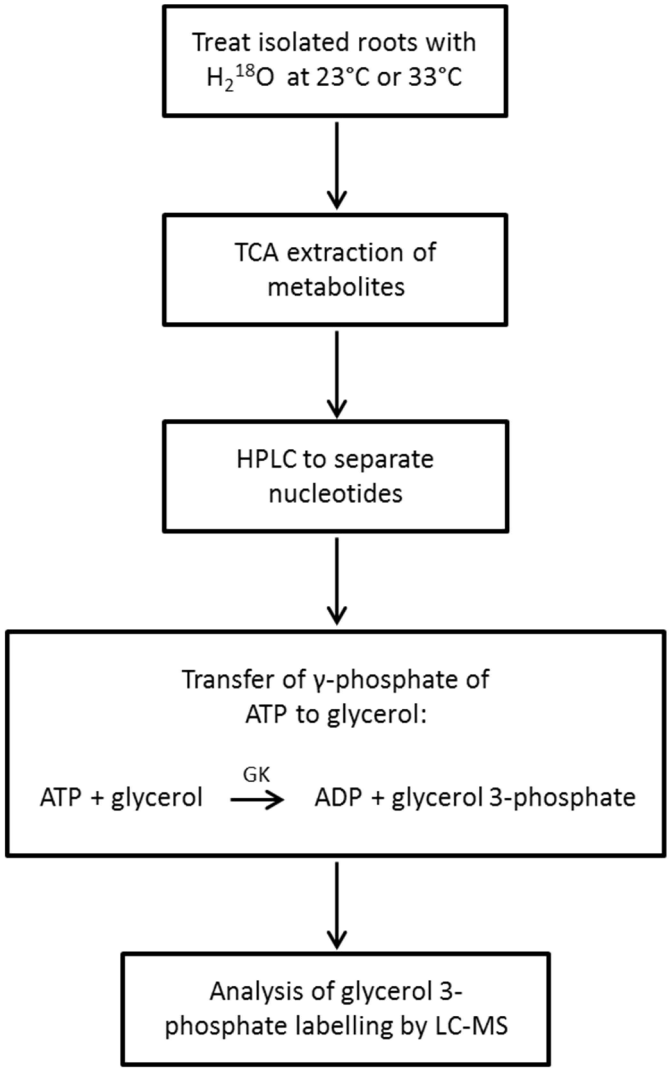


Figure 2.1. Work flow for the determination of ATP turnover rate using $H_2{}^{18}O$

Abbreviations: TCA = trichloroacetic acid, HPLC = high-performance liquid chromatography, GK = glycerokinase, LC-MS = liquid chromatography – mass spectrometry.

HPLC

Nucleotides were separated by HPLC, using a Partisil 10 SAX column (Hichrom, Reading, UK) and 0.3 M ammonium bicarbonate for gradient elution at a flow rate of 1 $ml.min^{-1}$. The gradient program used is shown in Figure 2.2. Fractions containing ATP were freeze dried and stored at –80°C.

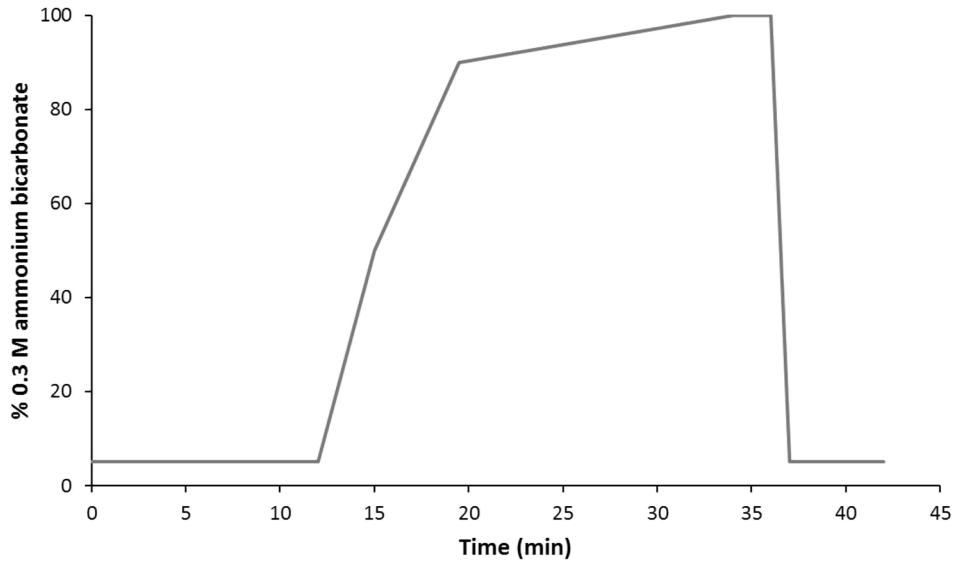


Figure 2.2 Gradient program for the separation of nucleotides by HPLC.

Glycerokinase reaction

Purified ATP was resuspended in 25 µl dH_2O. The glycerokinase reaction was initiated by adding 2.5 mM $MgCl_2$, 5 mM glycerol and 5 U glycerokinase to the ATP sample to a final volume of 100 µl, and incubating at 37°C for 30 minutes. Glycerokinase was removed from the samples by chloroform-methanol extraction; 350 µl of an ice-cold chloroform:methanol (3:7, v/v) mixture was added to each sample and the samples were incubated at –20°C with occasional mixing. 350 µl of water was added and the samples were warmed to 4°C with repeated shaking. The mixture was centrifuged at 420 *g* for 10 minutes and the upper aqueous-methanol phase retained. The chloroform phase was re-extracted with 300 µl cold water, centrifuged as before and the upper phase once again removed. The pooled aqueous-methanol extract was lyophilised.

LC-MS

^{18}O-labelling in glycerol 3-phosphate was quantified by LC-MS analysis in collaboration with John Lunn, Max Planck Institute of Molecular Plant Physiology, Potsdam, Germany.

3. The effect of short-term temperature increase on respiration rate and carbon use efficiency

Introduction

It is widely recognised that respiration is sensitive to short-term changes in temperature such as those experienced by plants on a daily basis, and increases as temperature rises with a Q_{10} of between 1.1 and 2.9 (Atkin et al., 2000). Growth rate also increases with short-term increases in temperature, which explains a proportion of the increase in respiratory CO_2 production as energy and carbon skeletons required for the biosynthesis of cellular components are supplied by respiration. However, a proportion of respiration originates from processes not associated with growth: resulting from uncoupling of the mtETC, cell maintenance costs such as protein turnover and ion gradient homeostasis, and futile cycles of ATP synthesis and hydrolysis (Penning de Vries, 1974; Amthor 2000). Non-growth respiration leads to carbon loss as CO_2 without contributing to biomass synthesis and is an inefficient use of substrate carbon that limits the carbon available for growth. The proportion of respiration that does not contribute to growth has been estimated to be high (Masakapalli et al., 2010), however, a thorough assessment of the efficiency of carbon use at a range of temperatures has not been undertaken. This can be assessed using two parameters: carbon conversion efficiency (CCE) and coefficients of growth and maintenance.

Carbon conversion efficiency

Plant growth is dependent on the quantity of substrate available and the efficiency with which it is converted into biomass. CCE, the proportion of substrate carbon passing through metabolism that is converted into biomass (Hansen et al., 2009), is a measure of this efficiency. A reduction in CCE demonstrates that there is an increase in respiratory costs relative to carbon incorporation

into biomass; such costs result from an increase in the specific respiratory cost for growth or an increase in non-growth respiration.

Two general approaches are used to calculate CCE: carbon balance and calorimetry. Carbon balance directly accounts for carbon entering respiratory metabolism and lost as CO_2. One method to measure this is to calculate the ratio of respiration to photosynthesis. CCE is calculated as net daily carbon gain divided by gross daily photosynthesis. This method is suitable for long-term measurements of CCE, however, as measurements of carbon gain and photosynthesis over the course of a day are required, this method is not suitable for taking short-term measurements of CCE necessary to study the response of CCE to changes in temperature over a few hours. For instance, CCE was calculated from gas exchange measurements taken over four weeks in lettuce (van Iersel, 2003a) or over 42 days in tomato (Frantz and Bugbee, 2005). Another method to account for carbon entering and leaving respiratory metabolism is to feed ^{14}C-labelled substrate and determine the fate of substrate carbon by measuring radioactivity in biomass components and CO_2. This approach has been used to measure CCE of small tissue samples over a relatively short time frame; CCE during oil production in *Brassica napus* embryos was measured by feeding uniformly labelled substrate for three days (Schwender et al., 2004), and in a heterotrophic arabidopsis cell suspension culture, CCE was determined by feeding with uniformly labelled glucose for 24 hours (Masakapalli et al., 2010). The second approach for calculating CCE is calorimetry. The metabolic heat rate, the sum of heat rates from anabolism and catabolism, is measured alongside the rate of CO_2 production, which is assumed to measure the rate of catabolism. However, CO_2 is also released from anabolic processes, such as lipid synthesis, and so the CO_2 production rate may not always be a good measure of the catabolic rate. CCE is calculated from the ratio of rates of catabolism and anabolism (Hansen at al., 2005). Like radioisotope feeding studies, this method has been used to measure the CCE of small tissue samples over a short time frame (Criddle et al., 1990; Smith et al., 2001). A further drawback of this technique is that it cannot be used on tissues in the light.

A small number of studies have previously measured CCE at elevated temperature. From a survey of calorimetric data from which CCE could be calculated at a range of temperatures, it was hypothesised that there is a general response of CCE to short-term changes in temperature, in which CCE remains fairly stable at temperatures spanning the normal growth range of a species and declines rapidly once the temperature limits for growth are reached (Hansen et al., 2009). The underlying biochemical reasons behind the drop in CCE beyond the temperature limits for growth were not established, but it was suggested that the decline in CCE is potentially due to uncoupling of the mtETC via AOX, limiting carbon availability for growth (Hansen et al., 2009). In a separate study, CCE was shown to decrease from 58% to 21% in arabidopsis cells in culture when growth temperature was increased from 21°C to 29°C. The decrease in CCE could be accounted for by a two-fold increase in TCA cycle flux and was accompanied by partial mitochondrial depolarisation, resulting from increased ATP production or mtETC uncoupling (Williams et al., 2010). However, the behaviour of a cell culture may not be representative of that of intact plant tissues: in a carrot cell culture, CCE was shown to be constant at temperatures ranging from 20°C to 35°C, whereas in carrot plantlets it was found that CCE changes across this temperature range, mirroring the response of growth to different temperatures (Nogales et al., 2013).

Further measurements of CCE are required at a range of temperatures in order to assess how short-term temperature changes affect CCE in an intact plant system, and how CCE changes relate to changes in non-growth respiration. For the experiments presented in this chapter, feeding with ^{14}C labelled substrate was used to determine CCE. This was the most appropriate method as CCE can be measured over short time frames allowing the short-term response to temperature to be established. Additionally, unlike calorimetry, this method allows direct measurement of the fate of metabolised carbon, allowing assessment of carbon partitioning to different biomass components and calculation of the specific respiratory cost of biomass synthesis and subsequent calculation of non-growth respiration.

Growth and maintenance coefficients

A second approach to assess the efficiency of carbon use under different conditions is to separate respiration into two components: respiration associated with growth and respiration associated with maintenance (Amthor, 1984). Estimates of growth and maintenance respiration at elevated temperature are limited, but have shown that the specific costs for growth are temperature insensitive, whereas costs for maintenance increase (van Iersel et al., 2003b; Szaniawski & Kietkiewicz, 1982; Marcelis & Baan Hofman-Eijer, 1995). However, the methods used to estimate maintenance respiration in previous work may be flawed. As there is no clear biochemical distinction between respiration to support growth and maintenance, it is difficult to separate respiration that is required to fuel the two processes. One method previously used to separate these components is by regression of relative growth rate and respiration; maintenance respiration is taken to be the value of respiration when relative growth rate equals zero (Gifford, 2003). This method requires variation in relative growth rate, which is often achieved by varying light intensity; however, this assumes a constant specific rate of maintenance respiration under different environmental conditions, which is unlikely given the role of maintenance processes in adaptation to changing environmental conditions. A second method is to measure the respiration rate of mature tissues (Wilson, 1982). As no growth is occurring in mature tissues, all respiration is assumed to come from maintenance. However, changes in biomass composition over the lifetime of a plant will alter maintenance costs: for instance, protein turnover is a significant contributor to maintenance costs whereas lignin does not turn over (Penning de Vries, 1975) resulting in lower specific maintenance costs as plants age (Jones et al., 1978), thus maintenance respiration rates of mature tissues may not reflect those in growing tissues.

Furthermore, the separation of respiration into growth and maintenance components has been criticised largely due to the existence of processes that do not easily fit entirely into either category. For example, costs for ion transport have previously been considered as either growth or maintenance, or treated as a separate component (Scheurwater et al., 1998). Nutrient uptake

is clearly necessary for growth, however, it can also form part of the maintenance cost when active ion transport is required to replace ions that have leaked back across the membrane (Amthor, 2000). A further criticism of the separation of respiration into growth and maintenance components is the assumption that all residual respiration after costs for growth have been accounted for results from maintenance processes (Thornley, 2011). Some respiration may occur as a result of ATP-consuming substrate cycles, in which metabolites are degraded and reformed (Kruger et al., 2007). Equally, uncoupling of the mtETC is not associated specifically with either growth or maintenance, but it does affect the rate of respiratory CO_2 loss to support these processes. In this chapter, these issues are minimised by calculating growth costs using a stoichiometric metabolic model that incorporates transport costs for growth into overall respiratory cost for the production of experimentally determined biomass, and assumes a constant P/O value (Cheung et al., 2013). Subtracting the model-generated value for biomass-associated respiration from total respiration does not give a value of maintenance respiration, but rather a value of non-growth respiration. Non-growth respiration encompasses the respiratory cost of all processes that do not contribute to growth, including uncoupling of the mtETC, maintenance processes and ATP consumption by substrate cycling.

Chapter aims

The aim of the work described in this chapter was firstly to characterise the effect of short-term changes in temperature on respiration and CCE of excised arabidopsis roots, and secondly to determine the origin of increased respiration at elevated temperature in terms of growth and non-growth respiration. The use of arabidopsis roots has a number of advantages. Firstly, as a heterotrophic system, determination of respiration rates and CCE is not complicated by the fixation of CO_2 by photosynthesis. Secondly, the existence of a genome scale metabolic model of heterotrophic arabidopsis metabolism (Williams et al., 2010; Cheung et al., 2013), which includes

costs for solute uptake and intracellular transport, facilitates determination of respiratory costs for growth and the separation of respiration into growth and non-growth components.

Results

Establishing an experimental system for the determination of CCE

Previously, CCE has been determined by feeding [U-^{14}C]glucose to arabidopsis suspension cells and determining ^{14}C incorporation into CO_2 and biomass components (Masakapalli et al., 2010). Initial experiments were designed to optimise and adapt this technique for arabidopsis roots. The optimum time for incubation with ^{14}C glucose was first determined; this had to be long enough for ^{14}C to permeate to the metabolic network and become linearly incorporated into all biomass components, but not so long that the excised roots begin to die. Roots of 14-day-old arabidopsis (ecotype Col-0) seedlings grown in liquid culture were removed and labelled with [U-^{14}C]glucose for 12, 18 and 24 hours at 23°C and ^{14}C incorporation into CO_2 and biomass components was determined. ^{14}C was incorporated linearly into major biomass components (Figure 3.1) and CO_2 (Figure 3.2) between 12 and 24 hours, signifying that pools of metabolic intermediates had reached isotopic steady state. No slowing of metabolism was observed, suggesting that cell death was not occurring in the excised roots within this time frame. Carbon partitioning to different biomass components was similar to that found in arabidopsis cell suspensions; in arabidopsis roots at 18 hours, 18% of carbon was partitioned to soluble sugars, 6% to organic acids, 8% to amino acids, 3% to starch, 8% to protein, 14% to cell wall, 4% to lipid and 40% to carbon dioxide, compared with carbon partitioning of 15% to sugars, 5% to organic acids, 16% to amino acids, 4% to starch, 7% to protein, 11% to cell wall, 2% to lipid and 39% to carbon dioxide in a heterotrophic arabidopsis cell suspension (Masakapalli et al., 2010). Carbon partitioning did not differ significantly between time points, with the exception of a small decrease in the proportion of ^{14}C that entered soluble

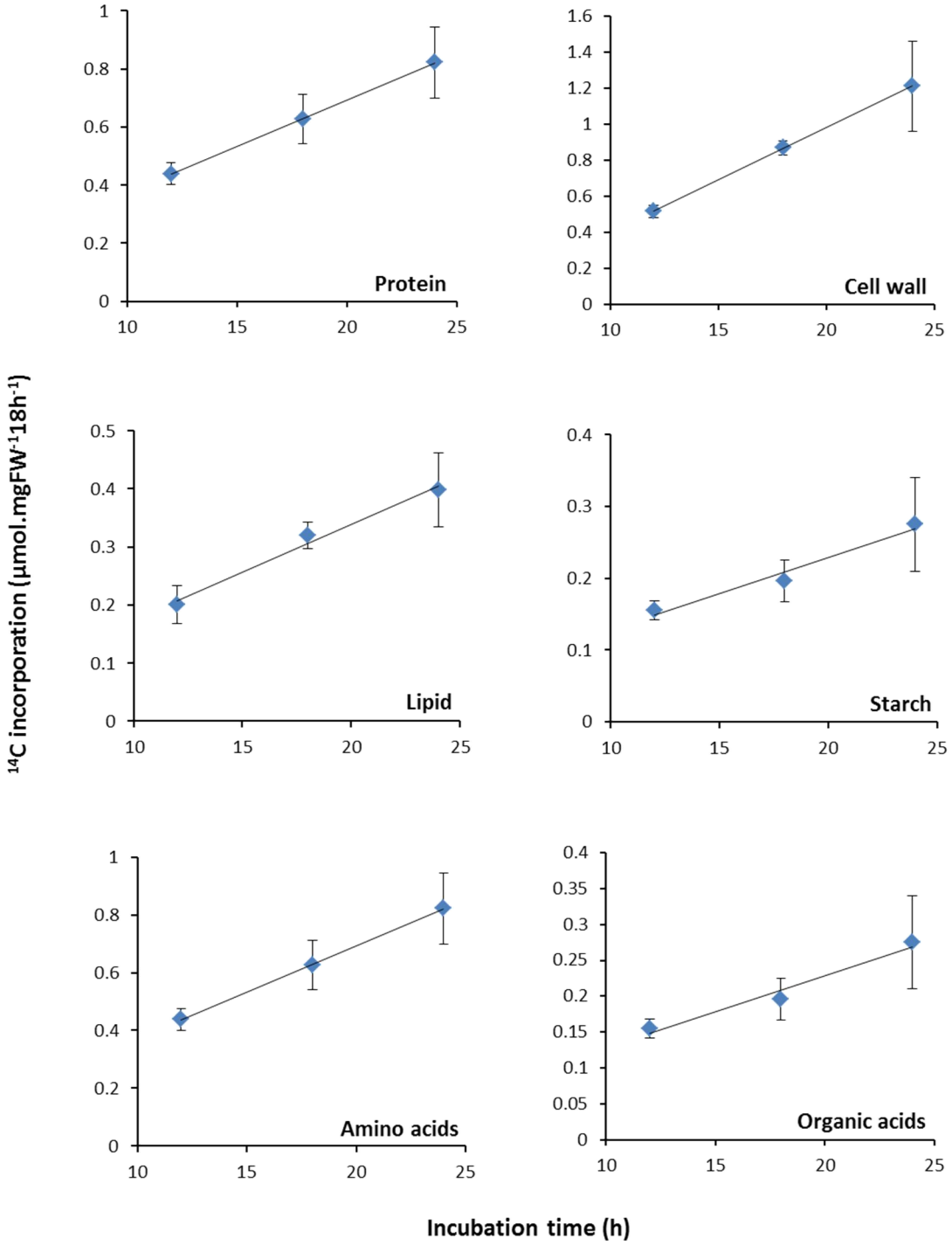


Figure 3.1. Time course of ^{14}C incorporation into root biomass fractions during incubation with [U-^{14}C]glucose.

Excised arabidopsis roots were supplied with [U-^{14}C]glucose (74 kBq in 5 ml of medium containing 170 mM glucose, 2.56 mM MES pH 5.7 and 0.22% [w/v] Murashige & Skoog) for either 12, 18 or 24 hours at 23°C. Label incorporation into major biomass components (protein, cell wall, lipid, starch, amino acids, organic acids and sugars) was measured at each time point. Data are the mean (n=4) ± SEM.

sugars and a small increase in labelling of cell wall components at 24 hours relative to the other time points (significant at p=0.05; Figure 3.3).

CCE was calculated from the ratio of ^{14}C incorporation into CO_2 to incorporation into total biomass:

$$CCE = \frac{B}{CO_2 + B} = \frac{1}{1 + (\frac{CO_2}{B})}$$

where CO_2 and B refer to ^{14}C incorporation into CO_2 and total biomass (µmol.mgFW^{-1}18h^{-1}), respectively. The CCE values for arabidopsis roots obtained here were 57.7 (54.7–61.3)% at 18 hours and 54.7 (50.8–59.1)% for 24 hours (the 68% confidence interval is shown in brackets; calculated from the standard error of the CO_2/B ratio). This is within the range of CCE values for heterotrophic tissues obtained in previous studies, with arabidopsis heterotrophic cell suspension culture having a CCE of 58-60% (Williams et al., 2010; Masakapalli et al., 2010). The difference between values obtained at 18 hours and 24 hours is not statistically significant (p=0.59).

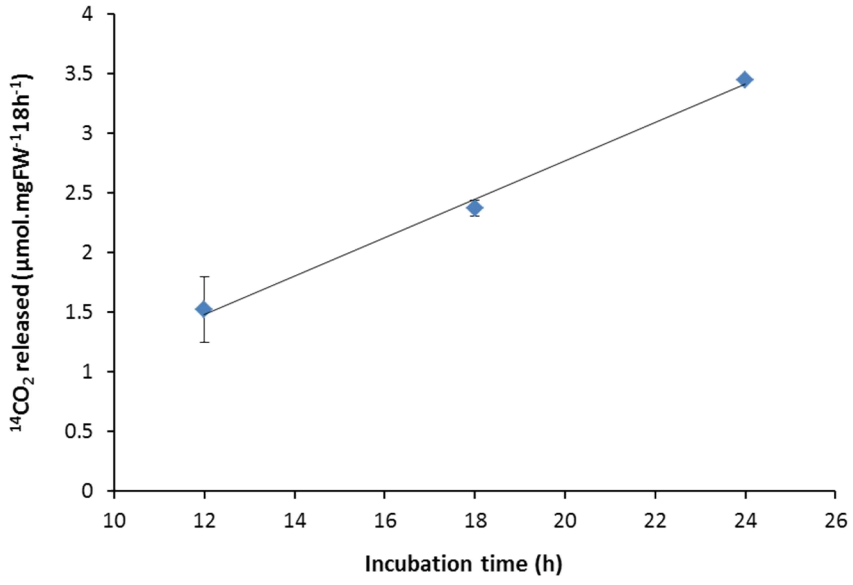


Figure 3.2. Time course of $^{14}CO_2$ release from root tissue during incubation with [U-^{14}C]glucose.
Excised arabidopsis roots were incubated with [U-^{14}C]glucose as described in Figure 3.1. $^{14}CO_2$ released during incubation was collected and radioactivity determined. Data are the mean (n=4) ± SEM for each time point.

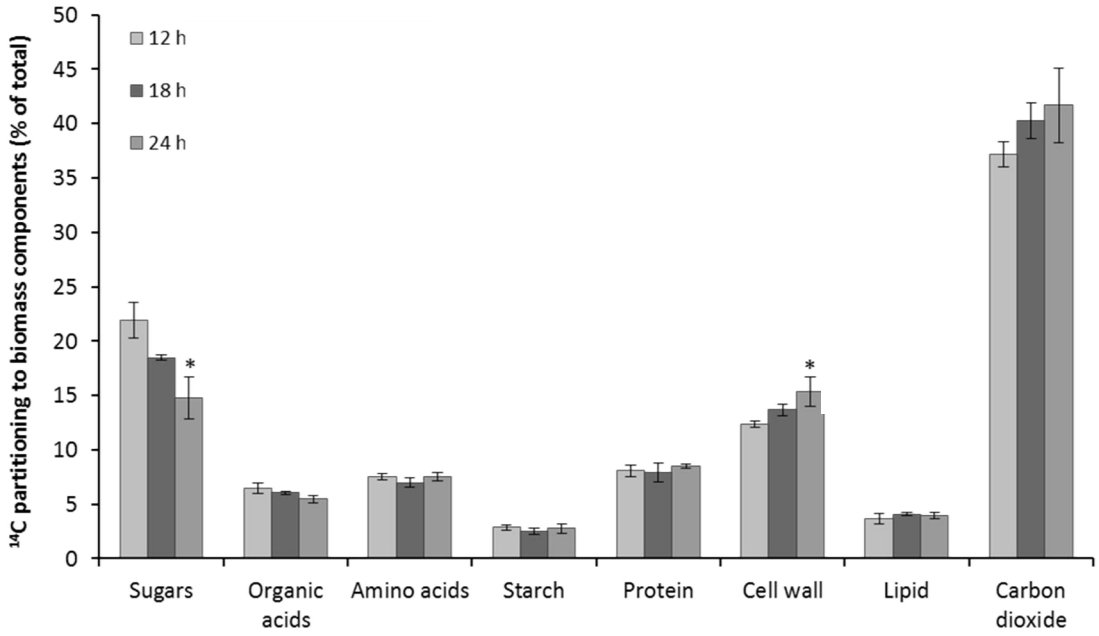


Figure 3.3. Carbon partitioning to biomass components and carbon dioxide after incubation with [U-^{14}C]glucose for 12, 18 or 24 hours.

^{14}C incorporation data for biomass components and CO_2 from Figures 3.1 and 3.2 presented as a percentage of total ^{14}C incorporation. Data are the mean (n=4) ± SEM. * denotes $p<0.05$ at 24 h compared with 12 h.

These initial experiments demonstrate that the ^{14}C feeding strategy is suitable for the determination of CCE in excised arabidopsis roots, and that after a feeding time of 18 hours, measurements of carbon partitioning to biomass components and CCE are stable.

The short-term temperature response of growth, respiration and CCE

To investigate the effect of short-term increases in temperature on the CCE of arabidopsis roots, excised roots from 14 day-old plants grown at 23°C were fed with [U-^{14}C]glucose for 18 hours at a range of temperatures from 23°C to 39°C. ^{14}C incorporation into total biomass and CO_2 was measured. A two-phase response of growth to temperature was observed: there was an increase in ^{14}C incorporated into both biomass and CO_2 with increasing temperature up to 37°C, with ^{14}C incorporation into biomass increasing 1.5-fold and incorporation into CO_2 increasing 2.7-fold from

23°C to 37°C (Figure 3.4A). However, at temperatures above 37°C, there was a rapid decline in ^{14}C incorporation into both biomass and CO_2. The response of CCE to short-term changes in temperature also followed a two-phase pattern with a gradual decrease in CCE from 60.2% at 23°C to 49.0% at 37°C (p=0.002) and a more rapid decline in CCE from 37°C to 39°C down to 15.6% (Figure 3.4B).

There are two possible explanations for the rapid decline in CCE and growth at temperatures above 37°C. The first is that CCE falls as a consequence of increased ATP consumption for cell maintenance or inefficient ATP production and this in turn limits the carbon available for growth. Alternatively, growth might cease due to factors other than CCE, such as regulation by growth regulators or cell death, and this growth cessation is the primary cause of reduced CCE. In order to differentiate between these possibilities, rates of non-growth respiration were calculated. If CCE was reduced as a consequence of maintenance costs and uncoupling of the mtETC, then it would be expected that the rate of non-growth respiration would increase at temperatures above 37°C.

Estimation of non-growth respiration using a flux-balance model

Respiration was separated into growth and non-growth components by using ^{14}C feeding data on carbon partitioning into biomass components (Figure 3.5) as constraints in a flux balance model of heterotrophic arabidopsis metabolism (Cheung et al., 2013). To understand the extent that biomass composition impacts on respiratory costs for growth, carbon partitioning to biomass components was assessed at 23°C and 39°C. These temperatures were selected to maximise differences in carbon partitioning. There were a number of significant changes in carbon

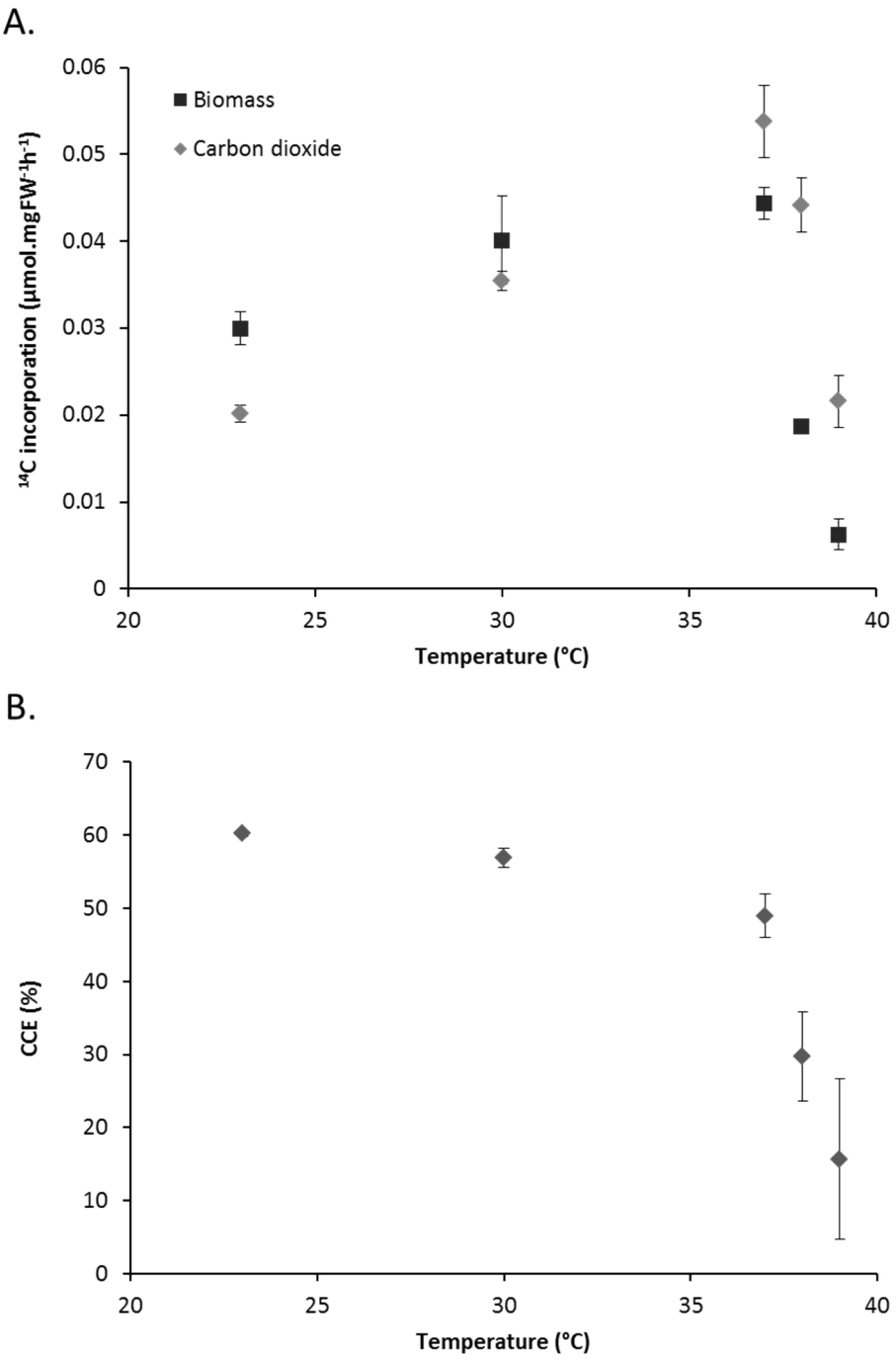


Figure 3.4 The effect of 18 hour elevated temperature treatment on the rate of $^{14}CO_2$ evolution, ^{14}C incorporation into biomass and CCE of roots from 23°C grown arabidopsis plants.

Excised roots were supplied with [U-^{14}C]glucose for 18 hours at 23°C, 30°C, 37°C, 38°C or 39°C. A. Relative incorporation of ^{14}C into total biomass and CO_2. B. The effect of temperature on CCE, calculated from the data presented in A. Data presented are the weighted means of independent experiments, Data are the mean ± SEM, 23°C n= 6 ; 30°C n= 3; 37°C n= 3; 38°C n= 3; 39°C n= 4.

partitioning. In particular, decreased synthesis of cell wall components and protein and increased synthesis of organic acids and starch as a percentage of total biomass production at 39°C. ^{14}C data were further fractionated into individual sugars, lipid, organic acids and amino acids according to proportions of these obtained from a heterotrophic arabidopsis cell culture (Masakapalli et al., 2010, Appendix Table 1). Using these biomass values as constraints, and assuming a constant value for the P/O ratio, the model predicted CO_2 release for the production of biomass. This value was subtracted from the experimentally determined CO_2 production rate, to provide a value of non-growth respiration. Despite some significant differences in carbon partitioning at 23° and 39°C, the specific respiratory cost for growth processes was calculated to be similar; 0.23 carbons

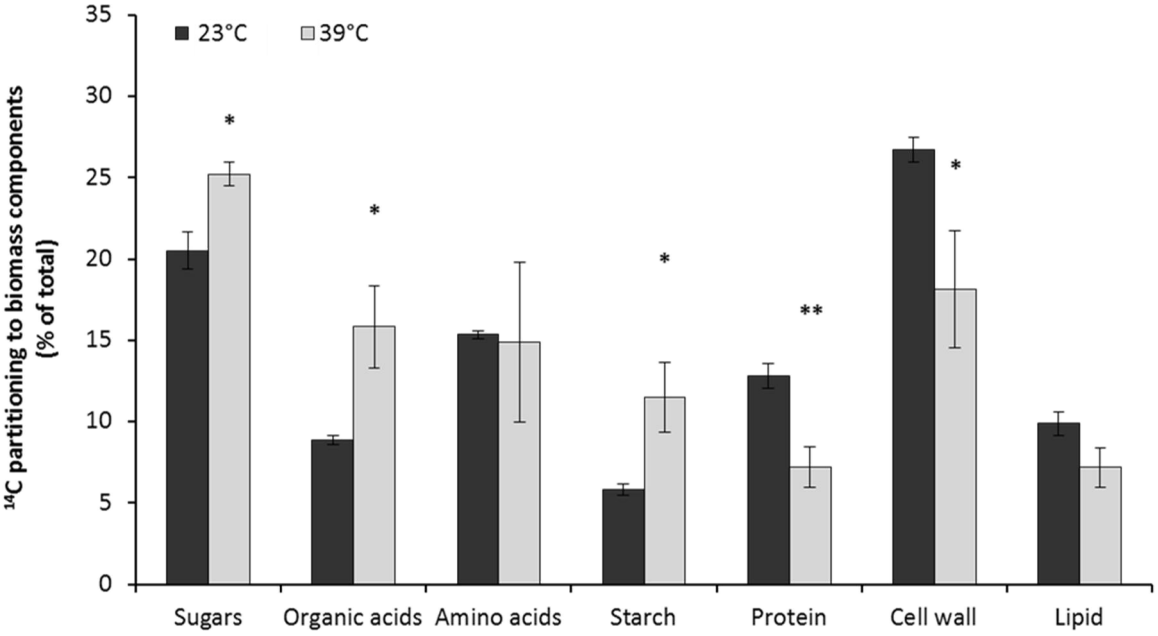


Figure 3.5. Carbon partitioning to biomass components at 23°C and 39°C.

Excised arabidopsis roots were supplied with [U-^{14}C]glucose (74 kBq in 5 ml of medium containing 170 mM glucose, 2.56 mM MES pH 5.7 and 0.22% [w/v] Murashige & Skoog) for 18 hours. Label incorporation into biomass components was determined after the 18 hour incubation and expressed as a percentage of total ^{14}C entering biomass. Data are the mean (n=4) ± SEM. Student's *t*-test * $p < 0.05$, ** $p < 0.01$.

were released as CO_2 per carbon incorporated into biomass at 23°C and 0.19 at 39°C. The specific respiratory cost for growth was assumed to be 0.23 carbons into CO_2 per carbon into biomass for temperatures between 23°C and 37°C. Table 3.1 shows calculation of non-growth respiration. Non-growth respiration increased 3.3-fold from 23°C to 37°C. Above these temperatures, non-growth respiration declined sharply (Figure 3.6A). When the rate of CO_2 release for non-growth processes is compared with total CO_2 and CO_2 for biomass production in the range of temperatures 23°C to 37°C, non-growth respiration dominates the increase in total CO_2 production; increasing from 65.9% of total respiration at 23°C to 81.0% at 37°C (Figure 3.6B).

Table 3.1. Calculation of non-growth respiration

Temperature (°C)	$^{14}CO_2$ production (nmol.mgFW^{-1}18h^{-1})	^{14}C in biomass (nmol.mgFW^{-1}18h^{-1})	$^{14}CO_{2(B)}$ (nmol.mgFW^{-1}18h^{-1})	$^{14}CO_{2(NG)}$ (nmol.mgFW^{-1}18h^{-1})	$^{14}CO_{2(NG)}$ (% of total $^{14}CO_2$)
23	20.1±0.9	30.0±1.9	6.9±0.4	13.3±1.1	65.9±3.3
30	35.4±1.1	40.1±5.1	9.2±1.2	26.2±1.9	74.0±3.5
37	53.7±4.1	44.4±1.8	10.2±0.4	43.5±4.1	81.0±7.1
38	44.2±3.1	18.7±0.8	4.3±0.2	39.8±3.1	90.3±7.4
39	21.6±3.1	6.3±1.8	1.2±0.4	20.4±3.0	94.5±13.4

$^{14}CO_2$ production and ^{14}C in biomass were determined by [U-^{14}C]glucose feeding experiments, described earlier. $^{14}CO_{2(B)}$ is the rate of $^{14}CO_2$ production attributable to growth, and is calculated by multiplying ^{14}C entering biomass by 0.23 (or 0.19 at 39°C), the model-generated specific respiratory costs for biomass synthesis. $^{14}CO_{2(NG)}$ is $^{14}CO_2$ production associated with non-growth processes, and is calculated by subtracting $^{14}CO_{2(B)}$ from total $^{14}CO_2$ production. Data are the mean ± SEM, 23°C n= 6 ; 30°C n= 3; 37°C n= 3; 38°C n= 3; 39°C n= 4.

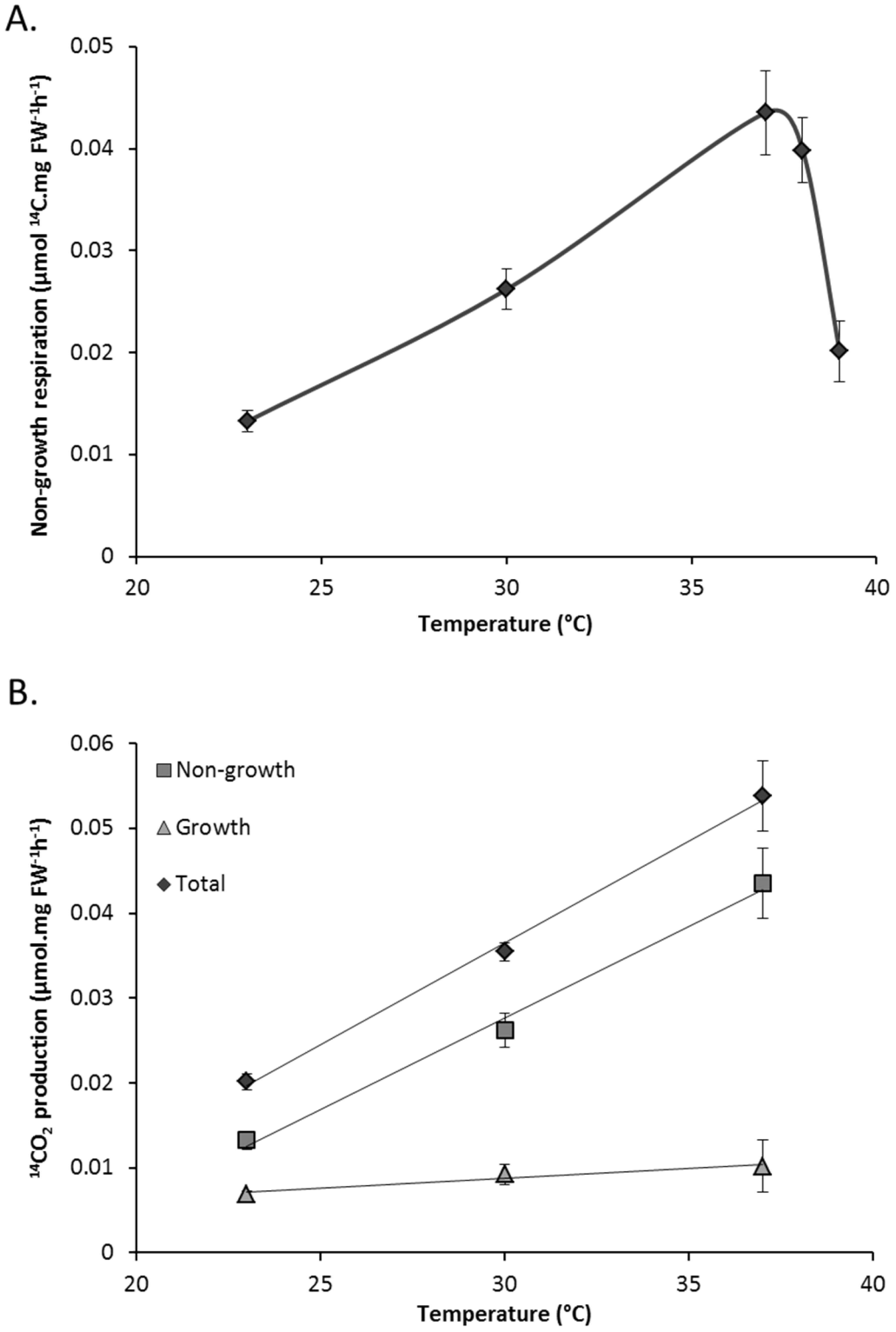


Figure 3.6. The effect of temperature on non-growth respiration.

A. Non-growth respiration in response to short-term changes in temperature up to 39°C. B. Respiration associated with growth and non-growth processes at temperatures ranging from 23°C to 37°C. Data are the mean ± SEM, 23°C n=6, 30°C n=3, 37°C n=3, 38°C n=3, 39°C n=4.

Determination of the source of non-growth CO_2 production

The major sites of CO_2 production in heterotrophic arabidopsis cells are the OPPP and the TCA cycle (Sweetlove et al., 2013). The TCA cycle activity provides reductant for ATP synthesis by the mtETC, whereas OPPP activity generates reductant in the form of NADPH. If non-growth respiration is increasing as a result of uncoupling of the mtETC or because of increased ATP consumption for cell maintenance processes, then it might be expected that CO_2 production by the TCA cycle would increase relative to CO_2 production by the OPPP. Two temperatures, 23°C and 33°C, were selected to further investigate the underlying causes behind the increase in non-growth respiration. These were selected because there is a significant increase in CO_2 release between the two temperatures, and higher temperatures at which growth ceases are avoided. The relative contribution to CO_2 production of the two pathways was tested by feeding excised arabidopsis roots with glucose ^{14}C labelled at the C1, C2, C3,4 or C6 positions for 18 hours and collecting the $^{14}CO_2$ emitted. CO_2 released from the C1 and C2 positions of glucose is associated with both the OPPP and the TCA cycle, whereas CO_2 release from C3,4 and C6 positions, primarily arises from the TCA cycle (ap Rees and Beevers 1960).

The amount of CO_2 released from all positions at 33°C was approximately double that of roots treated at 23°C (Figure 3.7), this is consistent with the CO_2 released from [U-^{14}C]glucose (Figure 3.4A). If there was an increase in the proportion of CO_2 released from the TCA cycle, then it would be expected that there would be a decrease in the ratios of CO_2 from C1/C6, C1/C3,4, C2/C3,4 and (C1-C6)/C3,4 (Averill et al., 1998). The small, although insignificant increase in C2/C3,4 (Table 3.2) is consistent with a greater proportion of the carbon entering the TCA cycle being completely oxidised to CO2 and a smaller proportion being withdrawn for biosynthesis. All other differences in the ratios were insignificant.

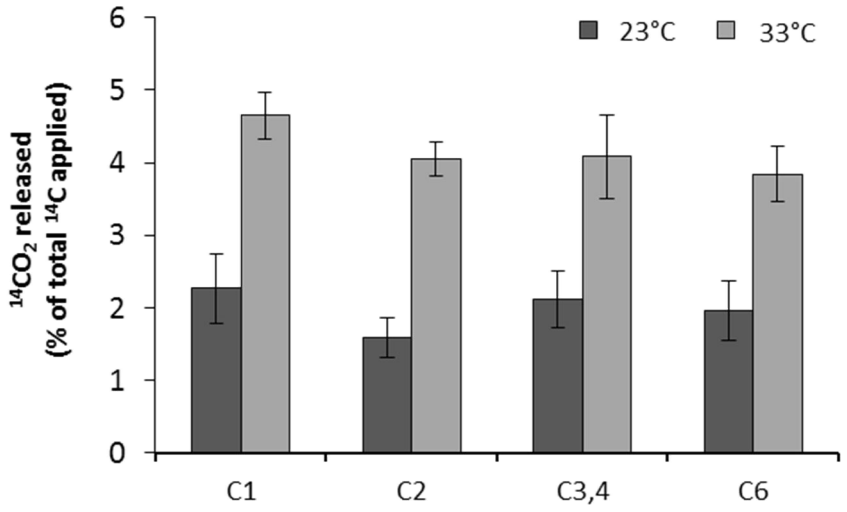


Figure 3.7. CO_2 release from different carbon positions of glucose

Excised arabidopsis roots from 23°C grown plants were incubated in 0.22% [w/v] Murashige & Skoog medium with 2.56 mM MES (pH 5.7), supplemented with 170 mM glucose containing 7.4 kBq [1-^{14}C]-, [2-^{14}C], [3,4-^{14}C]- or [6-^{14}C]-glucose. Feeding was for 18 hours in a sealed flask, after which, total CO_2 was collected in a KOH trap and radioactivity determined by scintillation counting.

Table 3.2. Ratios of CO_2 released from different carbon positions of glucose

	23°C	33°C	p value
C1/C6	1.27 ± 0.06	1.28 ± 0.09	0.95
C1/C3,4	1.04 ± 0.03	1.18 ± 0.12	0.35
C2/C3,4	0.79 ± 0.04	1.12 ± 0.15	0.08
(C1-C6)/C3,4	0.14 ± 0.04	0.24 ± 0.08	0.53

Calculated from data presented in Figure 3.7. Data are the mean (n=6) ± SEM. The p value was determined using a *t*-test.

Discussion

CCE decreases with temperature with a two-phase response

The ^{14}C feeding strategy used here was suitable for the calculation of CCE in arabidopsis roots; feeding [U-^{14}C]glucose for 18 hours generated a CCE value of 57.7-60.2% at 23°C, which is comparable to previous CCE estimates in heterotrophic systems: CCE was found to be 58-60% in heterotrophic cell suspension cultures (Williams et al., 2010, Masakapalli et al., 2010), 50% in sunflower embryos (Alonso et al., 2007), 50% in maize embryos (Alonso et al., 2011) and 52-68% in a tomato cell suspension culture (Rontein et al., 2002). When feeding experiments were conducted on excised roots from 23°C grown plants at a range of temperatures, $^{14}CO_2$ production increased with temperature with a Q_{10} of 1.93 between 23°C and 37°C. The Q_{10} value for arabidopsis roots presented here is in good agreement with previously published values of approximately 2.0 (Tjoelker et al., 2001). There was also an increase in ^{14}C incorporation into biomass at temperatures up to 37°C. This may reflect the fact that the roots are supplied with non-limiting substrate, assuming that they are able to take up sufficient glucose from the medium, causing the effect of temperature on enzyme kinetics to act to increase the rate of biomass synthesis in the short-term. From 37°C to 39°C, there is a decrease in the rate of ^{14}C incorporation into biomass and CO_2 as the temperature optimum for growth is exceeded. There is an overall decline in CCE from 23°C to 39°C, however, the decline in CCE has two phases; a slow decline in CCE in the temperature range at which growth is increasing with temperature and a more substantial decline once the temperature limits for growth are reached. This supports previous observations that CCE remains high until the temperature limits of growth are reached, at which point CCE declines rapidly (Criddle et al., 1997).

Despite increased ^{14}C incorporation into both CO_2 and biomass, there is a gradual decrease in CCE of 33% from 23°C to 37°C, demonstrating that there is an increasingly wasteful use of carbon in arabidopsis roots as temperature increases. Previously, it was calculated that even small changes

in CCE can have a large impact on productivity over the course of a growing season: a change in CCE from 70% to 80% would change growth over a unit of time by a factor of five, assuming that the specific rate of CO_2 production is constant (Hansen et al., 2009). In the results presented here, the rate of biomass production increases with temperature despite decreasing CCE. arabidopsisAssuming that glucose supply id non-limiting in this system, the abundance of substrate eases the potential competition between growth and maintenance processes for substrate. In a situation where substrate was limiting, and competition did exist, it is likely that substrate would be preferentially used to fuel maintenance at the expense of growth. Supporting this proposal, when substrate was limited in barley by transferring plants to dark conditions over a period of days, maintenance respiration in non-growing mature tissue proceeded as normal, however, growth in non-mature tissue ceased, alongside a simultaneous decrease in respiration (Robson and Parsons, 1981).

At temperatures above 37°C, there is a sudden drop in CCE that coincides with a similar drop in growth rate and CO_2 production. A reduction in CCE that mirrors a decline in growth rate in response to temperature has been observed by calorimetric methods in several other systems, including tomato and cabbage leaves (Criddle et al., 1997), maize (Smith et al., 2001), carrot plantlets (Nogales et al., 2013), winterfat (Thygerson et al., 2002) and cheatgrass (Mccarlie et al., 2003). One potential explanation for this drop in growth and CCE is that respiratory costs increase at temperatures above 37°C, either as a result of uncoupling of the mtETC or because of increases in maintenance processes. Activity of such processes then limits carbon availability for growth, and this leads to the simultaneous reduction in growth rate. Hansen et al. (2009) suggested that the large reduction in CCE above the temperature limits for growth may be at least partly because of increased AOX activity: they demonstrated a close relationship between the COX/AOX activity ratio and CCE by calculating that CCE would drop from 85% to 65% if all oxygen reduction switched from COX to AOX. However, for this to explain such a precipitous drop in CCE, a sudden switch on of AOX activity at a particular temperature would be required alongside abrupt

activation of other energy-wasting processes, and there is no published evidence that this actually occurs (Gonzalez-Meler et al., 1999; Searle et al., 2011; Vanlerberghe, 2013). A different explanation for the drop in CCE and growth at temperatures above 37°C relies on the interdependence of CCE and growth; CCE will decrease with growth cessation, even if that growth cessation is due to factors other than a direct result of CCE on growth. Growth cessation independent of lower CCE could occur because of cell death, or because of the activation of growth regulators such as DELLA proteins, which inhibit growth in response to abiotic stresses (Achard et al., 2008).

Non-growth respiration increases with temperature up to 37°C

By looking at the effect of increased temperature on non-growth respiration, it is possible to understand in more detail the relationship between growth, respiration and CCE. Non-growth respiration was calculated by subtracting a model-generated value of growth respiration from experimental values of total respiration. The specific costs for growth will only change if the biomass composition alters and changes in growth respiration with temperature have long been assumed to reflect changes in growth rate rather than changes in the specific cost of producing biomass (Penning de Vries et al., 1974). There was a small decrease in the specific cost for growth at 39°C compared with 23°C and the use of the specific cost for growth at 23°C to calculate non-growth respiration for all temperatures up to 37°C may result in a slight underestimation of non-growth respiration at the higher temperatures. However, specific respiration for growth was shown to be the same across a range of moderate growth temperatures in cucumber fruit and sunflower roots (Marcelis and Baan Hofman-Eijer, 1995; Szaniawski and Kietkiewicz, 1982). Additionally, the very slow growth rate at 39°C may indicate that the roots were severely stressed at this temperature and this might explain the change in carbon partitioning to biomass components; in heterotrophic arabidopsis cells at 29°C, a similar reduction in specific ATP cost

was observed alongside a decline in the growth rate, relative to cells at 21°C (Williams et al., 2010).

The observed relationship between temperature and non-growth respiration highlights the importance of non-growth respiration to the overall carbon budget of the plant across a range of temperatures. At 23°C, 65.9% of CO_2 was released from non-growth respiration, signifying that cell maintenance and mtETC uncoupling make up the majority of the overall respiratory cost even at low temperatures. This corroborates results from a heterotrophic arabidopsis cell culture, in which non-growth respiration was found to account for over half of total respiration (Masakapalli et al., 2010). There was a dramatic increase in the rate of non-growth respiration from 23°C to 37°C, with a Q_{10} of 2.45. Similarly, in four bedding species, it was calculated that maintenance respiration increased with temperature with a Q_{10} of between 2.5 and 2.6 (Van Iersel, 2003) and a Q_{10} of two for maintenance respiration was calculated in ryegrass (Jones et al., 1978). The increase in the rate of non-growth respiration with temperature was not matched by the increase in the rate of growth respiration, which increased with temperature with a Q_{10} of 1.31. Thus, as temperature increased, non-growth respiration became more dominant, making up 81.0% of total respiration at 37°C. This increase in non-growth respiration explains the decrease in CCE observed between 23°C and 37°C

The relationship between non-growth respiration and CCE also provides some insight into the rapid decline in CCE at temperatures above 37°C. If the drop in CCE at this point was due to the switching on of some process resulting in increased maintenance costs or uncoupling of the mtETC, and this in turn was driving a reduction in growth due to competition for substrate, then it would be expected that the rate of non-growth respiration would continue to increase beyond this. However, at temperatures of 38°C and 39°C, there was a sharp decrease in the rate of non-growth respiration from a maximum at 37°C, following the pattern of the response already observed for CCE and ^{14}C incorporation into biomass and total CO_2 (Figure 3.4). It is, therefore,

most likely that the reduction in CCE is caused by growth cessation from an overall slowing of metabolism, possibly indicative of cell death, and it can be concluded that this observed drop in CCE is not relevant as part of the normal physiological response of the system.

CO_2 release from the TCA cycle and the OPPP increases proportionally at elevated temperature Determining the sites of CO_2 production can give insight into the underlying processes driving an increase in non-growth respiration at high temperature. The TCA cycle produces reductant that fuels ATP synthesis by the mtETC; if the increase in non-growth respiration resulted entirely from mtETC uncoupling processes and ATP consumption by cell maintenance processes and substrate cycles, then it would be expected that the proportion of CO_2 released from the TCA cycle relative to the OPPP would increase. Results from feeding glucose labelled at different positions suggested that while CO_2 production from both pathways was increased at 33°C relative to 23°C, there was no significant change in the proportion of CO_2 that originated from the TCA cycle and the OPPP. There are a number of potential reasons for increased OPPP activity: firstly, the OPPP supplies reductant for many biosynthetic reactions, so the increase in growth at the higher temperature would partly explain the increased OPPP activity. Secondly, there is a requirement for reductant for certain cell maintenance processes such as lipid turnover and ROS detoxification pathways. Cheung et al. (2013) predicted that 50% of total NADPH produced was used for maintenance in an arabidopsis cell suspension culture. Despite this, the relative consumption of NADPH for maintenance is low compared with ATP consumption for maintenance; in arabidopsis heterotrophic cell suspension cultures, it was predicted that NADPH costs for maintenance were 35% that of ATP costs for maintenance (Cheung et al., 2013), and 15% of total CO_2 was produced by the OPPP compared with approximately 58% for the TCA cycle (calculated from data in Williams et al., 2010). This suggests that while the rate of CO_2 production by both pathways is increasing with temperature to a similar extent, it is likely that the TCA is dominating overall CO_2 production at both 23°C and 33°C. Therefore, the source of non-biomass respiration is likely to be primarily an increase in ATP consumption for maintenance processes or uncoupling of the mtETC.

Summary

The aims of this chapter were to characterise the response of respiration and CCE to increasing temperature, and to establish the metabolic origin of changes in respiration and CCE in terms of growth and non-growth respiration. The data presented in this chapter show that, as expected, there was an increase in total respiration with increasing temperature. CCE declined with increasing temperature up to 37°C, and it was shown that this decrease was due to an increase in non-growth respiration with temperature. Increased non-growth respiration is a consequence of both increased TCA cycle and OPPP activity, but it is likely to be dominated by changes in processes involved with ATP production and consumption.

4. Identifying ATP-consuming processes that contribute to increased ATP consumption

Introduction

In previous chapters, an increase in non-growth respiration at high temperatures was demonstrated. It was shown that the majority of non-growth CO_2 production originated from the TCA cycle and is a result of decreased mtETC coupling or increased ATP consumption for non-growth processes. This chapter looks at the effect of temperature on ATP consumption and aims to dissect the individual processes contributing to overall ATP consumption at high temperature.

Major ATP-consuming processes

Protein turnover and the maintenance of ion gradients across cellular membranes are frequently cited as being the most important maintenance processes in terms of energy requirement (Amthor, 2000; Scheurwater et al., 2000; Penning de Vries, 1975). Protein turnover is essential to replace damaged proteins and to change the protein complement of cells to deal with environmental change (Huffaker and Peterson, 1974). In leaves it was found that protein turnover consumed 34% of total ATP produced in wheat (Zagdanska, 1995) and 17–37% of respiratory costs in potato (Bouma et al., 1994). Furthermore, in both wheat roots and *Petunia* x *hybrida* petals, it was demonstrated that increased temperature lead to a higher rate of protein turnover (Ferguson et al., 1990; Hachiya et al., 2007).

Maintenance of ion gradients also contributes significantly to non-growth respiration (Scheurwater et al., 1998; Zagdanska, 1995). Furthermore, the cost of maintaining ion gradients is likely to increase at elevated temperature as membrane fluidity increases, resulting in greater ion leak (Los and Murata, 2004). Therefore, to account for the increase in non-biomass respiration

observed in Chapter 3, the effect of temperature on protein turnover and ion gradient homeostasis will be considered.

Methods for studying protein turnover

Protein turnover is the degradation and re-synthesis of proteins, although it is often assessed as the rate of protein degradation, which can be determined by performing pulse-chase experiments. Commonly, amino acids labelled with either radioactive or stable isotopes are fed to plant tissue and become incorporated into protein. The rate of loss of label from the protein fraction after transfer to non-labelled media is used to calculate the degradation rate (Huffaker and Peterson, 1974). This approach was used to calculate a mean cellular protein half-life of 4–6 days in two grass species (Scheurwater et al., 2000). However, there are problems with this approach: the incorporation of exogenously supplied amino acids into protein may be inefficient as plants are able to synthesis all amino acids *de novo*, thus diluting labelled amino acids (Gruhler et al., 2005; Yang et al., 2010). For instance, it was found that exogenous sugar is a more direct source of amino acids for protein than amino acids applied exogenously (Bidwell et al., 1964). The presence of inactive storage pools of amino acids also presents a problem as metabolically active pools may not be in rapid equilibrium with storage pools, and this limits the incorporation of exogenously supplied label into protein (Oaks and Bidwell, 1970). Additionally, labelled amino acids liberated from protein can be reincorporated into newly synthesised protein during the chase period resulting in an underestimation of the degradation rate, and accounting for this recycling is not possible unless the size of the precursor pool is known.

Labelling experiments using ^{15}N have been performed to overcome the problems of *de novo* amino acid synthesis and inactive storage pools. By switching plants to ^{15}N substrate, for instance $^{15}NH_4{}^{15}NO_3$ and $K^{15}NO_3$ (Li et al., 2012), label is incorporated into amino acids synthesised de novo. The rate of protein degradation is then calculated by tracking the decrease in the

proportional size of natural abundance amino acids in protein (Nelson et al., 2014). However, this method is associated with some disadvantages. Firstly, there is a lag from initial ^{15}N feeding to the label appearing in amino acids as a consequence of ^{15}N substrate uptake and amino acid synthesis, and accounting for this complicates experimental design and analysis (Nelson et al., 2014). Additionally, as with pulse-chase experiments using exogenously supplied labelled amino acids, reincorporation of unlabelled amino acids into protein is possible. Despite this, advances are currently being made in the analysis of data from such experiments to counteract these problems and this technique has been used to determine protein turnover in 84 proteins in arabidopsis (Li et al., 2012), as well as determining the degradation rate for proteins in the mitochondrial proteome (Nelson et al., 2013).

Methods using tritiated water (^3H_2O) were developed also to avoid the issues associated with pulse-chase experiments using exogenously supplied labelled amino acids. ^3H_2O rapidly equilibrates with water in all cellular compartments. Subsequently the action of transaminases transfers ^3H onto the α-carbon of amino acids. Once the amino acid has been incorporated into protein, this ^3H cannot be removed by the reverse reaction, although it can be removed from free amino acids once the protein has been degraded and consequently reincorporation of labelled amino acids is reduced. This approach was used to assess total protein degradation in *Lemna minor*, and a half-life of 3–7 days was calculated (Humphrey and Davies, 1975). More recently, the same principles were applied to labelling with deuterated water (D_2O; Yang et al., 2010). However, deuterium can be toxic to living systems and this may have an effect on protein turnover rates; 50% D_2O caused protein synthesis to be inhibited by 20% (Cooke et al., 1979), and 60% D_2O was lethal to *Nicotiana tabacum* plants (Uphaus et al., 1975). Yang et al. (2010) characterised the effect of D_2O in arabidopsis and found that D_2O stress was concentration dependent and transient: 30% D_2O inhibited hypocotyl and root growth by approximately 27%, and 10% D_2O inhibited growth by 10%. In the same study, microarray data demonstrated a moderate stress response to D_2O, however, this appeared to be short-term with initial changes in

gene expression dissipating over time. Additionally, expression of most genes upregulated in response to D_2O exposure decreased after four hours of recovery in H_2O.

Whilst using tracers to measure protein degradation rates is useful to determine the half-lives of proteins under different conditions, this alone does not give any indication of the contribution that protein turnover has on the overall ATP budget and respiration. The significance of protein turnover has been assessed by taking measurements of respiration in the presence of the protein synthesis inhibitor, CHI. This method relies on the principle that inhibition of a process that consumes ATP will lead to a corresponding decrease in respiratory O_2, and has been used in several studies to calculate ATP consumption for protein turnover (Zagdanska, 1995; Bouma et al., 1994; Hachiya et al., 2007).

Methods to assess ATP cost for maintaining ion gradients

Membrane ATPases are essential for maintaining ion gradients across plant membranes; ATP hydrolysis is coupled to proton-pumping to generate a proton gradient that drives secondary transport of ions. Previously, the effect of different treatments on membrane integrity has been inferred by looking at the activity of membrane ATPases in microsomal extracts after different temperature treatments; chilling and heat treatments led to increased ATPase activity in grape plants and this was accompanied by an increase in electrolyte leakage (Zhang et al., 2006). Additionally, a transient increase in ATPase activity was observed in response to chilling stress in cucumber roots (Ahn et al., 2000). These studies highlight the potential impact that ATPase may have on the ATP budget under short-term changes in temperature. However, whilst measurement of ATPase activity can be a useful indicator of membrane state, it is a measure of enzyme capacity rather than *in vivo* activity, and ATP consumption for ion gradient homeostasis *in vivo* depends on both ATPase protein abundance and *in vivo* regulation. For instance, the stoichiometry of ATPases has been shown to change under certain conditions; in membrane vesicles isolated from lemon

fruit (Müller & Taiz, 2002) and yeast (Kettner et al., 2003), the stoichiometry of the V-ATPase decreased as ΔpH across the membrane increased. Variable stoichiometry of the plasma membrane H^+-ATPase was also demonstrated in response to salinity stress in cucumber roots, with an increased H^+/ATP coupling ratio under salinity stress (Janicka-Russak et al., 2013). Therefore, to calculate how temperature affects ATP consumption for ATPase activity *in vivo*, it is necessary to use an inhibitor approach similar to that previously described for protein turnover. This has been previously attempted for P-ATPase in wheat leaves using vanadate as an inhibitor and it was found that P-ATPase consumes 13% of total ATP consumed (Zagdanska, 1995). However a similar approach has not been attempted for V-ATPase in plants.

Chapter aims

The aim of this chapter is to assess whether changes in ATP-consuming cell maintenance processes are responsible for the increase in non-growth respiration at high temperature found in Chapter 3. This will be achieved firstly by determining the protein turnover rate and ATPase activities at 23°C and 33°C, and secondly by constructing an ATP budget at these temperatures to measure the relative contribution of these processes to overall ATP consumption.

Results

Calculation of the protein turnover rate at 23°C and 33°C

Establishing a D_2O feeding method to measure protein turnover

When plants are grown in D_2O containing media, ^2H is incorporated into all amino acids. To ensure that labelled amino acids are not reincorporated into newly formed protein during the chase period, the labelling of only amino acids that are rapidly de-labelled after release from protein

must be considered. To this end, plants were grown in media containing 20% D_2O and transferred to D_2O-free media after 14 days. Free amino acids were extracted from roots 1, 2 , 4, 8 and 24 hours after transfer to the unlabelled media and labelling of amino acids detected by GC-MS. Labelling in nine amino acids was detected and the half-life of label in free amino acids calculated. The relative abundance of deuterium in each amino acid fragment, R, was calculated by:

$$\boldsymbol{R = \frac{\sum_{i=0}^{n}(M_i - NA_i)\, x\, i}{n}}$$

where *n* is the number of hydrogen atoms that can be labelled in a particular fragment, M_i is the proportion of heavy mass isotopomers determined by GC-MS, *NA* is the natural abundance of mass isotopomers and *i* is the number of labelled hydrogens. For time point zero, the relative abundance of heavy mass isotopomers was set at 1.0. For all amino acids detected except alanine, label was linearly removed with half-lives ranging from 18.8 hours to 96.2 hours (Figure 4.1). The slow removal and incomplete removal of label reflects the fact that ^2H is incorporated into some amino acids at positions from which it cannot be removed by transamination. Removal of label from alanine was much faster, with a half-life of 2.0 hours and 84% of label had been removed after 24 hours. Therefore, to study protein turnover with minimal reincorporation of labelled amino acids into protein, loss of labelled alanine from protein was examined.

The rate of protein turnover is similar at 23°C and 33°C

Arabidopsis plants were grown in 20% $D_2O$for 14 days at 23°C before transfer to D_2O-free media at 23°C and 33°C for 0, 24, 48 and 72 hours. Protein was extracted from roots and ^2H labelling in alanine determined to give the rate of label loss from protein (Figure 4.2A). However, the rate of label loss is not equivalent to the protein degradation constant (K_D), as incorporation of newly synthesised amino acids into protein after transfer to D_2O-free media acts to dilute the labelling in protein. To account for this dilution effect, total protein content was measured at the same time

points (Figure 4.2B), and K_D was calculated by determining the quantity of labelled protein at each time point, expressed as a proportion of the quantity of protein at t_0 (L), according to the following equations:

$$L = \frac{(L_{obs}\ x\ Pt_n)}{Pt_0}$$

$$K_D = \frac{L}{time}$$

L_{obs} is the proportion of ^2H label in protein alanine from experimental data, Pt_n is the protein content in the root sample at t_n and Pt_0 is the protein content at t_0. Small differences were found in the observed rate of protein loss and the rate of protein accumulation at 23°C and 33°C (Figure 4.2A). There was a 1.2-fold increase in the rate of protein accumulation at 33°C compared with 23°C (Figure 4.2B). It is surprising that there was not a greater increase in the rate of protein accumulation at 33°C, given the increased growth rate demonstrated in Chapter 3. This may be explained by an erroneous result at 72 hours, as the rate of protein increase is 1.7-fold higher at 33°C compared with 23°C when this point is excluded, which is consistent with results from Chapter 3. The calculated rate of protein degradation was the same at 23°C and 33°C (Figure 4.2C), with both treatments having a K_D of 0.0055 h^{-1} (0.13 day^{-1}).

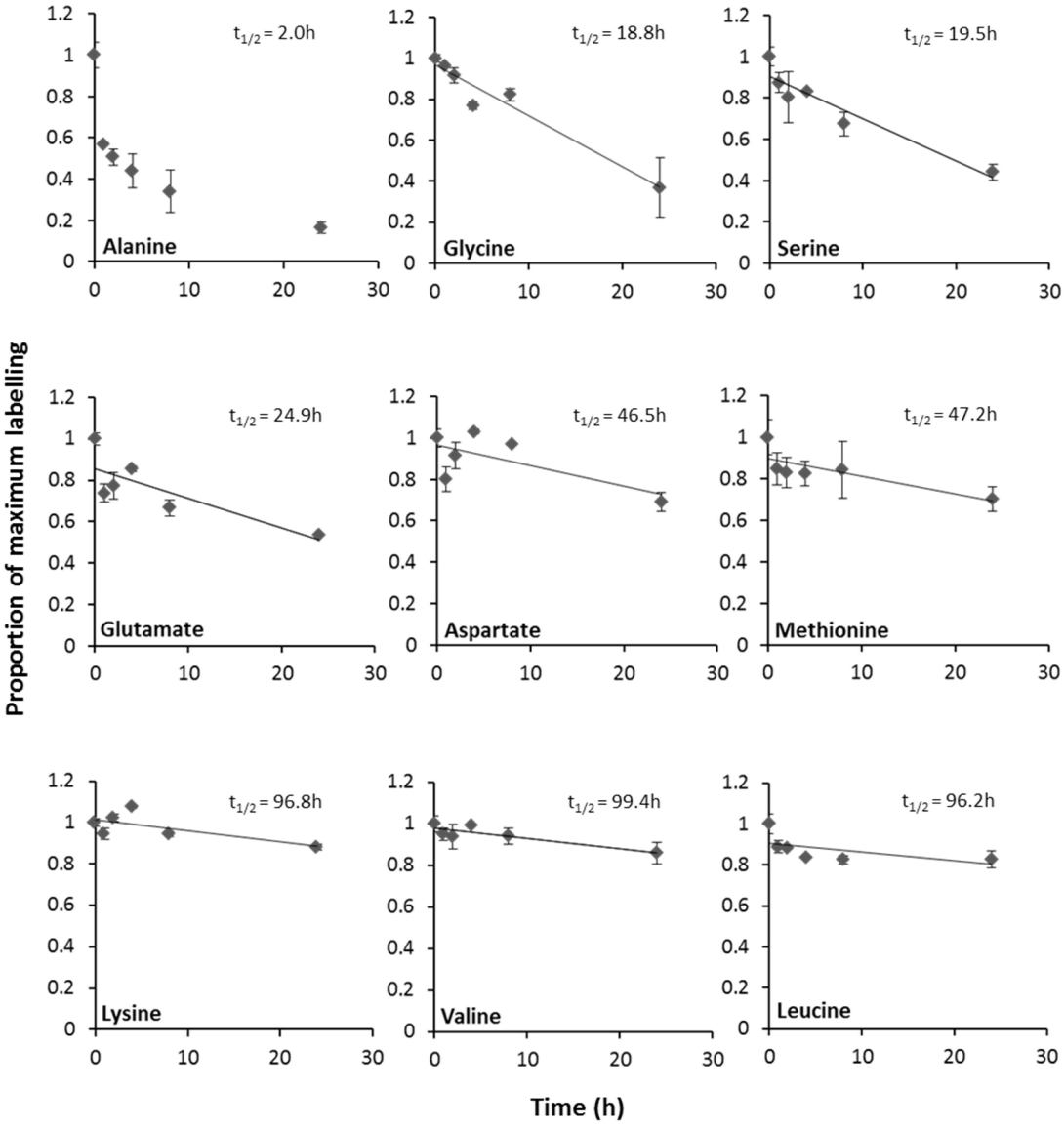


Figure 4.1. Loss of ^{2}H label from amino acids after switching from D_2O to H_2O media

Arabidopsis plants were grown on 0.22% [w/v] Murashige & Skoog media with 170 mM glucose and 2.56 MES, pH 5.7, containing 20% **D_2O**. After 14 days of growth, plants were transferred to **D_2O**-free media for 1, 2, 4, 8 and 24 hours and the ^{2}H label in free amino acids, as a proportion of maximum labelling, was determined by GC-MS. Data are mean (n=4) ± SEM.

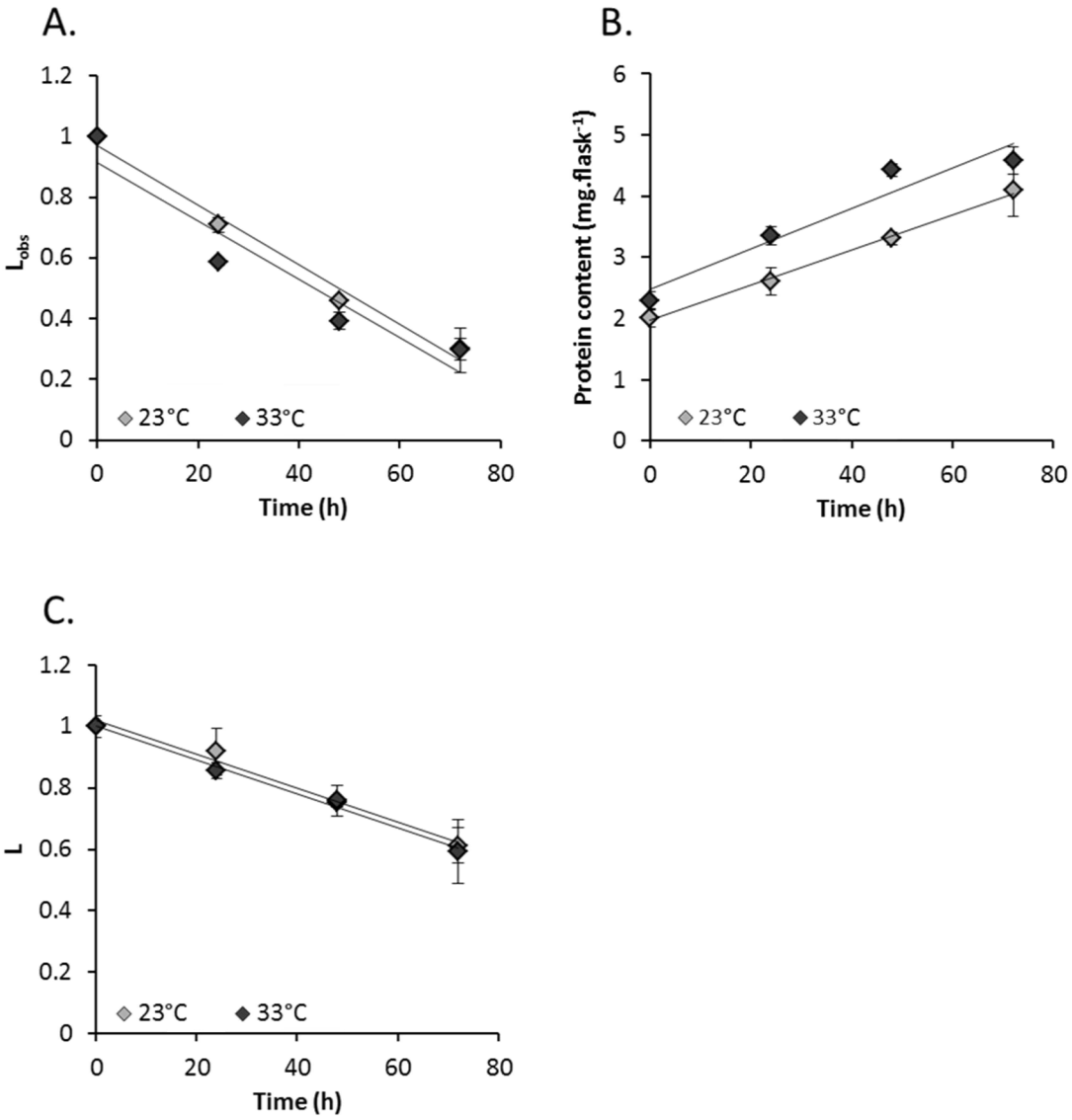


Figure 4.2. Rate of label loss and protein degradation at 23°C and 33°C.

Plants were grown at 23°C in media containing 20% **D_2O**. At day 14, they were transferred to **D_2O**-free media and either kept at 23°C, or transferred to 33°C. Root protein was extracted and labelling of alanine determined by GC-MS. A) Loss of label from alanine. B) Rate of protein accumulation in roots. C) Rate of label loss attributed to protein degradation. L_{obs} = the proportion of ^2H label in protein alanine from experimental data, L = corrected rate of label loss due to protein turnover. Data are the mean (n=6) ± SEM.

Estimation of the cost of maintaining ion gradients

Activities of membrane ATPases are increased after treatment at 33°C

To examine how high-temperature treatment affects the capacity for proton-pumping across the vacuolar and plasma membranes, V-ATPase, P-ATPase and PPase activities were measured in microsomal fractions extracted from arabidopsis roots treated for 18 hours at either 23°C or 33°C. Microsomal extracts from 33°C treated roots showed increased activity of V-ATPase, P-ATPase and PPase compared with 23°C treated roots (Figure 4.3). This suggests that there is an increase in membrane leak at high temperature leading to dissipation of ion gradients that must be counteracted by increased ATPase activity.

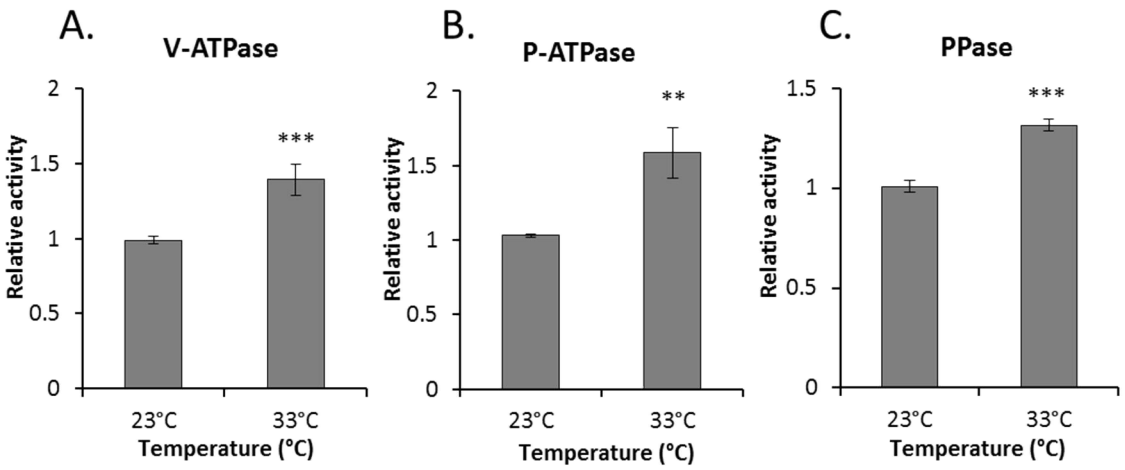


Figure 4.3. Relative activities of V-ATPase, P-ATPase and PPase from root microsomal fractions.
Microsomal fractions were isolated from roots excised from arabidopsis plants treated for 18 hours at either 23°C or 33°C. A) V-ATPase activity measured as decrease in total ATPase activity after inhibition with 100 nM Concanamycin A (1=12.50 µmol Pi.mg protein^{-1}h^{-1}), B) P-ATPase activity measured as the difference in ATPase activity before and after inhibition with 500 µM vanadate (1=20.27 µmol Pi.mg protein^{-1}h^{-1}), C) PPase activity measured as increase in PPase activity after addition of 50 mM KCl (1=21.37 µmol Pi.mg protein^{-1}h^{-1}). Data are the mean (n=9) ± SEM. **p=<0.01, ***p=<0.001.

The rate of ion leakage from roots is increased at 33°C compared with 23°C

To assess whether there is increased membrane leakage at high temperatures, ion conductance measurements of roots from 23°C grown plants were taken at 23°C and 33°C and the relative electrical conductivity (REC) was calculated as the conductivity relative to maximum conductivity after killing the tissue. In agreement with the increased ATPase activities shown previously, the rate of ion leakage was 1.6-fold higher when measured at 33°C compared with 23°C (Figure 4.4A and B). To determine whether the increase in REC was a result of increased membrane fluidity or because of permanent membrane damage, arabidopsis roots from 23°C grown plants were treated at either 23°C or 33°C for two hours, washed with distilled H_2O and ion leakage determined at 23°C for the following two hours. There was no difference in ion leakage between roots that had been treated at 23°C or 33°C (Figure 4.4C and D), indicating that the increase in ion leakage observed at 33°C was a consequence of transiently increased membrane fluidity rather than permanent membrane damage.

Construction of an ATP budget

The above data reveal the effect that high-temperature treatment has on individual cell maintenance process in arabidopsis. However, these data do not demonstrate the importance of each process with respect to overall ATP consumption. To investigate this, an ATP budget was constructed that included values for protein turnover and maintenance of ion gradients, as well as values for growth processes.

The general approach used here to construct the ATP budget was to measure oxygen consumption before and after inhibition of individual maintenance processes. ATP consumption for growth was determined by inputting biomass data into a genome-scale flux balance model for heterotrophic arabidopsis metabolism (Cheung et al., 2013).

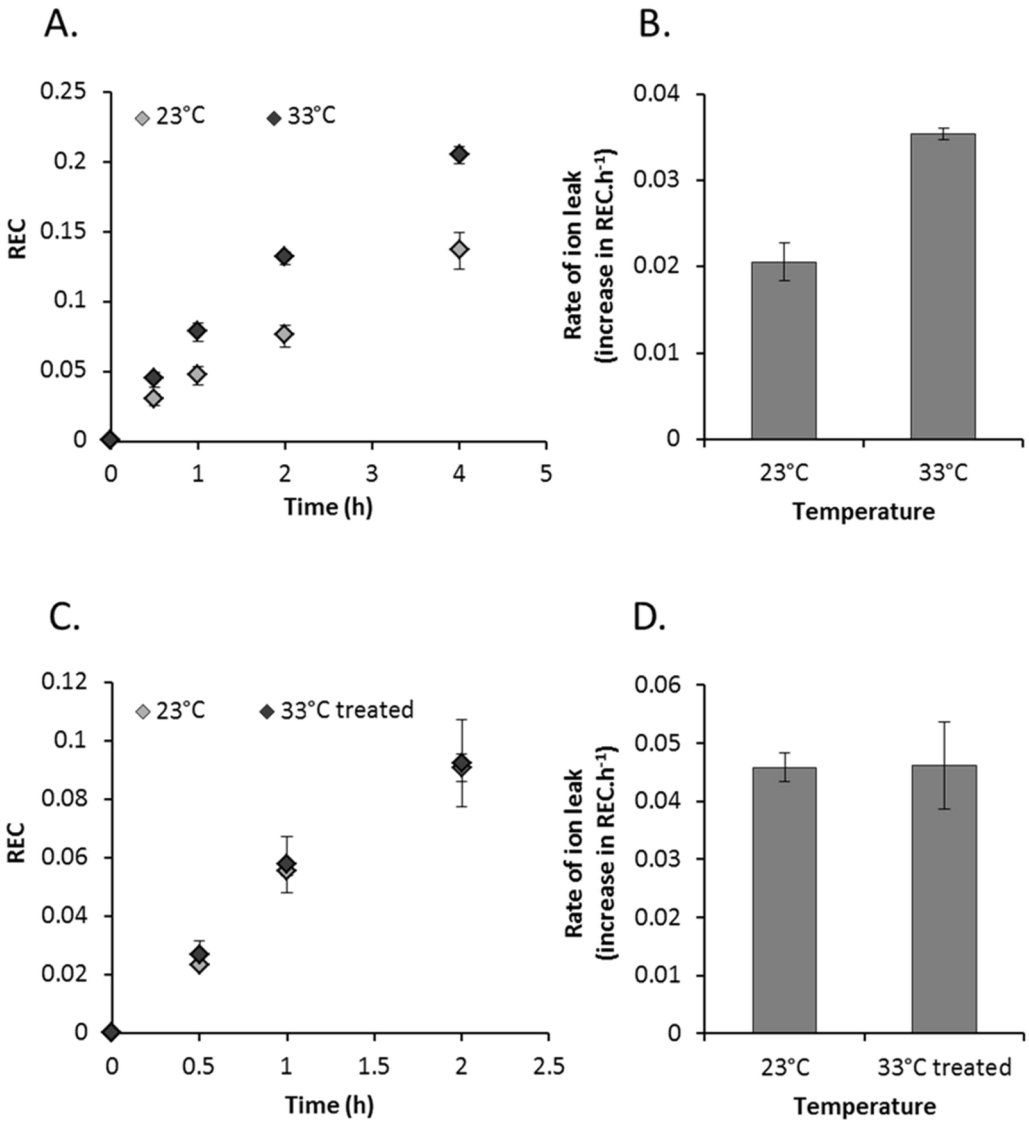


Figure 4.4. Rate of ion leakage from roots at 23°C and 33°C.

Roots were excised from arabidopsis plants grown at 23°C and REC determined in media containing 3% (w/v) glucose and 0.5% (w/v) MES, pH 5.7. Ion conductance measurements were taken time intervals from 0–4 hours. A. Relative electrical conductivity (REC) at 23°C and 33°C. B. Initial rate of ion leakage calculated from the slope in Figure 4.4A from 0–1 hours. C. Rate of ion leakage from roots at 23°C after prior treatment for two hours at 23°C and 33°C. D. Initial rate of ion leakage calculated from the slope of Figure 4.4C. Data are the mean (n=4) ± SEM. **p=<0.01.

ATP consumption for growth processes was higher at 33°C than at 23°C.

Carbon partitioning to biomass components at 23°C and 33°C was determined by performing ^{14}C feeding experiments (see Chapter 3 for details). There were no significant differences in carbon partitioning at 23°C and 33°C (Figure 4.5), and therefore changes in ATP cost for growth reflect differences in growth rate between the two temperatures rather than differences in the specific cost for growth assuming that the cost of synthesis is the same at the two temperatures. Biomass data were used as constraints in a heterotrophic arabidopsis genome scale model, using minimisation of total flux as the objective function (Cheung et al., 2013). The model generated values of ATP consumption for biomass synthesis of 168.68 nmol ATP.gFW-^{1}min-^{1} at 23°C and 276.63 nmol ATP.gFW-^{1}min-^{1} at 33°C. These values include the ATP costs of synthesising biomass components, as well as transport costs involved in their synthesis.

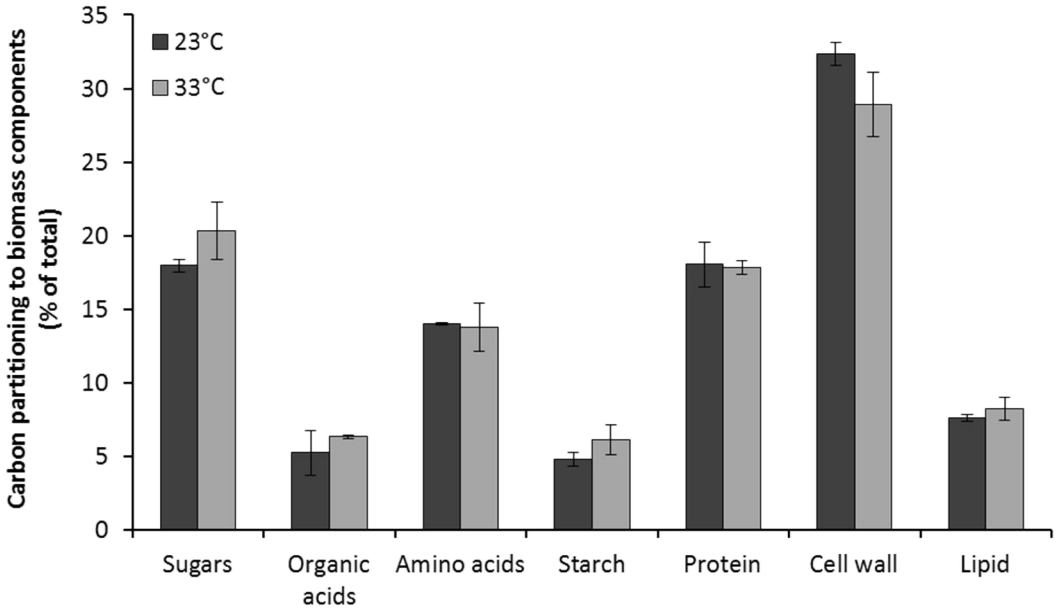


Figure 4.5. Carbon partitioning to biomass components at 23°C and 39°C.

Excised arabidopsis roots were supplied with [U-^{14}C] glucose (74 kBq in 5 ml of media containing 170 mM glucose, 2.56 mM MES pH 5.7 and 0.221% [w/v] Murashige & Skoog) for 18 hours. Label incorporation into biomass components was determined and expressed as a percentage of total ^{14}C entering biomass. Data are the mean (n=4) ± SEM.

Oxygen consumption by roots is greater at 33°C than at 23°C

Oxygen consumption of excised 23°C grown arabidopsis roots was 205.00 nmol O_2.$gFW^{-1}min^{-1}$ at 23°C, compared with 409.59 nmol O_2.$gFW^{-1}min^{-1}$ at 33°C. These values were used to calculate a value for total ATP production, assuming a P/O value of 2.12, which was the P/O ratio of mitochondria generated by the metabolic model. Values for ATP production were 869.20 nmol ATP.gFW-^{1}min-^{1} at 23°C and 1736.66 nmol ATP.$gFW^{-1}min^{-1}$ at 33°C.

Treatment with CHI results in a reduction in root oxygen consumption at 23°C and 33°C

CHI is an inhibitor of cytosolic protein synthesis and was used here to estimate the ATP cost for protein turnover. In order to ensure maximum inhibition of protein synthesis by CHI, roots were treated for 0.5, 1 and 2 hours with 0.5mM CHI, a concentration used to inhibit protein synthesis *in vivo* in wheat roots and *Petunia x hybrida* petals (Hachiya et al., 2007; Zagdanska, 1995), and O_2 consumption was measured. After inhibition of protein synthesis, O_2 consumption decreased by 46.6% at 0.5 hours, and inhibition did not increase with further incubation time (Figure 4.6A).

To determine the ATP cost for protein turnover at 23°C and 33°C, excised roots were treated with CHI for 0.5 hours. Reduction in O_2 uptake after incubation with CHI was 82.02 nmol O_2.$gFW^{-1}min^{-1}$ at 23°C and 116.94 nmol O_2.$gFW^{-1}min^{-1}$ at 33°C (Figure 4.6B). These data were converted into values of ATP consumption for protein synthesis by multiplication with the P/O ratio to give values of ATP consumption of 347.76 nmol ATP. $gFW^{-1}min^{-1}$ at 23°C and 495.82 nmol ATP. $gFW^{-1}min^{-1}$ at 33°C.

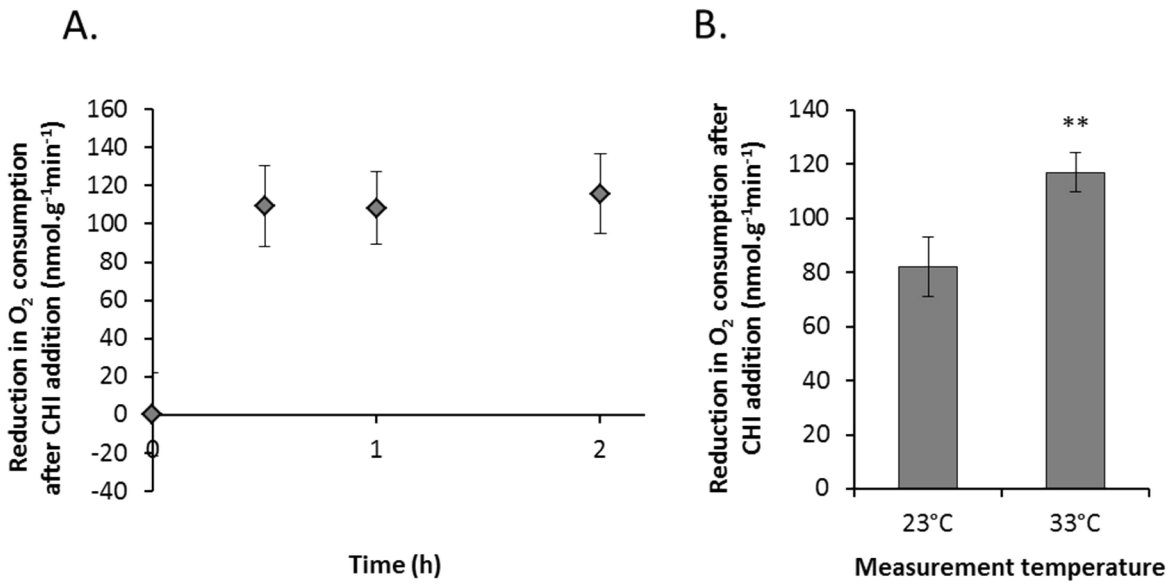


Figure 4.6. Effect of CHI on oxygen consumption rate.

Oxygen consumption of excised roots from 23°C-grown plants was measured in the absence and presence of 0.5 mM CHI at 23°C. A. Time course of CHI effect on oxygen consumption rate. Data are mean (n=8) ± SEM. B. Reduction in O_2 consumption rate after treatment with 0.5 mM CHI for 0.5 hours at 23°C and 33°C. Data are mean (n=20) ± SEM. **p=<0.01.

To convert ATP costs for total protein synthesis into values of protein turnover, ATP cost for the net accumulation of protein (i.e. growth) was subtracted, and the ATP cost for processes that are associated with protein turnover, but not inhibited by CHI, were added (Bouma et al., 1994; Hachiya et al., 2007). To calculate this, theoretical values of ATP consumption for processes involved with protein turnover were used (Visser & Bouma, 1992; Table 4.1).

Energy for net protein synthesis, E_{PS} was calculated as:

$$E_{PS} = \Delta P \; x \; E_{specPS} \; x \frac{1}{1 - F_{org}}$$

where E_{specPS} is the specific cost of protein synthesis (Table 4.1), ΔP is the rate of increase in amino acid residues in protein and F_{org} is the proportion of total protein synthesis that occurs in organelles. ΔP was calculated from ^{14}C feeding data as the sum of all amino acids in the protein

fraction to be 5.78 nmol.min^{-1}g^{-1} at 23°C and 9.42 nmol.min^{-1}g^{-1} at 33°C. F_{org} was assumed to be 0%, as approximately 95% of mitochondrial and plastid proteins are synthesised in the cytosol (Hachiya et al., 2007; Nelson et al., 2014). ATP consumption for protein turnover, E_{PT}, was then calculated (Table 4.2):

$$E_{PT} = (E_{CHI} - E_{PS})\, x \frac{E_{specPT}}{E_{specCHI}}\, x \frac{1}{1 - F_{org}}$$

where E_{CHI} is ATP production inhibited by CHI, E_{specPT} is the theoretical specific cost for protein turnover and $E_{specCHI}$ is the theoretical specific cost for CHI inhibited processes. ATP consumption for protein turnover was found to be 327.78 nmol ATP.min^{-1}gFW^{-1} at 23°C and 445.53 nmol ATP.min^{-1}gFW^{-1} at 33°C.

Table 4.1. Theoretical specific energy costs for processes involved with protein turnover.

	Specific energy costs (mol ATP. mol^{-1} peptide bond)		**CHI inhibited?**
	Min	**Max**	
Protein biodegradation	1.0	2.0	No
Amino acid activation	2.0	2.0	Yes
Error correction by aminoacyl tRNA synthetases	5.0	8.0	Yes
Peptide bond formation and translocation	2.0	2.0	Yes
Tool maintenance	1.0	1.0	Yes
Signal sequences	0.6	1.9	Yes
Amino acid turnover	0.0	3.5	No
Post translational processing	0.2	0.4	Yes
E_{specPT}	**11.8**	**20.8**	
E_{specPS}	**10.8**	**18.8**	
$E_{specCHI}$	**10.8**	**15.3**	

Data taken from de Visser (1992). E_{specPT} = Specific cost of protein turnover, E_{specPS} = Specific cost of protein synthesis, $E_{specCHI}$ = Specific cost of CHI inhibited processes.

ATP consumption for V-ATPase and P-ATPase activities

ATP consumption due to V-ATPase activity was measured using Concanamycin A (ConcA), a specific inhibitor of the V-ATPase (Drose and Altendorf, 1997). Whether ConcA is able to penetrate the cell wall and fully inhibit V-ATPase *in vivo* has not been tested previously, and so initial experiments were designed to test whether ConcA is able to fully inhibit V-ATPase *in vivo*, and to determine the incubation time necessary to achieve this. Arabidopsis roots were treated with 100nM ConcA (Robinson et al., 2004) for 0–120 minutes followed by washing under running water for 15 minutes to remove exogenous ConcA from the roots. The microsomal fraction was extracted and V-ATPase activity measured (Figure 4.7A). After a 30 minute incubation with ConcA, V-ATPase activity was inhibited by 89.1% and was fully inhibited after two hours. An incubation time of 30 minutes was selected to minimise any non-specific effects of the inhibitor.

To determine the ATP consumption for V-ATPase activity, reduction in oxygen consumption after incubation with 100 nM ConcA was measured (Figure 4.7B), and converted to a value of ATP consumption by multiplying by the P/O ratio value. This gave an ATP consumption rate of 201.39 nmol ATP.$g^{-1}min^{-1}$ at 23°C and 602.10 nmol ATP.$g^{-1}min^{-1}$ at 33°C. Using [U-^{14}C]-glucose feeding data on carbon partitioning to biomass components, the genome scale model of heterotrophic arabidopsis metabolism was used to calculate the cost for transport across the tonoplast associated with growth. The genome scale model calculated the cost for all sucrose, glucose, fructose, citrate, malate, succinate and isocitrate molecules synthesised to be transported across the tonoplast once. Additional transport of these metabolites was considered to be maintenance as this most likely results from the leakage of ions and solutes back across the membrane. The ATP consumption rate for V-ATPase activity associated with biomass production was calculated to be 6.16 nmol ATP.$gFW^{-1}min^{-1}$ at 23°C and 10.10 nmol ATP.$gFW^{-1}min^{-1}$ at 33°C. After subtraction of the growth related V-ATPase ATP cost from total ATP cost, values of ATP consumption for V-ATPase activity associated with maintenance of 195.23 nmol ATP.$g^{-1}min^{-1}$ at 23°C and 592.00 nmol ATP.$g^{-1}min^{-1}$ at 33°C were obtained.

Table 4.2 Values for the calculation of protein turnover

	23°C	**33°C**
ΔP (nmol.min^{-1}g^{-1})	5.78	9.42
E_{specPS} (ATP.mol^{-1}peptide bond)	14.80	14.80
F_{org} (%)	0	0
R_{CHI} (nmol O_2.gFW^{-1}min^{-1})	82.02	116.94
E_{CHI} (nmol ATP. gFW^{-1}min^{-1})	347.76	495.82
E_{PS} (nmol ATP. gFW^{-1}min^{-1})	85.54	139.41
E_{specPT} (mol ATP.mol^{-1}peptide bond^{-1})	16.30	16.30
$E_{specCHI}$ (mol ATP.mol^{-1}peptide bond^{-1})	13.05	13.05
E_{PT} (nmol ATP.min^{-1}gFW^{-1})	**327.78**	**445.53**

Where maximum and minimum values are available (see Table 4.1), average values are presented.

Using a similar approach, the ATP cost for P-ATPase activity was determined using the P-ATPase inhibitor, vanadate. The binding affinity for P-ATPase is much lower than that of ConcA and V-ATPase; Jacobs & Taiz (1980) demonstrated that vanadate inhibition of P-ATPase was fully reversible within five minutes of vanadate removal. Therefore, it was not possible to determine whether P-ATPase in microsomes extracted from vanadate treated roots was inhibited, as the vanadate would simply wash off during the extraction process. However, vanadate has been used to inhibit P-ATPase *in vivo* in previous studies; phosphate transport in aged potato tuber discs was inhibited by 0.5 mM vanadate (Poder and Penot, 1992) and 1 mM vanadate was used to inhibit auxin-enhanced H^+ secretion in pea and oat epicotyls, with inhibition occurring after five minutes

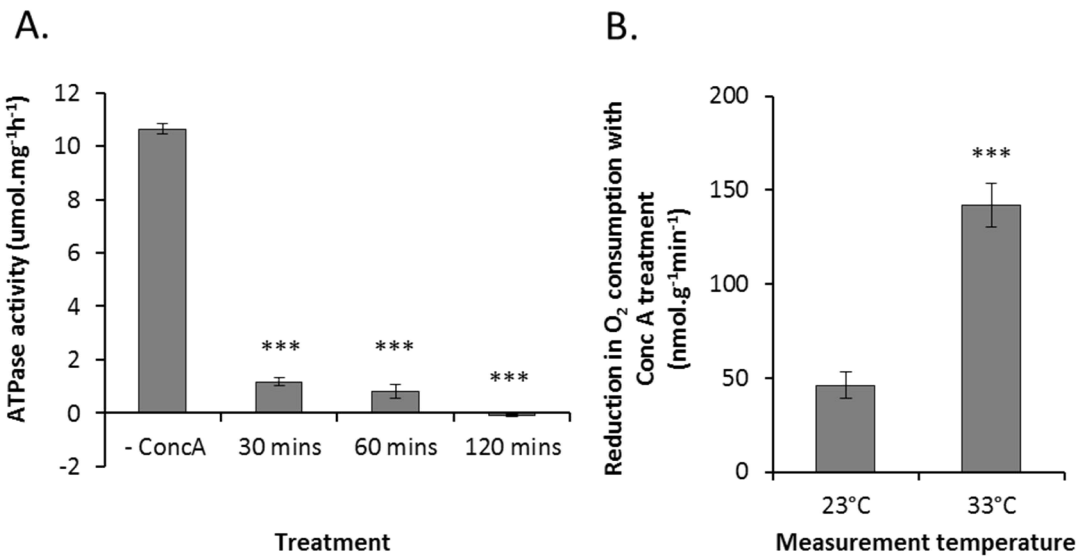


Figure 4.7. Inhibition of V-ATPase by ConcA.

A. V-ATPase of microsomal fractions extracted from 23°C-grown roots pretreated with 100 nM ConcA. Data are the mean (n=4) ± SEM. B. Reduction in oxygen consumption rate after treatment with 100 nM ConcA for 30 minutes. Data are the mean (n=16) ± SEM. ***p=<0.001 from control.

and maximum inhibition after 10–15 minutes (Jacobs and Taiz, 1980). Using 1 mM vanadate, a time course of the effect of vanadate on respiration was performed. Consistent with previous work, vanadate rapidly reduced O_2 consumption rate and maximum inhibition was reached after five minutes (Figure 4.8A).

Inhibition of O_2 consumption after incubation with vanadate was measured (Figure 4.8B) and converted to ATP consumption values for P-ATPase activity of 198.00 nmol ATP.$gFW^{-1}min^{-1}$ at 23°C and 358.27 nmol ATP.$gFW^{-1}min^{-1}$ at 33°C. The arabidopsis genome scale model was used to calculate ATP consumption for P-ATPase activity associated with growth processes; the model calculated the cost of transporting across the plasma membrane the glucose, nitrate, phosphate and sulphate necessary to synthesise the biomass produced. Additional ATP cost for transport across the plasma membrane is necessary to replace molecules and ions that have leaked back across the membrane and is considered a maintenance cost. The ATP cost for growth-associated

P-ATPase activity was 57.28 nmol ATP.gFW^{-1}min^{-1} at 23°C and 93.39 nmol ATP.gFW^{-1}min^{-1} at 33°C. This was subtracted from total ATP consumption, to give values of P-ATPase activity for maintenance of 140.72 nmol ATP.gFW^{-1}min^{-1} at 23°C and 264.91 nmol ATP.gFW^{-1}min^{-1} at 33°C (Table 4.3).

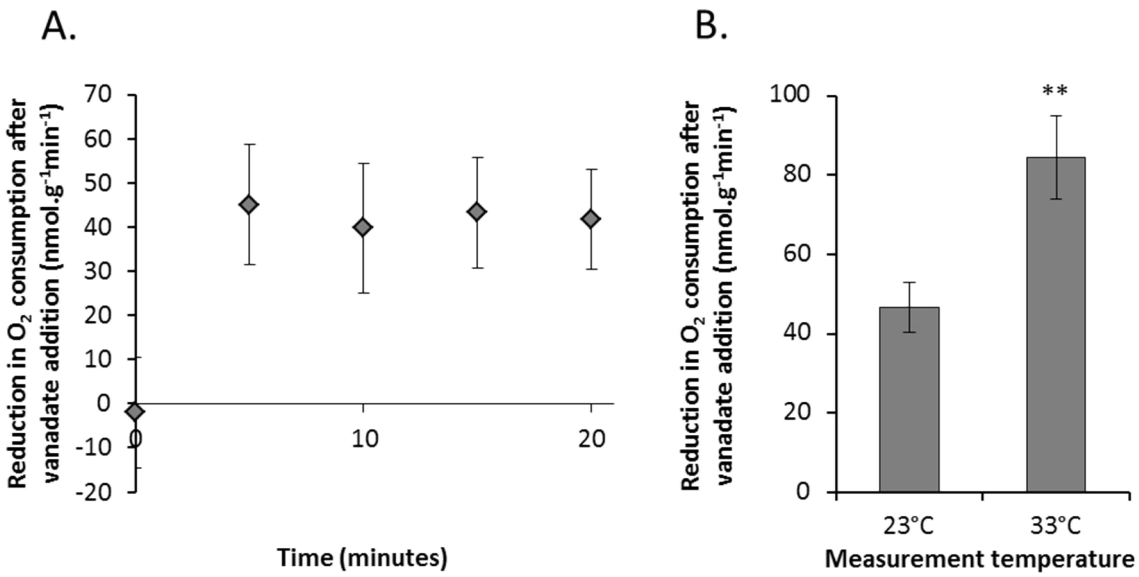


Figure 4.8. Effect of P-ATPase inhibition by vanadate on oxygen consumption.

Oxygen consumption of excised roots from 23°C-grown plants was measured in the absence and presence of 1 mM vanadate. A. Time course of vanadate effect on oxygen consumption rate. Data are mean (n=8) ± SEM. B. Reduction in oxygen consumption rate after treatment with 1 mM vanadate for 10 minutes at 23°C and 33°C. Data are the mean (n=18) ± SEM. **p=<0.01.

ATP budget summary

There was a small but insignificant decrease in the proportion of ATP consumption for growth at 33°C compared with 23°C. (p=0.07). The percentage of total ATP consumption for protein turnover decreased from 37.7% at 23°C to 25.7% at 33°C (p=0.015). Overall, the proportion of

Table 4.3. Calculation of ATP cost for V-ATPase and P-ATPase activities.

	23°C		33°C	
Parameter	**V-ATPase**	**P-ATPase**	**V-ATPase**	**P-ATPase**
$\mathbf{R_{inhibitor}}$ (nmol O_2. $gFW^{-1}min^{-1}$)	46.04	46.70	142.00	84.50
$\mathbf{E_{inhibitor}}$ (nmol ATP. $gFW^{-1}min^{-1}$)	201.39	198.00	602.10	358.27
$\mathbf{E_{TG}}$ (nmol ATP. $gFW^{-1}min^{-1}$)	6.16	57.28	10.10	93.36
$\mathbf{E_{TM}}$ (nmol ATP. $gFW^{-1}min^{-1}$)	**195.23**	**140.72**	**592.00**	**264.91**

$R_{inhibitor}$ =the decrease in O_2 consumption with inhibitor treatment; $E_{inhibitor}$ = the decrease in ATP production with inhibitor treatment, E_{TG} = ATP consumption for growth related transport processes, E_{TM} = ATP consumption for maintenance transport processes.

total ATP consumption attributed to the maintenance of ion gradients increased from 38.0% to 49.8%, however this increase was driven by a large proportional increase in the ATP demand for V-ATPase activity from 21.8% at 23°C to 34.0% at 33°C (p=0.018), while the proportion of total ATP demand attributed to P-ATPase remained approximately the same (Table 4.4; Figure 4.9)

Table 4.4. ATP budget.

	23°C		33°C	
	ATP consumption (nmol.gFW-^{1}min-^{1})	**% of total ATP**	**ATP consumption (nmol.gFW-^{1}min-^{1})**	**% of total ATP**
Total	869.2 ± 53.2	-	1736.7 ± 124.4***	-
Growth	168.7	19.4 ± 1.20	276.6	15.9 ± 1.14^{ns}
V-ATPase	195.2 ± 19.7	22.46 ± 3.01	592.0 ± 66.0***	34.0 ± 2.82*
P-ATPase	140.7 ± 26.8	16.19 ± 3.04	264.9 ± 44.6*	15.81 ± 2.43^{ns}
Protein turnover	327.8 ± 57.3	37.71 ± 6.52	445.5 ± 41.4^{ns}	25.65 ± 2.10*

Values presented are mean ± SEM. Total, n=6; V-ATPase, n=16; P-ATPase, n=18; protein turnover, n=20. Significance from 23°C: *p=<0.05, **p=<0.01, ***p=<0.001, ns non-significant.

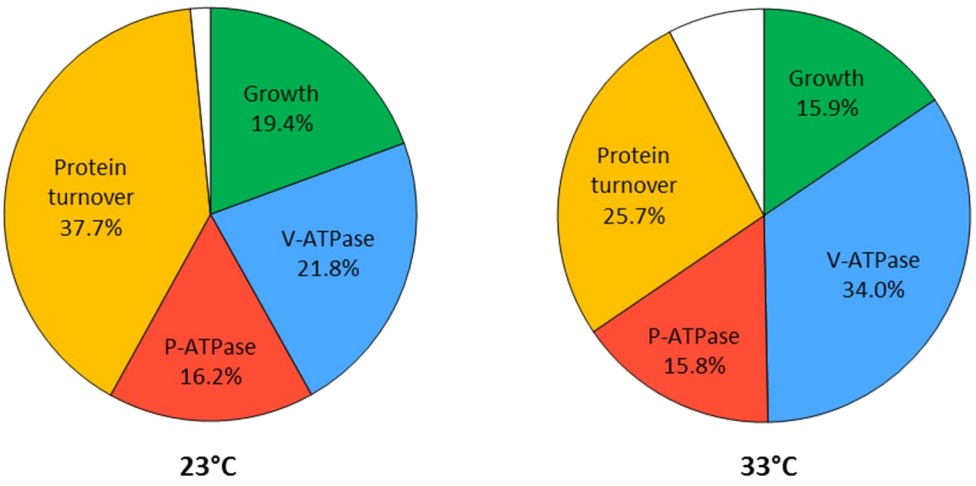


Figure 4.9. Summary of ATP budget.

ATP consumption for ATP-consuming processes at 23°C and 33°C presented as a percentage of total ATP consumption. From data presented in Table 4.4. The white section represents ATP consumption that was not accounted for by the budget.

The effect of P/O ratio on the ATP budget

To convert values of oxygen consumption into ATP consumption throughout calculation of the ATP budget, a P/O ratio of 2.12 was assumed. To test the impact that this assumption has on the conclusions drawn from the ATP budget, the budget was recalculated assuming P/O ratios of 1.5, 2.0 and 2.5. Figure 4.10 demonstrates that changing the P/O ratio within this range does not change the conclusions drawn from the ATP budget; in all cases, there is a large increase in ATP consumption for V-ATPase activity, and a decrease in ATP consumption for protein turnover at 33°C relative to 23°C as a proportion of overall ATP consumption.

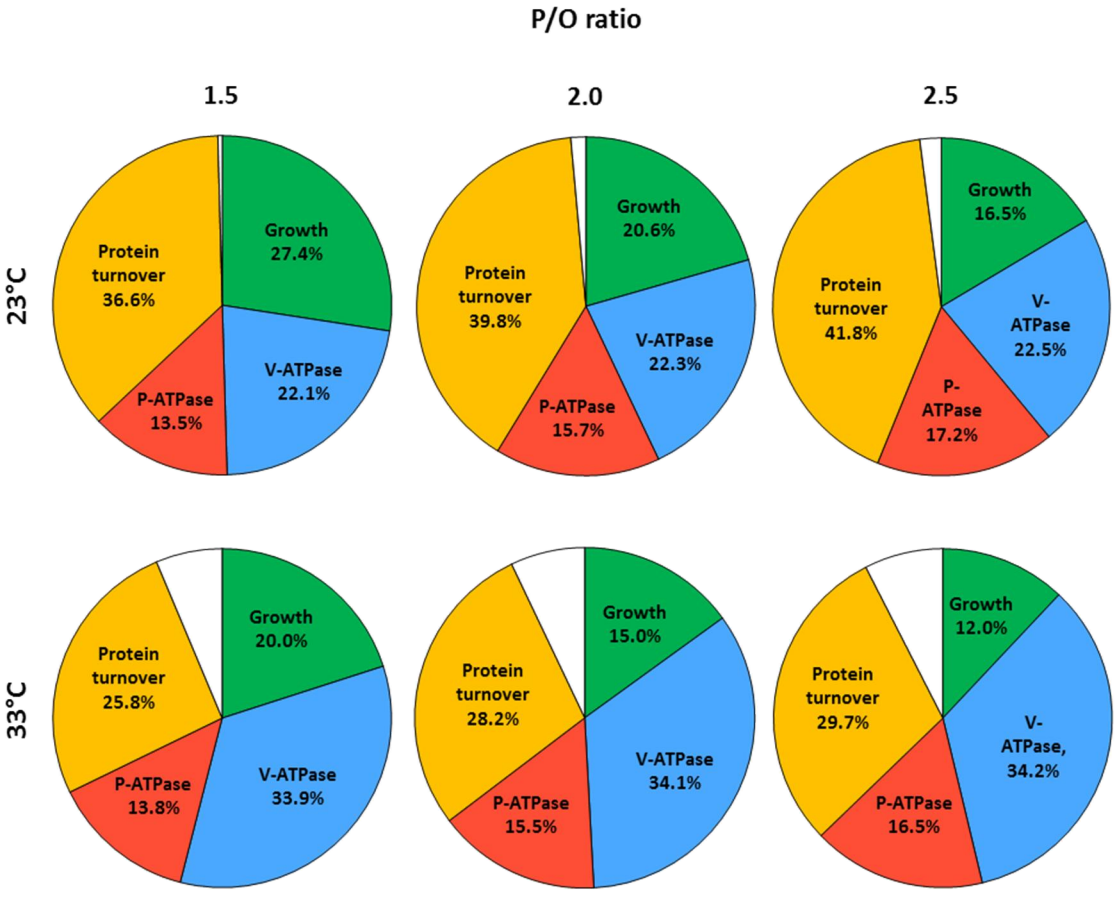


Figure 4.10. Effect of P/O ratio on the ATP budget.

Using the same experimental data as for the ATP budget shown in Figure 4.9, the ATP budget was recalculated assuming a range of P/O ratios from 1.5–2.5. White sections represent ATP consumption that is unaccounted for by the ATP budget.

Discussion

There was no difference in the rate of protein turnover at 23°C and 33°C

Plant proteins exhibit a wide range of turnover rates (Li et al., 2012). To study global protein turnover, it is necessary to ensure that label is incorporated into all proteins, including those that turn over very slowly. To achieve this, plants were germinated and grown in media containing D_2O, as opposed to short-term labelling over a few days or hours, which favours the labelling of proteins with fast turnover rates (Humphrey and Davies, 1976; Yang et al., 2010). The use of D_2O to study protein turnover relies on aminotransferase activity to exchange ^2H with ^1H on the α, and sometimes β, carbon of soluble amino acids during the chase period, to prevent reincorporation of labelled amino acids into protein (Humphrey and Davies, 1975). However, over a long incubation time with D_2O, new amino acids are synthesised *de novo* (Humphrey and Davies, 1976). Therefore, it was necessary to ensure that label was being removed from soluble amino acids during the chase period. ^2H was lost from soluble alanine much faster than from the other amino acids studied; the half-life of ^2H in soluble alanine was 2.0 hours, compared with half-lives of over 18 hours for other amino acids. This reflects the fact that, through amino acid synthesis and aminotransferase activity, four deuterium atoms can be incorporated into alanine on the α and β carbons, all of which can be exchanged by aminotransferase activity (Oshima and Tamiya, 1961). Thus, all of the ^2H labelling in alanine can be quickly removed by aminotransferases during the pulse period. Slower removal of ^2H from the other amino acids is most likely occurring because, while ^2H on the α carbon on many amino acids can be exchanged by aminotransferases, ^2H in other positions cannot be exchanged and the removal of this label reflects the rate of amino acid degradation (Humphrey & Davies, 1976). Therefore, to ensure that recycling of labelled amino acids did not affect measurements of protein turnover, the labelling of alanine was traced.

Values for protein degradation obtained here were 0.13 day^{-1} (half-life of 3.79 days) for both 23°C and 33°C. This is within the range of values previously attained; Li et al. (2012) determined that

the degradation rate of 84 different proteins from an arabidopsis cell culture ranged between 0.05-0.8 day^{-1}. The degradation rate obtained here is at the lower end of this range, this may reflect the presence of structural proteins with slow turnover rates in arabidopsis roots that were not considered in the study by Li et al. (2012). Consistent with this, studies of global protein turnover have revealed lower degradation rates: in two grass species, the protein half-life was calculated to be 4–6 days (Scheurwater et al., 2000) and in 7 days in *Lemna minor* (Cooke et al., 1975). However, it is surprising that the measured rates of protein degradation were the same at 23°C and 33°C as an increase in protein turnover might have been expected to occur at high temperatures to change the protein complement of the cells to deal with a change in environmental conditions. Previously, increased protein turnover rate has been demonstrated upon exposure to high-temperature treatment; in wheat roots, the protein half-life was calculated to be 51 hours at 22°C, decreasing to 41 hours at 32°C (Ferguson et al., 1990). Although this study used ^3H_2O labelling – a similar approach to the D_2O labelling strategy used here - this discrepancy might reflect differences in the labelling protocol and subsequent analysis. Ferguson et al. (1990) fed ^3H_2O for 48 hours and this shorter feeding time may result in turnover times reflecting those of proteins with a faster turnover time. Additionally, the effect of label dilution from *de novo* amino acid synthesis was not taken into consideration; a faster growth rate at the higher temperature would lead to a greater dilution effect, thus giving a faster apparent rate of protein turnover at the higher temperature.

Results from the pulse-chase experiment presented in this chapter were consistent with results from the ATP budget for protein turnover: the ATP consumption for protein turnover was slightly, but not statistically, higher at 33°C than at 23°C. The value obtained for ATP consumption for protein turnover of 327.8 nmol $ATP.gFW^{-1}min^{-1}$ at 23°C was of the same magnitude to that of equivalent studies on other plants, where the ATP consumption for protein turnover was found to be 166.7–194.4 nmol $ATP.gFW^{-1}min^{-1}$ (2.4–2.8 mmol $ATP.gDW^{-1}day^{-1}$) in roots of *Dactylis glomerata* and *Festuca ovina* (Scheurwater et al., 2000) and 150 nmol $ATP.gFW^{-1}min^{-1}$ (25 nmol

ATP.gDW^{-1}s^{-1}) in wheat roots (Zagdanska, 1995). The ATP budget data demonstrated that, as expected, protein turnover consumes a major proportion of the total ATP produced. At 23°C, protein turnover consumed 37.7% of total ATP, this is comparable with results in wheat roots (22.2%, Zagdanska, 1995), potato leaves (17–37%, Bouma et al., 1994) and roots of two grass species (22–90%, Scheurwater et al., 2000). However, protein turnover consumed less ATP as a percentage of total ATP consumption at 33°C compared with 23°C. From this it can be concluded that, although protein turnover is major source of ATP consumption in arabidopsis roots, it does not contribute significantly to the increase in ATP consumption and non-growth respiration at high temperature.

Increased ion leakage leads to greater ATP consumption for ATPase activity in arabidopsis roots at high temperature.

There was an increase in the maximum extractable activities of V-ATPase, P-ATPase and PPase in microsomes isolated from roots treated at 33°C compared with 23°C. Changes in membrane ATPase activity have been demonstrated previously in response to changes in temperature; in grape plants, both hot and cold treatments lead to increased plasma membrane ATPase activity as well as increased membrane leakage (Zhang et al., 2006). This suggests that the increase in ATPase activity is necessary to counteract the increased ion leakage. Consistent with this, ion conductance measurements made on arabidopsis roots demonstrated an increase in ion leakage at 33°C compared with 23°C. The ATP cost for ion gradient homeostasis is the sum of the energy to maintain all cellular membranes, however, measurement of ion conductance of the media surrounding the roots reflects membrane leak from just the plasma membrane. Despite this, it is likely that these results can be extrapolated to other biological cellular membranes as the fluidisation of membranes at high temperatures is a general property of biological membranes, and temperature effects on membrane fluidity have been shown in fish, bacteria, yeast and plants (Los and Murata, 2004; Cossins, 1977; Sinensky, 1974; Carratù et al., 1996; Martinière et al., 2011).

Consistent with the data discussed above, ATP consumption for ATPase activity assessed by inhibition with ConcA and vanadate showed that there was an increase in ATP consumption for both V-ATPase and P-ATPase, with V-ATPase displaying a much larger increase in activity at 33°C than P-ATPase. Data from the ATP budget demonstrate that ion gradient homeostasis is an appreciable proportion of total ATP consumption; at 23°C, P-ATPase activity consumed 16.2% and V-ATPase activity consumed 21.8% of total ATP. This is consistent with the limited published data on ATP consumption by ATPase activities in plants. Zagdanska (1995) measured ATP consumption by P-ATPase to be 13% of total ATP production. At 33°C, P-ATPase consumed 15.8% and V-ATPase consumed 34.0% of total ATP. Although there was an increase in P-ATPase activity at 33°C, the proportion of ATP for P-ATPase remained constant at both temperatures whereas the proportion of total ATP consumed by V-ATP increased at the higher temperature. The large increase in ATP consumption for V-ATPase activity relative to P-ATPase is not supported by data from the ATPase activity assays on extracted microsomes (Figure 4.3.), which suggested that the increase in the activities of V-ATPase and PPases, which are also located in the vacuole, were similar to the increase in the activity of P-ATPase. However, as discussed in the introduction, ATPase activity data from extracted microsomes only gives an indication of the maximum catalytic capacity related to protein content, and this cannot always be extrapolated to *in vivo* activity. The large increase in ATP consumption for V-ATPase activity relative to P-ATPase activity may be explained by the relative size of the ion gradients across the tonoplast and plasma membranes; a primary role of the vacuole is the storage of metabolites and inorganic ions, resulting in a high concentration gradient across the tonoplast membrane (Wink, 1993). As an example, the concentration of nitrate in the cytosol was shown to be 5 mM whereas the concentration in the vacuole was 39 mM (Miller and Smith, 1996), the value of obtained for the apoplast was 4 mM (Solomon and Oliver, 2001). The steep electrochemical gradient across the tonoplast compared with the smaller concentration gradient across the plasma membrane means that as membranes become more fluid and leakier at high temperature, there will be a greater leakage of ions from

the vacuole, down the electrochemical gradient, and the V-ATPase will have to operate faster to maintain ion gradients than the P-ATPase at the plasma membrane. However, it also remains a possibility that this result is a consequence of incomplete inhibition of P-ATPase as P-ATPase inhibition could not be tested as rigorously as V-ATPase inhibition by ConcA. Nevertheless, despite these uncertainties, the overall proportional increase in ATP consumption to maintain ion gradients, from 38.0% to 49.8%, highlights that ion gradient homeostasis is an important contributor to increased ATP consumption and non-growth respiration at high temperature in arabidopsis roots.

Protein turnover, ion gradient homeostasis and growth are sufficient to explain the majority of ATP consumption at 23°C and 33°C

As previously discussed, the ATP budget showed that as a proportion of the total, the ATP consumption for protein turnover decreased, while the ATP consumption for the maintenance of ion gradients increased. Consistent with findings in Chapter 3 that demonstrated a decrease in the proportion of total CO_2 release from growth processes as temperature increased, there was a small, although insignificant, decrease in the proportion of total ATP consumption that could be attributed to growth at 33°C compared with at 23°C. Here, ATP consumption for growth was shown to account for 19.4% of total ATP consumption at 23°C. In arabidopsis suspension cultures, it was calculated that the energy requirements for growth were much higher, with 84% of glucose consumption attributed to growth processes (Cheung et al., 2013). This discrepancy can be explained by differences in growth between the two systems; in cell cultures, all cells are rapidly dividing, requiring a large amount of energy for growth. In contrast, a small proportion of cells are undergoing cell division in roots, and the majority of ATP is therefore required to maintain existing cells.

ATP cost for protein turnover, ion gradient homeostasis and growth accounted for 95.1% of total ATP consumption at 23°C and 91.4% of ATP consumption at 33°C, leaving a small amount of ATP

consumption unaccounted for. There are three factors that could lead to errors in the ATP budget leading to this gap: the assumed P/O ratio used to convert values of oxygen consumption into ATP production, the presence of ATP-consuming processes not considered in the calculation and experimental errors in constructing the budget. The ATP budget was calculated assuming a P/O ratio of 2.12, this is the P/O ratio of the mtETC generated by the genome scale model used to calculate the growth costs for the ATP budget, and is within the expected range of P/O ratios (Hinkle, 2005). Recalculation of the ATP budget at 23°C and 33°C, assuming a range of different ATP ratios demonstrated that the P/O ratio does not dramatically change the ATP budget, thus incorrect assumption of the P/O ratio within the range of commonly assumed P/O ratios will not affect the main conclusions. Incorrect assumption of the P/O ratio may explain the gap in the ATP budget at 23°C, where assuming a P/O ratio of 1.4 accounts for 100% of ATP consumption, however a P/O ratio of 1.4 is low, especially under non-stressful conditions. At 33°C, 100% of ATP production is accounted for only when the P/O ratio is 0.45. This is extremely low and therefore it is highly unlikely that solely incorrect assumption of the P/O ratio is able to explain the gap in the ATP budget.

There are a number of additional ATP-consuming processes that were not considered during the construction of the ATP budget. Turnover of cellular components other than protein was not considered, however these costs are thought to be low (Penning de Vries, 1975). The rate of DNA turnover has been shown to be very slow in leaves (Dyer & Osborne, 1971), although published estimations of the ATP cost are not available. Equally, it was estimated that the ATP cost of lipid turnover was just 3–6% of the ATP cost of protein turnover (Kawaga et al., 1973; Penning de Vries, 1975). A further ATP-consuming process, not associated with cell maintenance, is substrate cycling. Attempts have been made to quantify the ATP expense of sucrose cycling, and a wide range of values have been obtained from 3% to 62% of total ATP produced (Alonso et al., 2007; Hatzfeld & Stitt, 1990; Hill & ap Rees, 1994; Rontein et al., 2002). It has since been shown that the higher values in this range are likely to be an overestimate (Kruger *et al.*, 2007). Nevertheless,

there does seem to be variation in the extent of substrate cycling between tissues (Hatzfeld and Stitt, 1990) and substrate cycling remains a possible cause for the gap in the ATP budget.

Lastly, there may be experimental errors associated with the construction of the ATP budget leading to inaccurate results. The use of inhibitors to calculate the ATP cost for different processes assumes that after the elimination of a process by inhibition, ATP synthesis is reduced by the ATP demand for that process. This assumption has been tested in a number of cell systems including rat hepatocytes and Ehrlich ascites tumour cells (Müller et al., 1986; Schneider et al., 1990). However, non-specific effects of inhibitors that may affect energy use cannot be ruled out; such effects may include stress response from a depletion in protein after CHI inhibition (Bouma et al., 1994), or inability to maintain ion gradients. The impact of non-specific effects of the inhibitors used was limited as much as possible by treating roots with inhibitors for shortest time necessary to achieve full inhibition, nevertheless, the possibility of such effects cannot be excluded.

Summary

Data presented in this chapter demonstrate that protein turnover and the maintenance of ion gradients are quantitatively the most important ATP-consuming maintenance processes in terms of energy consumption. The rate of protein turnover shows no significant change, whereas ion leakage and ATP consumption for ATPase activity increase with high temperature. This suggests that reducing ATPase activities may be effective in reducing the rate of non-growth respiration at high temperature. Given the likelihood that ATPase activity increases to deal with enhanced membrane fluidity and ion leakage at high temperature, a potential approach to achieve this is to modify membrane properties to reduce fluidity at high temperature.

5. Is increased non-growth respiration at elevated temperature caused by a reduction in mitochondrial coupling?

Introduction

The mtETC couples the oxidation of NADH, as well as other substrates, to the production of ATP. NADH is derived from the TCA cycle and consequently, decreased coupling of NADH oxidation to ATP production results in a greater rate of CO_2 production. Many studies have focused on various mitochondrial uncoupling mechanisms under different stress conditions, however, no consensus on the effect of high temperature on mitochondrial coupling has been reached. In this chapter, the effect of mtETC coupling at 23°C and 33°C will be investigated.

Assessing uncoupling by studying the activity of uncoupling mechanisms

One approach to assess the level of mtETC coupling is to study the activity of different uncoupling mechanisms in the plant mtETC. Individual uncoupling mechanisms are discussed in detail in the General introduction and so just a brief overview of the methods used to estimate their activity will be provided here.

Estimating AOX activity

The most straightforward approach for estimating AOX activity is to measure the abundance of AOX protein, either directly, or indirectly by studying gene expression of AOX family members. For instance, expression of AOX genes and protein levels were both found to be increased under chilling stress (Mizuno et al., 2008; Vanlerberghe & Mcintosh, 1992). A similar approach is to

measure AOX capacity, which is an estimate of maximum possible electron flux through AOX, by measuring cyanide resistant O_2 consumption by either whole tissue or isolated mitochondria (Mcdonald et al., 2002; Møller et al., 1988). However, this approach does not necessarily give a good approximation of *in vivo* AOX activity as once the cytochrome pathway is inhibited, electrons are forced through the alternative pathway, resulting in overestimation of electron partitioning to AOX (Millenaar and Lambers, 2003). Additionally, *in vivo* activity of AOX is dependent on post-translational regulation, such as dimerization under reducing conditions (Umbach et al., 1994; Umbach & Siedow, 1993), activation by pyruvate (Hoefnagel et al., 1997; Umbach et al., 1994) and AOX activity will also depend on the *in vivo* activation of COX. The simplicity of these measurements allows easy approximation of changes in AOX activity under different conditions, however, such an approach will not provide a complete picture of *in vivo* AOX engagement.

A more recent technique to assess electron partitioning between AOX and COX is the ^{18}O fractionation technique, based on the fact that AOX discriminates against ^{18}O to a greater extent than the COX (Guy et al., 1989). This method is non-invasive and does not directly involve the use of inhibitors. As such it provides a more accurate assessment of *in vivo* partitioning between AOX and COX. Using this technique, it was found that under certain conditions over 50% of electron flux is via AOX (Millar et al., 1998). Additionally, this method allows comparison of AOX capacity or protein levels with *in vivo* AOX activity. For instance, it was shown that AOX protein levels were two-fold higher in mung bean grown at 19°C compared with 28°C, and 19°C grown plants were able to maintain higher flux through AOX at measurement temperatures below 28°C than 28°C-grown plants (Gonzalez-Meler et al., 1999). However, other studies have shown little agreement between AOX protein levels and partitioning to AOX (Guy and Vanlerberghe, 2005; Vidal et al., 2007).

Alternative NAD(P)H dehydrogenase activity

Activity of alternative NAD(P)H dehydrogenases has previously been assayed in isolated mitochondria. By providing mitochondria with NADH or NADPH as an electron donor, and inhibiting complex 1 with rotenone, the rate of external NAD(P)H dehydrogenases can be measured. Determining the activity of NAD(P)H dehydrogenases located on the matrix facing side of the inner mitochondrial is more challenging, but can be achieved by either using inside-out submitochondrial particles (Melo et al., 1996), or by permeabilising the inner mitochondrial membrane to NAD(P)H (Svensson and Rasmusson, 2001). *In vivo*, external alternative NAD(P)H dehydrogenases are regulated by intracellular Ca^{2+} (Cottingham & Moore, 1984; Geisler et al., 2007), and therefore activity may differ from that measured in isolated mitochondria. There are currently no published attempts to measure the rate of alternative NAD(P)H dehydrogenase activity in intact plant tissues; however, the activity of NAD(P)H dehydrogenases has been studied in active isolated mitochondria and cells cells after membrane permeabilisation with alamethicin (Johansson et al., 2004; Matic et al., 2005).

UCP activity

UCP allows the passage of protons from the intermembrane space back into the matrix, thus dissipating the proton gradient necessary to drive ATP synthesis (Nicholls and Bernson, 1977). It has been shown to have a role in stress tolerance and consistent with this, it is activated by oxidation products of fatty acids when there is an abundance of ROS (Considine et al., 2003). One factor affecting activity of UCP is protein abundance; transgenic tobacco overexpressing UCP had better tolerance to oxidative stress, suggesting that protein levels may be at least partly responsible for UCP activity (Brandalise et al., 2003). Additionally, in potato tubers stored in the cold (4°C or 5°C), UCP protein levels increase with time compared with potato tubers stored under control conditions of 20°C or 25°C (Calegario et al., 2003; Laloi et al, 1997). Maximum UCP

activity is determined by measuring oxygen uptake of isolated mitochondria; UCP activity is measured as ROS-stimulated, nucleotide-inhibited O_2 uptake (Smith et al., 2004). However, as with other uncoupling mechanisms, UCP is subject to post-translational regulation that means that determination of protein levels or maximum activity does not necessarily indicate the extent of UCP activity *in vivo*. UCP is activated by ROS *in vivo* and cellular levels of ROS will therefore affect the actual contribution of UCP to *in vivo* mitochondrial uncoupling.

Basal proton leak

Previously, basal proton leak has been studied by measuring the state 4 respiratory rate (Stuart et al., 1999). When mitochondria are in state 4, mitochondrial respiration is used solely to drive basal proton leak, provided that UCP is inhibited. However, proton flux across the inner membrane increases at higher membrane potentials (Nicholls and Bernson, 1977) and therefore measuring the proton leak in isolated mitochondria only provides a rough estimate of the proton leak *in vivo*, where the membrane potential is dependent on factors such as ATP turnover and substrate availability (Brand & Nicholls, 2011). Furthermore, it has been demonstrated that while proton leak accounts for total respiratory rate in state 4, it only accounts for a small proportion of respiratory rate in state 3 as membrane potential is so much higher during state 4 respiration (Brand, 1990). Thus, measuring state 4 respiration measures the maximum leakage rate possible, which is almost certainly an overestimation of the proton leak when ATP synthesis is occurring.

Basal proton leak has been estimated *in vivo* in rat liver cells (Nobes et al., 1990). The relationship between membrane potential and respiration rate was assessed by titrating with oligomycin to inhibit ATP synthesis, and it was demonstrated that, like in isolated mitochondria, increased proton conductance in situ is increased at high values of membrane potential. By assessing the respiration rate and mitochondrial membrane potential in the absence of oligomycin, the authors demonstrated that 20–40% of total respiratory rate can be attributed to basal proton leak.

Mitochondrial pulsing

Schwarzländer et al., 2012 recently described a novel uncoupling mechanism involving transient depolarisation of the inner mitochondrial membrane due to influx of Ca^{2+}. This mitochondrial 'pulsing' was found to occur more frequently during high-temperature stress and upon treatment with peroxide or cadmium ions in arabidopsis roots, suggesting that it may have a role in stress tolerance under conditions leading to ROS accumulation. The impact of mitochondrial pulsing on oxygen uptake of isolated mitochondria can be studied using lanthanum to inhibit calcium ion channels responsible for allowing the calcium ion influx. This technique is limited to use on isolated mitochondria as the effects of $LaCl_3$ on calcium ion channels in whole tissues will reduce ATP consumption by ATP-dependent Ca^{2+} channels (Zagdanska, 1995), and therefore O_2 consumption will be affected by both mitochondrial pulsing and altered ATP turnover rate.

P/O ratio

Estimating the activities of various mtETC uncoupling processes as described above can give some insight into how coupled NADH oxidation is to ATP synthesis in the mtETC. However, it is preferable to look at the mtETC as a whole and quantitatively assess mtETC coupling by determination of the ADP/O ratio, the number of oxygen atoms consumed for every ATP produced. Generally accepted values for the P/O ratio are 2.5–3.0 for NADH oxidation and 1.5–2.0 for succinate oxidation, however, numerous estimated have been made on isolated mitochondria, ranging from 0.96–3.5 (Hinkle, 2005). Variation of the ADP/O ratio results from the action of the mtETC uncoupling mechanisms described above; a good example of how mtETC uncoupling can lower the ADP/O ratio was demonstrated by Day et al. 1988 in mitochondria isolated from soybean cotyledons. Addition of SHAM, an inhibitor of AOX, resulted in a small 1.1–1.4-fold increase in the ADP/O ratio with succinate as a substrate. Additionally, inhibition of complex 3 by

antimycin A, therefore forcing electrons through AOX, resulted in a decrease in the ADP/O ratio from 2.16 to 0.71. The ADP/O ratio of isolated mitochondria has been previously determined at different temperatures: in mitochondria isolated from chilling sensitive and chilling tolerant species, the ADP/O ratio was 1.35–1.76 and it was found to not be affected by measurement temperature (Lyons and Raison, 1970). Additionally, ADP/O ratios determined in isolated mitochondria from wheat and rye seedlings treated at 0–24°C showed no variation with temperature (Pomeroy and Andrews, 1975).

Calculation of the ADP/O ratio in isolated mitochondria involves simply determining oxygen uptake during consumption of a known quantity of ADP. While isolated mitochondria are a commonly used system to determine the ADP/O ratio under different conditions, ADP/O estimates in isolated mitochondria do not reflect the actual ADP/O ratio *in vivo*. Firstly, the *in vivo* ADP/O ratio is dependent on the activation status of uncoupling mechanisms such as AOX, UCP and alternative NAD(P)H dehydrogenases. As discussed in the General Introduction, the activation of these mechanisms is subject to control by post-translational mechanisms *in vivo*, and these mechanisms will be working at different rates in isolated mitochondria compared with *in vivo*, altering the ADP/O ratio. Secondly, the ADP/O ratio *in vivo* will be dependent on the rate of ATP turnover because as previously discussed, basal proton leak is dependent on the proton gradient across the inner mitochondrial membrane; when ATP turnover is rapid, movement of protons through ATP synthase dissipates the proton gradient thus reducing proton leak, however, when ATP turnover is slow, the proton gradient will increase leading to an increased rate of basal proton leak.

Measurement of *in vivo* P/O ratio requires measurement of both the O_2 uptake rate of a tissue and the rate of ATP turnover. Measurements of ATP turnover have been previously made using saturation transfer ^{31}P NMR. This technique relies on using radiofrequency radiation to saturate spins of a chemical group of interest, for instance the γ-phosphorous of ATP. Using this technique,

P/O ratios have been determined in animal systems that range from 1.29 to 2.46 (Brand et al., 1993; Freeman et al., 1983; Kingsley-Hickman et al., 1987). In plants, just one study has looked at the P/O ratio *in vivo*: in wheat roots, a P/O ratio of approximately 3 was determined when roots were supplied with glucose, and when wheat roots were supplied with succinate, the P/O ratio dropped to 2 (Roberts et al., 1984), values that are extremely close to commonly accepted P/O ratio values (Hinkle, 2005). A second approach that has been used to estimate ATP turnover rate is to use $H_2{}^{18}O$ water to label cellular Pi. Upon feeding, $H_2{}^{18}O$ rapidly equilibrates with cellular H_2O, and ^{18}O is incorporated into Pi upon ATP hydrolysis. Once Pi is labelled, incorporation of Pi into ATP, as well as other phosphometabolites, can be tracked (Nemutlu et al., 2012; Dawis et al., 1989). Advantages of this method are that feeding times are very short – in the range of seconds or minutes – and incubation with media containing $H_2{}^{18}O$ is the only perturbation experienced by the tissue, minimising experimental artifacts (Nemutlu et al., 2012). Additionally, the γ-phosphate of ATP can be enzymatically transferred to glycerol for GC-MS or LC-MS analysis of ^{18}O labelling, meaning that the high sensitivity of mass spectrometric techniques can be used to detect the labelling of extremely small quantities of ATP found in small tissue samples.

Chapter aims

The aim of this chapter is to assess whether there are changes in mitochondrial coupling that contribute to non-growth respiration and to identify potential uncoupling mechanisms responsible for any changes. This will be achieved firstly by experiments on isolated mitochondria to assess the capacity of individual uncoupling mechanisms and secondly by using an ^{18}O labelling approach to estimate the *in vivo* P/O ratio of excised arabidopsis roots at 23°C and 33°C.

Results

Experiments using isolated mitochondria

To gain insight into whether elevated temperature treatment increased the capacity of mitochondrial uncoupling mechanisms, experiments were performed on isolated mitochondria. Mitochondria were isolated from 14-day-old 23°C-grown arabidopsis seedlings that had been treated for 18 hours at 23°C or 33°C before mitochondrial extraction. Assays were then performed on extracted mitochondria at 23°C and 33°C. This approach allowed changes in capacity as a result of altered protein levels (i.e. after the 18 hour pre-treatment) to be distinguished from increased uncoupling activity as a result of the kinetic effects of assay at the higher temperature.

Determining the capacity of cytochrome oxidase pathway (COP) and and alternative oxidase pathway (AOP)

To assess AOP capacity, O_2 consumption was measured in state 3 before and after addition of cyanide. Cyanide-resistant O_2 consumption that was sensitive to n-propyl gallate, an AOX inhibitor, was considered to occur as a consequence of electron flow through AOP. When mitochondria isolated from plants grown at either 23°C or 33°C were assayed at a common temperature of 23°C, electron flow through COP was lower in plants treated at 33°C compared with plants treated at 23°C, whereas electron flow through AOP was unchanged (Figure 5.1A). Consequently, AOP capacity as a percentage of total O_2 uptake was increased after treatment at 33°C compared with 23°C, when assayed at 23°C (Figure 5.1C, dark bars). These results suggest that COP capacity is reduced after treatment at 33°C. However, western blots of subunits 1 and 2 of COX did not show a consistent decrease in protein content of isolated mitochondria.

When mitochondria isolated from plants treated at the two temperatures were assayed at a common temperature of 33°C, there were no significant differences between electron flow through COP and AOP (Figure 5.1B), and AOP capacity as a percentage of total uptake was similar (Figure 5.1C, light bars).

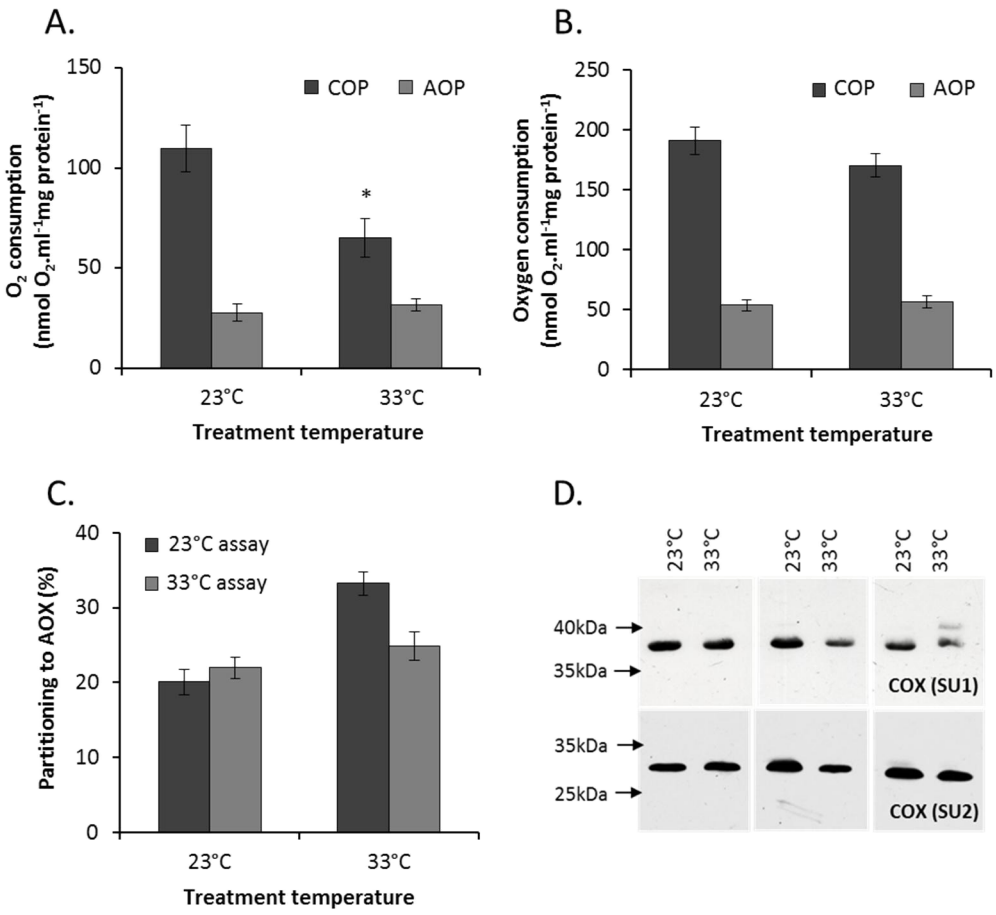


Figure 5.1 Electron flow through AOX and COX in isolated mitochondria

A. O_2 uptake in mitochondria isolated from 23°C and 33°C pre-treated plants was determined at 23°C before and after addition of 0.05 mM KCN. COP capacity = rate before KCN addition – rate after KCN addition. AOP capacity = rate after KCN addition – rate after n-propyl gallate addition (0.05 mM). B. AOP and COP capacities at 33°C assay temperature, calculated as before. C. AOP capacity expressed as a percentage of total O_2 consumption. D. Western blot of COX subunits (SU) 1 and 2. Data are mean ± SEM (n=3), Student's *t*-test, significance between treatment temperatures *p=<0.05, **p=<0.01.

Protein levels of alternative NAD(P)H dehydrogenases

Previously, alternative NAD(P)H dehydrogenase capacity has been measured by O_2 uptake measurements on isolated mitochondria as discussed in the Introduction. However the potential differences in COX capacity between mitochondria isolated from 23°C-treated and 33°C-treated plants would complicate results from such experiments, as it would not be possible to separate changes in alternative NAD(P)H dehydrogenase capacity from changes in COX capacity. Therefore, mitochondria isolated from 23°C and 33°C treated plants were analysed for protein content by western blot. There was no difference in the abundance of either NDA or NDB after treatment at 33°C, suggesting that the capacity of internal and external NAD(P)H dehydrogenases is not altered.

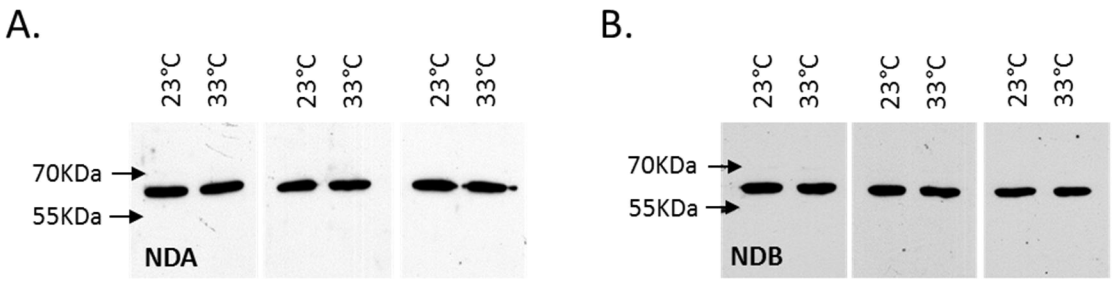


Figure 5.2 Western blots of alternative NAD(P)H dehydrogenases

Blots were carried out on mitochondrial samples isolated from arabidopsis seedlings treated at 23°C or 33°C. A Internal NAD(P)H dehydrogenase (NDA). B. External NAD(P)H dehydrogenase (NDB).

Estimating proton leakage rate

To estimate the rate of proton leakage, mitochondria were isolated from seedlings treated at 23°C and 33°C for 18 hours and provided with respiratory substrates and ADP to induce state 3 respiration. Proton leakage was determined as the rate of state 4 respiration as a percentage of state 3 respiration. Basal proton leakage was similar between 23°C and 33°C treated plants, when treated at a common measuring temperature of either 23°C or 33°. However, when assayed at

33°C, the basal proton leakage as a percentage of state 3 respiration increased by approximately 1.3-fold, from 47.2% to 75.7% in mitochondria from 23°C-treated plants and from 48.1% to 73.1% in mitochondria from 33°C-treated plants (Figure 5.3A).

The rate of basal proton leakage has been shown to correlate with ANT protein abundance (Brand et al., 2005). ANT protein levels determined by western blot were similar in mitochondria isolated from 23°c and 33°C treated plants (Figure 5.3B).

Protein abundance of UCP was also determined by western blot and it was found that there was a decrease in UCP protein after pre-treatment at 33°C (Figure 5.2B). Densitometry was used to quantify the difference in protein amount, and it was found that UCP protein content was approximately 34% less in mitochondria isolated from 33°C treated plants.

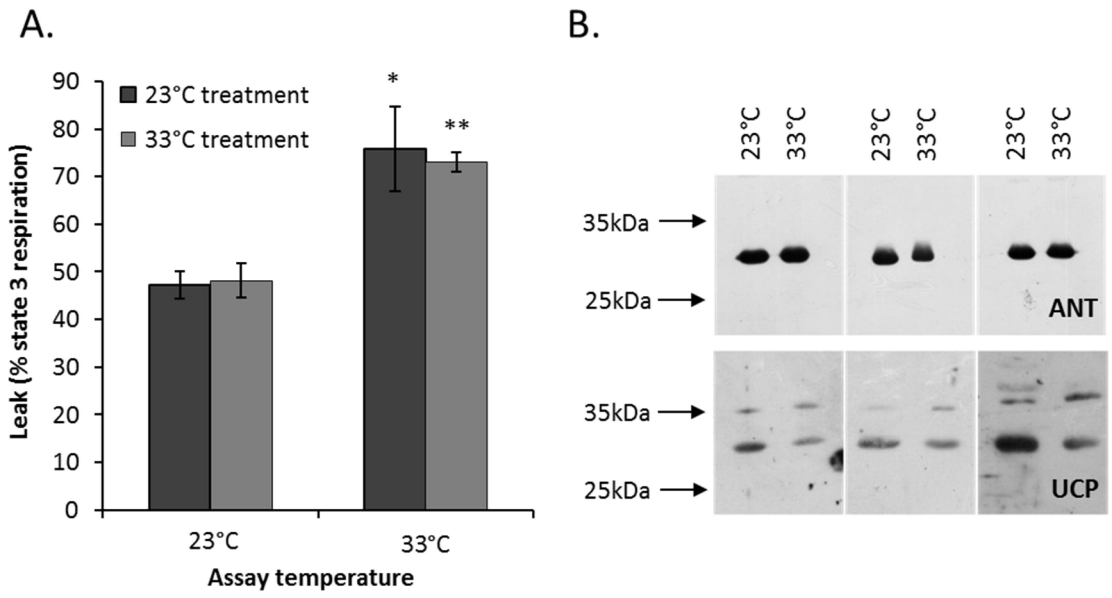


Figure 5.3. Proton leakage in isolated mitochondria at 23°C and 33°C

A. Rate of proton leakage measured as state 4 respiration as a percentage of state 3. B. Western blots of ANT and UCP. Data are mean ± SEM (n=3), Student's *t*-test, significance between treatment temperatures *p=<0.05, **p=<0.01.

Mitochondrial pulsing at 23°C and 33°C

Isolated mitochondria were provided with succinate and ADP to induce state 3 respiration. $LaCl_3$ was added to prevent mitochondrial pulsing and the percentage inhibition of O_2 uptake calculated. There was no difference in pulsing between either mitochondria isolated from plants treated at 23°C or 33°C, or mitochondria assayed at 23°C or 33°C (Figure 5.4).

Establishing a method for determination of the *in vivo* P/O ratio

The use of ^{18}O water has become an established method to determine the rate of ATP turnover *in vivo* for certain animal tissues (Dawis et al., 1989; Nemutlu et al., 2012; Zeleznikar et al., 1990). Initial experiments were done to determine whether this method could be adapted to plant tissues. The work flow for the determination of ATP turnover is described in Methods.

Separation of nucleotides by HPLC

The first step was to determine whether nucleotides could be separated by high-performance liquid chromatography (HPLC). Separation of nucleotides necessary to prevent transfer of phosphates from nucleotides other than ATP onto glycerol. ATP could be successfully separated from GTP and UTP, with ATP eluting at 25.5–26 minutes (Figure 5.6).

Time course of ^{18}O incorporation into ATP

To determine the optimum $H_2{}^{18}O$ incubation time for arabidopsis roots, a time course for $H_2{}^{18}O$ incubation was performed between 0 and 60 minutes. Figure 5.7 shows phosphate labelling by ^{18}O at one position ($^{18}O_1$), two positions ($^{18}O_2$) and three positions ($^{18}O_3$) on the γ-phosphate of ATP. Total percentage of phosphoryl oxygens replaced by ^{18}O was calculated as follows:

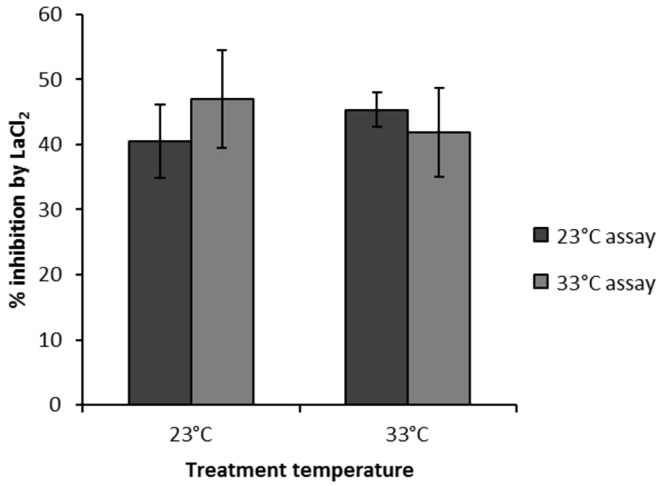


Figure 5.4 Mitochondrial pulsing of isolated mitochondria at 23°C and 33°C.

Pulsing measured as the decrease in oxygen consumption after addition of $LaCl_3$. Pulsing is presented as percentage inhibition after addition of 2 mM $LaCl_3$. Data are mean ± SEM (n=3).

$$Total = \frac{\%^{18}O_1 + 2(\%^{18}O_2) + 3(\%^{18}O_3)}{3(\%^{18}O\ in\ media)}$$

^{18}O labelling occurred rapidly, with the majority of ^{18}O being incorporated within the first two minutes. It was assumed that the rate of ^{18}O incorporation was linear from 0–2 minutes, and for calculation of ATP turnover rate, a labelling time of one minute was used.

Determination of in vivo ATP turnover rate and P/O ratio

ATP turnover rate was calculated as follows (Zeleznikar et al., 1990):

$$ATP\ turnover\ rate = F\ \times\ 3\ \times [ATP]$$

where F is the fraction of total phosphoryl oxygens replaced by ^{18}O. The percentage of ^{18}O labelling after one minute $H_2{}^{18}O$ feeding of excised roots at 23°C and 33°C was determined as before and was found to be 48.7 ± 2.0% at 23°C and 61.7 ± 1.5% at 33°C ($p<0.001$, Student's t-

test, n=6). ATP concentration was determined using HPLC and was 13.9 ± 0.9 nmol ATP.mg protein^{-1} at 23°C and 12.1 ± 1.4 nmol ATP.mg protein^{-1} at 33°C (ns, Student's t-test, n=6). Calculated rates of ATP turnover were 20.3 ± 1.3 nmol.mg protein^{-1}min^{-1} and 22.4 ± 2.5 nmol.mg protein^{-1}min^{-1} at 33°C (ns, Student's t-test, n=6). Although the rate of labelling of ATP was significantly higher at 33°C, the slightly lower ATP concentration at this temperature meant that the calculated ATP turnover rate was not significantly different.

Using these values of ATP turnover, as well as values for the rate of oxygen consumption (Table 4.1), the P/O ratio was calculated to be 0.78 at 23°C and 0.47 at 33°C ($p = 0.0047$, Student's *t*-test, n=6).

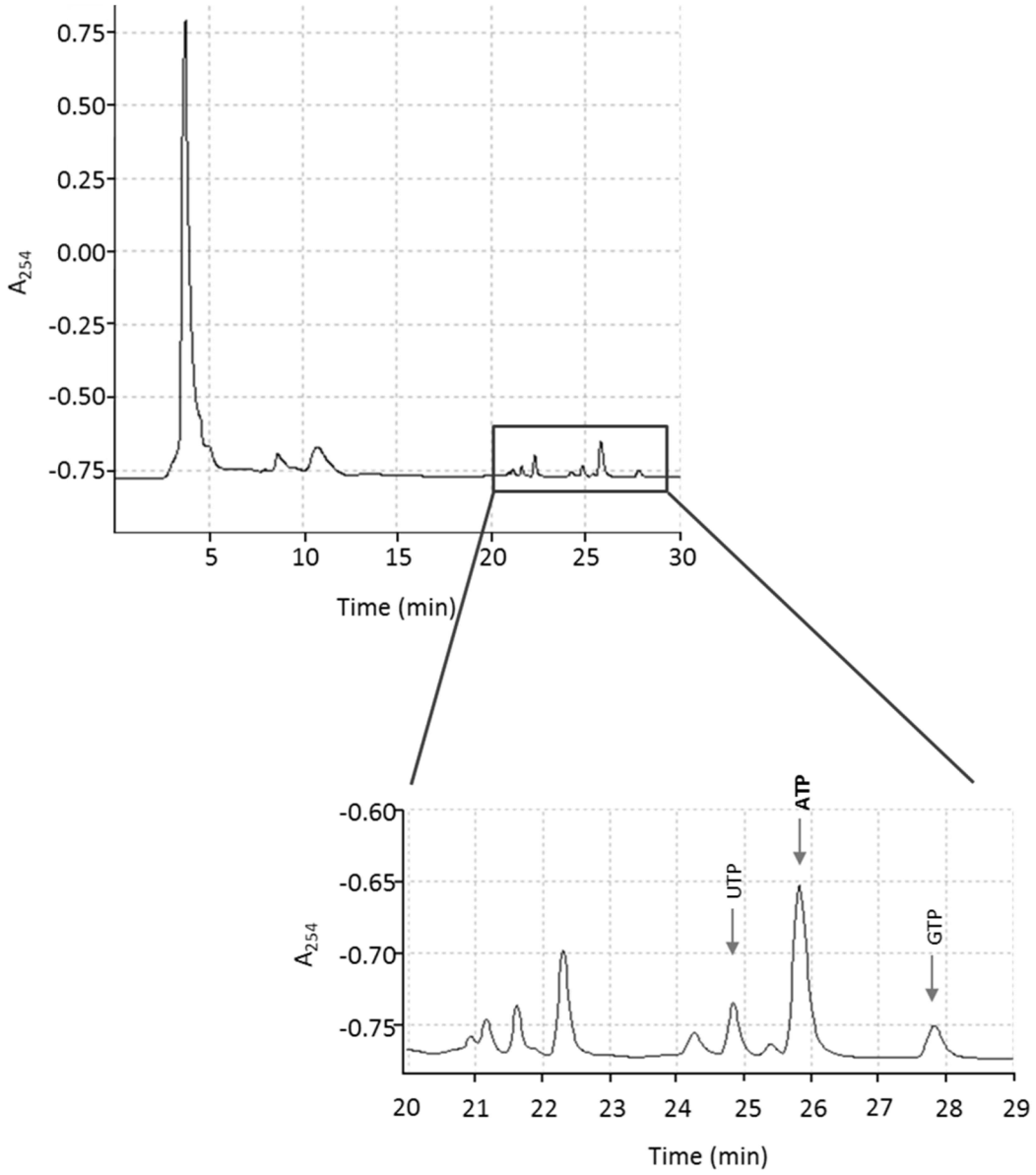


Figure 5.5. HPLC chromatogram of extracted metabolites.

Metabolites were extracted from arabidopsis roots by TCA extraction and fractionated by HPLC. Elution of nucleotide triphosphates is indicated.

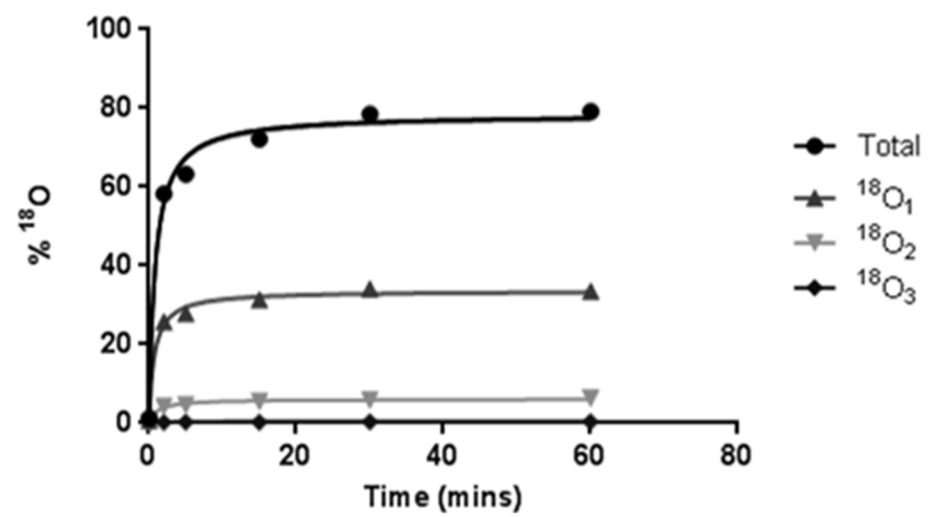


Figure 5.6 Time course of ^{18}O-phosphate incorportation into ATP

$H_2{}^{18}O$ was fed to excised Arabidopsis roots at 23°C for 2, 5, 15, 30, and 60 minutes, and ^{18}O incorporation into γ-phosphate of ATP determined. N=1 for each time point.

Table 5.5. Calculation of *in vivo* P/O ratio in arabidopsis roots at 23°C and 33°C

	23°C	**33°C**	**p value**
^{18}O labelling after 1 minute (%)	48.66 ±2.03	61.81 ± 1.47	0.0004
[ATP] (nmol ATP.mg protein^{-1})	13.91 ± 0.87	12.12 ± 1.42	0.33
ATP turnover (nmol.mg protein^{-1}min^{-1})	20.31 ± 1.30	22.47 ± 2.54	0.65
O_2 uptake (nmol.mg protein^{-1}min^{-1})	13.07 ± 0.80	23.72 ± 1.12	1.61 x 10^{-5}
O uptake (nmol.mg protein^{-1}min^{-1})	26.14 ± 1.60	47.43 ± 2.24	1.61 x 10^{-5}
P/O	**0.78 ± 0.064**	**0.47 ± 0.057**	**0.0047**

Values presented are mean ± SEM, n=6

Discussion

There is no evidence for changes in the capacity of AOP, alternative NAD(P)H dehydrogenases or mitochondrial pulsing consistent with decreased mitochondrial coupling at elevated temperature

When assays on isolated mitochondria were performed at the respective treatment temperatures, AOP capacity as a percentage of total state 3 oxygen consumption was similar between 23°C and 33°C, suggesting that electron partitioning to AOP does not increase at high temperature. This is supported by previous data; an $^{18}O/^{16}O$ discrimination study on *Cucurbita pepo*, *Nicotiana sativa* and *Vicia fabia* exposed to changes in temperature between 15°C and 30°C which showed no changes in electron partitioning between AOP and COP with temperature (Macfarlane et al., 2009). Additionally, it was observed that electron partitioning between AOP and COP remained stable at temperatures above 19–20°C in mung bean, although partitioning to AOP increased below these temperatures (Armstrong et al., 2008; Gonzalez-Meler et al., 1999). When mitochondria were assayed at a common temperature of 23°C, mitochondria from 33°C-treated plants displayed lower COP capacity, consequently AOP capacity as a percentage of state 3 respiration was higher, potentially suggesting greater electron partitioning to AOP. The decrease in COP capacity in mitochondria from 33°C treated plants assayed at 23°C may occur as a compensatory mechanism to maintain electron partitioning upon increases in temperature if the instantaneous temperature sensitivity of COP was greater than that of AOP. There is evidence that COP is more temperature sensitive than AOP (Kruse 2010); the Q_{10} for AOP was found to be higher than for COP in *Saxifraga cernua* (McNulty et al, 1987), *Cornus stolonifera* callus (Yoshida and Tagawa, 1979), soybean cotyledons (Gonzalez-Meler et al., 1999) and *Pinus radiata* needles (Kruse et al., 2008). However, results into the temperature sensitivity of AOP and COP are contradictory; in mung bean leaves, it was found that AOP is more temperature sensitive than COP (Gonzalez-Meler 1999), and in arabidopsis, AOP had greater temperature sensitivity that COP

at low temperatures, but not at temperatures above 21°C (Armstrong et al., 2008). The data presented in this chapter show that the Q_{10}s of COP and AOP (measured from mitochondria isolated from 23°C treated plants assayed at 23°C and 33°C) were similar at 1.8 and 1.9, respectively. Thus, compensation for the increased temperature sensitivity of COP does not easily explain the decrease in COP capacity in mitochondria isolated from 33°C treated plants assayed at 23°C. Additionally, there was no consistent decrease in COX protein from 33°C compared with 23°C treated plants. It is therefore possible that rather than indicating altered COP capacity after high-temperature treatment, oxygen consumption may be limited by other components in the COX pathway of the mtETC. Western blot analysis of other mtETC components, in particular complex III, would be necessary to test whether this is the case.

Protein abundance of alternative NAD(P)H dehydrogenases was shown to be similar in mitochondria isolated from plants treated at 23°C and 33°C. Whilst this an indication that alternative NAD(P)H dehydrogenase activity is similar between the two treatments, alternative NAD(P)H dehydrogenases are subject to post-translational regulation as discussed in the General Introduction, and protein amount may not be indicative of *in vivo* activation.

Reduction in O_2 consumption after inhibition of calcium ion channels by $LaCl_3$ was measured to assess the impact of mitochondrial pulsing on O_2 consumption. Treatment with $LaCl_3$ inhibited O_2 consumption by 40–46% for all treatments; this is very similar to the magnitude of inhibition found previously for isolated arabidopsis mitochondria of approximately 45% (Schwarzländer et al., 2012). Although it was previously found that exposure to high temperature lead to an increased rate of mitochondrial pulsing, in this study, pulsing was similar at 23°C and 33°C. This discrepancy may be explained by differences in the temperatures used for each study; previously, a more extreme temperature treatment of 42°C was used, and given the dependency of mitochondrial pulsing on mtETC redox poise, it is possible that treatment at 33°C did not cause sufficient oxidative stress to trigger increased levels of pulsing compared with treatment at 23°C.

Additionally, whether increased pulsing at 33°C occurs *in vivo* is unknown as isolated mitochondria display a pulsing frequency that is much higher than mitochondria in intact tissue (Schwarzländer et al., 2012).

Proton leakage is increased at 33°C compared with 23°C

The rate of proton leakage was significantly higher when mitochondria were assayed at 33°C compared with 23°C. There were no significant differences in basal proton leakage between mitochondria isolated from 23°C and 33°C treated plants, regardless of the assay temperature, indicating that increased proton leak with temperature is an intrinsic property of the mitochondrial membrane, such as a change in membrane fluidity, rather than mediated by changes in protein abundance. The abundance of one particular protein, ANT, has been shown to correlate with proton leakage rate (Brand, 2005). There was no change in ANT protein levels after treatment at 33°C, further suggesting that increased basal proton leakage was unlikely to be caused by changes in protein levels, but rather by changes in membrane fluidity at high temperature. It is well established that membrane fluidity is dependent on temperature (See General Introduction) and there is evidence that basal proton leakage depends on mitochondrial membrane fluidity: in arabidopsis cell lines, it was demonstrated that basal proton leakage was dependent on lipid composition of the inner mitochondrial membrane, being higher in membranes with greater fatty acid saturation and lower fluidity (Hourton-Cabassa et al., 2009).

Proton leakage was measured as state 4 O_2 consumption as a percentage of state 3. During state 4 respiration, protons are not passing through ATP synthase and consequently the proton gradient across the inner mitochondrial membrane increases. It is well established that the proton leakage rate is dependent on the proton gradient across the inner mitochondrial membrane (Nicholls and Bernson, 1977) and therefore measurement of O_2 consumption during state 4 is likely to be an overestimate of the rate of basal proton leakage during state 3. Therefore the

results presented here demonstrate that the maximum rate of proton leakage is increased with treatment at high temperature.

Assessment of the amount of UCP protein demonstrated that there was a decrease in UCP protein in mitochondria isolated from plants pre-treated at 33°C. The effect of high temperature on UCP levels has not previously been tested in plants; however, UCP protein levels have previously been shown to increase upon cold temperature treatment, consistent with the data presented here (Laloi et al., 1997). UCP has been shown to have a role in the reduction of ROS production by preventing over-reduction of the mtETC (Vercesi et al., 2006). It is possible that at high temperature, the level of UCP decreases because dissipation of the proton gradient through ATP synthase and basal proton leakage occurs at a greater rate at high temperature, and UCP activity is not required to dissipate the proton gradient to avoid ROS formation.

There is a decrease in *in vivo* P/O ratio at elevated temperature

Data from experiments performed on isolated mitochondria presented in this chapter provide no evidence for increased uncoupling by AOX, alternative NAD(P)H dehydrogenases , UCP or mitochondrial pulsing at 33°C relative to 23°C. However, there is evidence that the maximum rate of basal proton leakage increases at high temperature. Calculation of the *in vivo* P/O ratio allows the state of overall mitochondrial coupling to be assessed. The values of the in vivo P/O ratio of 0.78 and 0.47 are low compared with P/O ratios previously obtained by the ^{31}P saturation transfer technique for rat myocardium (2.34, Kingsley-Hickman et al., 1987), rat kidney (2.46, Freeman et al., 1983), resting hepatocytes (1.29, Brand et al., 1993) and maize root tips (2.0–3.2, Roberts et al., 1984). There are a number of reasons why the calculated P/O ratio might be underestimated; the first is that when determining the rate of ATP turnover, it was assumed that ^{18}O incorporation into ATP was linear from 0–2 minutes. The percentage of available oxygens labelled on γ-phosphate was 48.7% after one minute and 58.3% after two minutes, demonstrating

that labelling in this time frame was not linear. In order to get the most accurate rate of ATP turnover, the initial rate needs to be measured, and it was likely that the initial rates were faster than the rates measured in this experiment. The quick saturation of the γ-phosphate by ^{18}O is consistent with previous studies that have used this method; approximately 75% of oxygen atoms were labelled in rat myocardium (Nemutlu et al., 2012) and 55% were labelled in rat diaphragm muscle (Zeleznikar and Goldberg, 1991) after a two minute incubation with ^{18}O. This issue could be addressed by taking a greater number of time points from 0–2 minutes and fitting a curve to the data to obtain a more accurate estimate of the initial rate of ATP synthesis. A second potential source of error is that accurate measurements of ATP content in the tissue are required to calculate ATP synthesis rate. While the TCA extraction used here will denature ATPases, if ATP recovery from the tissue is not 100%, then this will have the effect of leading to an underestimated P/O.

These caveats aside, the data clearly show that while the rate of oxygen consumption is 1.8-fold higher at 33°C than at 23°C, the rate of ATP synthesis is similar at the two temperatures. Therefore, regardless of the actual P/O ratios obtained, the decrease in P/O ratio is likely to be a valid result. Data presented in this chapter show that at 33°C the P/O ratio decreases by 40% compared with 23°C. As the data from isolated mitochondria show that the maximum rate of basal proton leakage is higher at 33°C compared with 23°C, it is likely that the decrease in P/O ratio comes from a higher rate of proton leakage. The in vivo P/O ratio of mitochondria has not previously been investigated at different temperatures. However, the P/O ratio from a variety of plant species have been tested at different temperatures and it was found that temperature has no effect on P/O ratio (Lyons and Raison, 1970; Pomeroy and Andrews, 1975). This discrepancy may simply be a result of differences in mtETC uncoupling *in vivo* and in isolated mitochondria.

Summary

Data presented in this chapter demonstrate that there is a decrease in *in vivo* P/O ratio of excised arabidopsis roots at high temperature. Experiments performed on isolated mitochondria suggest that changes in AOP, alternative NAD(P)H dehydrogenase or UCP capacity, or increased pulsing are unlikely to contribute to reduced mitochondrial coupling at high temperature. However, an increase in maximum basal proton leakage was demonstrated at the high temperature and identified as a potential mechanism contributing to decreased P/O ratio.

6. Acclimation of non-growth respiration to temperature

Introduction

Data presented in previous chapters demonstrated that non-growth respiration is an important component of increased total respiratory rate upon short-term increases in temperature. However, longer term changes in the ambient temperature can lead to respiratory acclimation, which has the effect of reducing respiration upon sustained exposure to high temperature and increasing respiratory rate after sustained cold treatment (Atkin & Tjoelker, 2003). Although respiratory acclimation to temperature is a well-documented phenomenon, there is little published data on the biochemical processes that cause respiratory acclimation, in particular whether respiratory acclimation is due to acclimation of growth or non-growth respiration. In this chapter, the extent of acclimation of non-growth respiration and the underlying biochemical causes for respiratory acclimation will be investigated.

The extent of respiratory acclimation

There is great variation in the extent to which plants acclimate to temperature, with acclimation differing between species and tissues (Atkin & Tjoelker, 2003). In a study looking at respiratory acclimation in a range of alpine and lowland species, acclimation ranged from full to no acclimation, and the authors concluded that the extent of respiratory acclimation was dependent on genus (Larigauderie & Körner, 1995). Acclimation of boreal tree species (Tjoelker et al., 1999), tropical tree seedlings (Cheesman and Winter, 2013b) and plants differing in RGR (Loveys et al., 2003) was also found to vary widely. In some cases, complete respiratory homeostasis occurs, in

which plants grown at contrasting temperatures have identical respiration rates (Atkin et al., 2000).

Two approaches to measure respiratory acclimation were described by Loveys et al. (2003). The "homeostasis method" is the simplest and involves comparison of respiratory rates at the respective growth temperatures. This method is useful to establish whether respiratory homeostasis has occurred; the ratio of dark respiration at different temperatures is calculated and a ratio of one indicates full acclimation. The "set temperature method" involves measuring the ratio of respiratory rates of warm and cold grown plants at a common measuring temperature, for instance comparison of respiration at 23°C for plants grown at 18°C and 28°C (Loveys et al., 2003). Using this method, it is possible to compare results from different species as the degree of partial acclimation can be determined, however, it is not possible to identify cases in which respiratory homeostasis has occurred. Loveys et al. (2003) performed a comparison of the two methods on leaves and roots of plant species differing in relative growth rate grown at 18°C, 23°C and 28°C. As expected, the degree to which plants acclimated varied, but estimates using both methods had very good agreement for long-term acclimation. This suggests that the method selected to look at respiratory acclimation will not significantly affect the conclusions reached.

The biochemical causes of respiratory acclimation

The underlying mechanisms leading to respiratory acclimation have not previously been established. At moderate temperatures, respiratory flux is controlled by substrate availability and adenylate concentration (Covey-Crump et al., 2002), thus it is likely that respiratory acclimation to temperature is controlled by these same factors (Campbell et al., 2007). Therefore, in a system in which substrate is non-limiting, adenylate control will determine the extent to which respiration acclimates to temperature, and this in turn will be dependent on acclimation of ATP turnover rate. A decreased rate of ATP turnover at high temperature could result from reductions in ATP

consumption for growth or maintenance processes. For instance, in wheat and rice cultivars acclimated to low temperatures, it was demonstrated that plants with the greatest potential for respiratory acclimation to temperature are able to maintain similar rates of growth at a variety of temperatures (Kurimoto, et al., 2004), although this study did not investigate whether respiratory acclimation led to maintained RGR or whether ATP demand for growth was the driving force for respiratory acclimation. Additionally, whether growth acclimation is important in respiratory acclimation to high temperatures has not been investigated. Acclimation of ATP consumption by maintenance processes may also be important in respiratory acclimation to high temperature: one study demonstrated that roots of *Agrostis scabra* are able to acclimate to elevated temperature and acclimation was linked to a reduction in maintenance processes (Rachmilevitch et al., 2008). However, this study did not examine which individual maintenance processes may be important for respiratory acclimation.

There are a small number of studies that can provide some insight into whether the rates of individual maintenance processes acclimate to long-term changes in temperature. Whilst data presented in Chapter 4 demonstrate that protein turnover does not increase at high temperature in excised arabidopsis roots, increased protein turnover following short-term increases in temperature has been shown in other species (Ferguson et al., 1990, see Chapter 4 for discussion). One study looked at the effect of longer term high temperature treatments on protein turnover by studying the respiratory cost of protein turnover over the whole life of *petunia* x *hybrida* petals grown at 20°C, 25°C or 35°C (Hachiya et al., 2007). The respiratory cost at 35°C was found to be higher than that of petals grown at 20°C, or 25°C, over the whole life of the petal, suggesting that acclimation of protein turnover either does not occur or only partially occurs. Given that the rate of protein turnover was shown to be constant at 23°C and 33°C in Chapter 4, it seems unlikely that reduction in the rate of protein turnover is the driving force behind respiratory acclimation in excised arabidopsis roots.

The data presented in Chapter 4 suggest that a major contributor to increased respiration with short-term elevated temperature treatment is ATP consumption for the maintenance of membrane ion gradients. It is therefore possible that reduction in membrane ion leakage after sustained increases in temperature might contribute towards respiratory acclimation. As discussed in Chapter 4, ion leak at high temperature results from increased fluidity of cellular membranes (Los and Murata, 2004). Apart from temperature, another factor controlling membrane fluidity is the saturation levels of membrane fatty acids; the incorporation of more saturated fatty acids increases membrane viscosity resulting in reduced fluidity at high temperatures. There is evidence to suggest that plants regulate the saturation of membrane lipids in response to sustained changes in temperature: in arabidopsis, seedlings grown at 17°C had a higher content of 18:3 fatty acids (54%) than seedlings grown at 36°C (21%), meanwhile, the content of 18:2 fatty acids increased from 10.1% to 31.5% (Falcone et al., 2004). Additionally, the proportion of 18:3 fatty acids was found to increase in root tips as the growth temperature decreased (Horiguchi et al., 2000). These changes in membrane saturation are able to ameliorate ion leakage increases at unfavourable temperatures, thus reducing ATP consumption for the maintenance of ion gradients. Therefore, changes in membrane fluidity are a plausible candidate as a process that contributes to respiratory acclimation.

Membrane fluidity and *FAD* genes

If the modulation of membrane fluidity is important in respiratory acclimation to temperature, then artificially changing fluidity through temperature-independent means may be able to reduce non-growth respiration in non-acclimated plant tissues exposed to short-term increases in temperature. The saturation level of membranes is controlled by *FAD* genes; in non-green tissues, oleic acid (18:1) is produced by plastids and then further desaturated by *FAD2* to produce linoleic acid (18:2) followed by *FAD3* to produce α-linoleic acid (18:3, Ohlrogge & Browse, 1995). In plants

in which *FAD2* has been knocked out, membrane lipid desaturation from 18:1 to 18:2 and 18:3 is prevented, and membranes are more viscous as a result. Martinière et al. (2011) used fluorescence recovery after photobleaching (FRAP) measurements of lateral diffusion to demonstrate that membrane viscosity was increased in *fad2.2* mutants of arabidopsis, furthermore it was shown that membrane viscosity is the same at 12°C and 27°C in *fad2.2* plants. *fad2.2* plants are, therefore, a useful tool to test whether alteration of membrane fluidity is a potential strategy to reduce non-growth respiration at high temperatures.

Aims

The first aim of this chapter is to characterise the effect of long-term high temperature treatment on respiration of arabidopsis roots, and establish whether respiratory acclimation is a consequence of acclimation of growth- or non-growth respiration. Additionally, individual maintenance processes involved in driving respiratory acclimation will be identified. This will be achieved by growing arabidopsis seedlings at contrasting temperatures, and making measurements of respiration and maintenance processes at their respective growth temperatures. A second aim of this chapter is to determine whether increased membrane viscosity reduces the rate of non-growth respiration in plants exposed to short-term high-temperature treatments, by determining non-growth respiration in *fad2.2* mutant plants.

Results

Non-growth respiration in roots of 23°C and 30°C grown arabidopsis seedlings

Excised roots from arabidopsis plants grown in liquid culture at 23°C and 30°C were incubated with [U-^{14}C]glucose for 18 hours and ^{14}C incorporation into biomass fractions and CO_2 was determined at the respective growth temperatures. This is the same as the homeostasis method

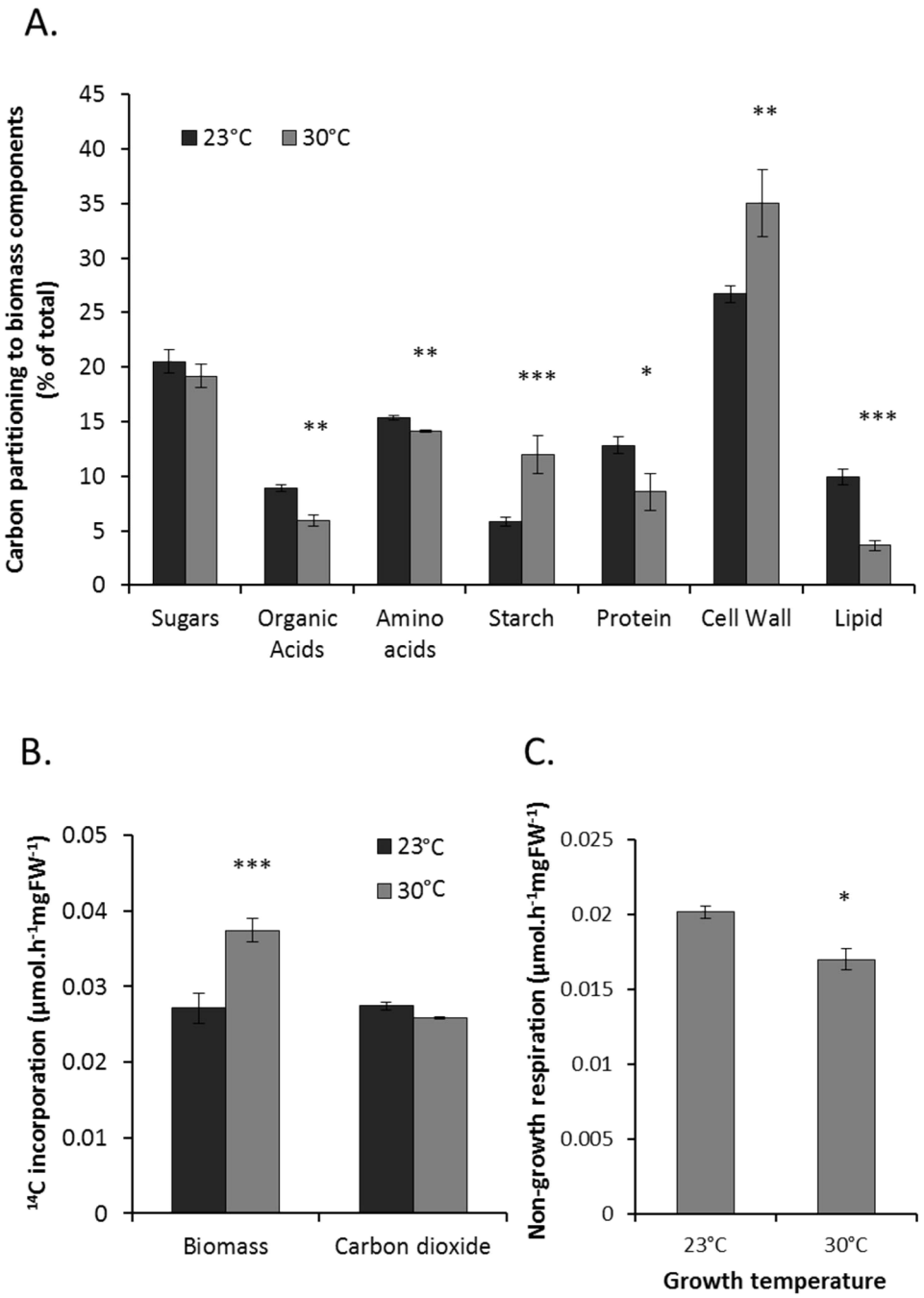


Figure 6.1. ^{14}C incorporation into biomass fractions, CO_2 and non-growth respiration in arabidopsis roots grown at 23°C and 30°C.

Excised arabidopsis roots were supplied with [U-^{14}C]glucose (148 kBq in 5 ml media containing 170 mM glucose, 2.56 mM [w/v] MES pH 5.7 and 0.22% [w/v] Murashige & Skoog) for 18 hours. A. Label incorporation into major biomass components (protein, cell wall, lipid, starch, amino acids, organic acids and sugars) as a percentage of total ^{14}C. B. ^{14}C incorporation into total biomass and carbon dioxide at 23°C and 30°C. C. Non-growth respiration. Data are mean (n=6) ± SEM. Student's *t*-test *p=<0.05, **p=<0.01, ***p=<0.001.

for measuring respiratory acclimation (Larigauderie & Körner, 1995, Loveys et al., 2003). Experiments were performed at 30°C instead of 33°C, as with other experiments presented in this thesis, because experiments were initially designed to be comparable to previous studies of CCE on arabidopsis cell cultures (Williams et al,. 2010). There was no significant difference between ^{14}C incorporation into CO_2 at 23°C and 30°C, indicating that full respiratory acclimation to the higher temperature had occurred. Significantly more ^{14}C entered biomass in roots grown at 30°C than roots grown at 23°C and there were differences in carbon partitioning to different biomass components between the two temperature treatments (Figure 6.1A). In particular, there was an increase in the proportion of cell wall and starch and a decrease in the proportion of lipids, organic acids and protein synthesised. By using the carbon partitioning data as constraints in a flux balance model of heterotrophic arabidopsis metabolism (Cheung et al., 2013), respiration was separated into growth and non-growth components (see Chapter 3 for details). Despite changes in carbon partitioning to biomass, the specific cost for growth was similar for both temperatures; 0.23 and 0.26 carbons released as CO_2 per carbon entering biomass, at 23°C and 30°C, respectively. Growth respiration accounted for 22.5% of total respiration at 23°C and 37.7% at 30°C. Consequently, non-growth respiration was slightly lower at 30°C than at 23°C (Figure 6.1C, p=0.04, Student's *t*-test n=6).

ATPase activities and ion leak of 23°C and 30°C grown arabidopsis roots

In Chapter 4, it was shown that an increase in non-growth respiration with short-term increase in temperature was attributed to increased ATPase activity to maintain ion gradients in the face of increased ion leakage at high temperature. To determine if there was an increase in ion leakage when plants were grown at 30°C compared with 23°C, ion conductance measurements were made on arabidopsis roots. There was no significant difference between the rate of ion leakage from roots grown and measured at 30°C and roots grown and measured at 23°C. As expected, the rate of ion leakage was greater when 23°C grown roots were measured at 30°C (Figure 6.2).

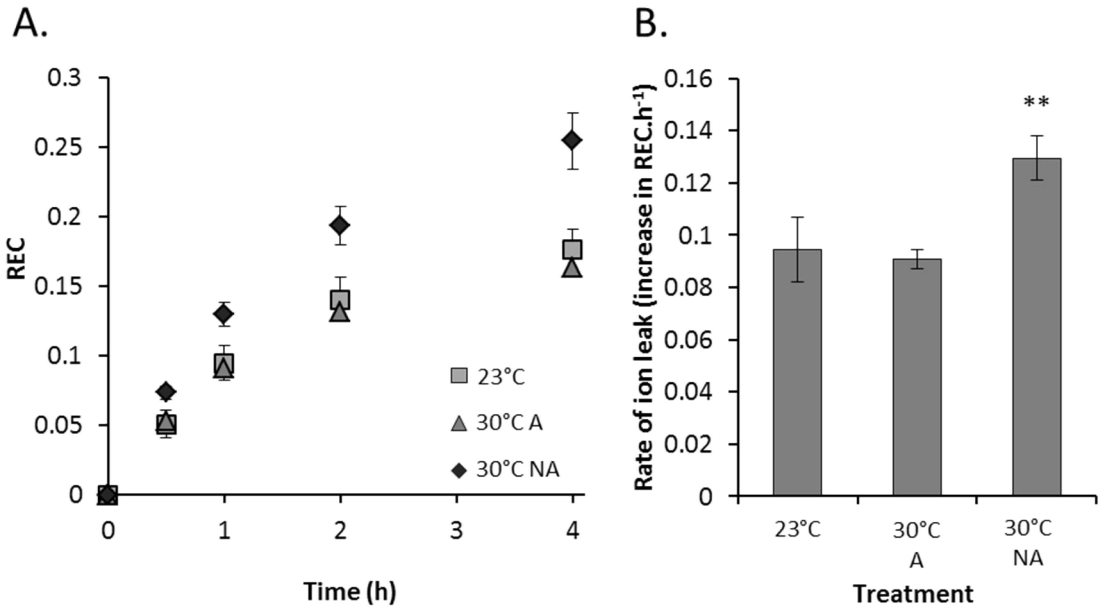


Figure 6.2. Rate of ion leakage from roots acclimated at 23°C and 30°C.

Roots were excised from arabidopsis plants grown at 23°C and 30°C and REC determined in media containing 170 mM glucose and 0.22% (w/v) MES, pH 5.7. Ion conductance measurements were taken at time intervals from 0–4 hours. A. REC at 23°C and 30°C ('30°C A' = 30°C grown roots assayed at 30°C, '30°C NA' = 23°C grown roots assayed at 30°C, '23°C' = 23°C grown roots assayed at 23°C). B. Initial rate of ion leakage calculated from the slope in Figure 6.2A from 0–1 hours. Data are the mean (n=4) ± SEM. Student's *t*-test **p=<0.01.

Additionally maximum extractable ATPase activities in microsomal fractions extracted from 23°C and 30°C grown plants were measured. There were small but significant decreases in ATPase activity from 30°C grown plants; activities of V-ATPase, P-ATPase and V-PPase from 30°C grown roots were 0.78-, 0.69- and 0.63- fold, respectively, that of 23°C grown roots (Figure 6.3).

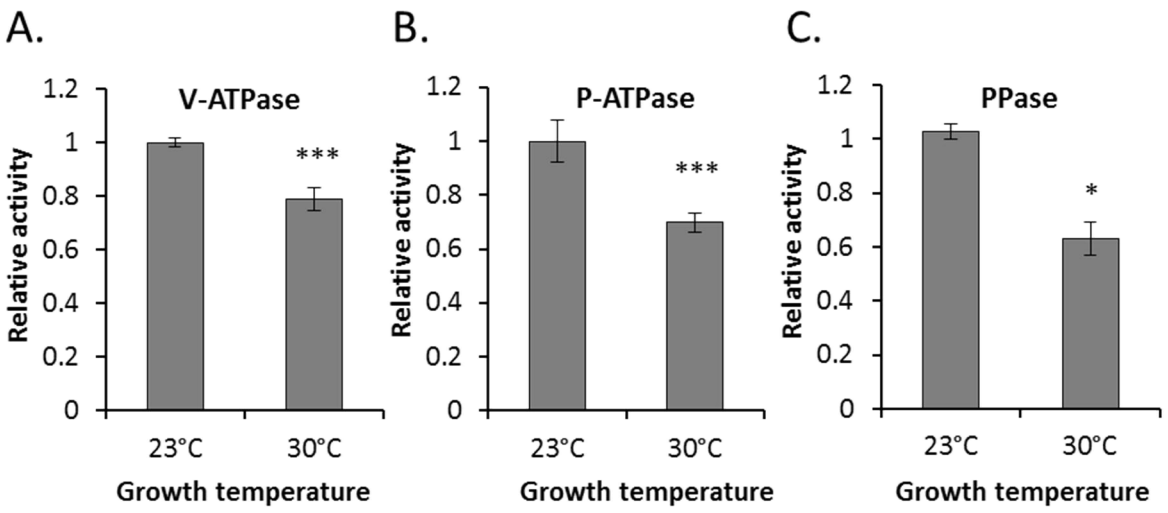


Figure 6.3 Relative activities of V-ATPase, P-ATPase and PPase from root microsomal fractions of arabidopsis plants grown at 23°C and 30°C.

Microsomal fractions were isolated from roots excised from arabidopsis plants grown at either 23°C or 30°C. A. V-ATPase activity measured as decrease in total ATPase activity after inhibition with 100 nM Concanamycin A (1=9.82 µmol Pi.mg protein^{-1}h^{-1}). B. P-ATPase activity measured as the difference in ATPase before and activity after inhibition with 500 µM vanadate (1=11.49 µmol Pi.mg protein^{-1}h^{-1}). C. PPase activity measured as increase in PPase activity after addition of 50 mM KCl (1=17.71 µmol Pi.mg protein^{-1}h^{-1}). Data are the mean (n=9) ± SEM. Student's *t*-test *p=<0.05, ***p=<0.001.

Protein turnover in arabidopsis roots grown at 23°C and 30°C

The rate of protein degradation was determined in roots of 23°C and 30°C grown plants as described in Chapter 4. The proportion of ^{2}H label in alanine was very similar between plants grown at 23°C and 30°C (Figure 6.4A). In contrast to data presented in Figure 6.1B, showing

increased biomass accumulation at 30°C, the rate of protein accumulation was slower at 30°C compared with 23°C (Figure 3.4B). After accounting for the dilution of label due to amino acid synthesis during the chase period, the protein degradation rate was not significantly different (p=0.119, Student's *t*-test n=4) between the two treatments: 0.0046 h^{-1} at 23°C and 0.0056 h^{-1} at 30°C.

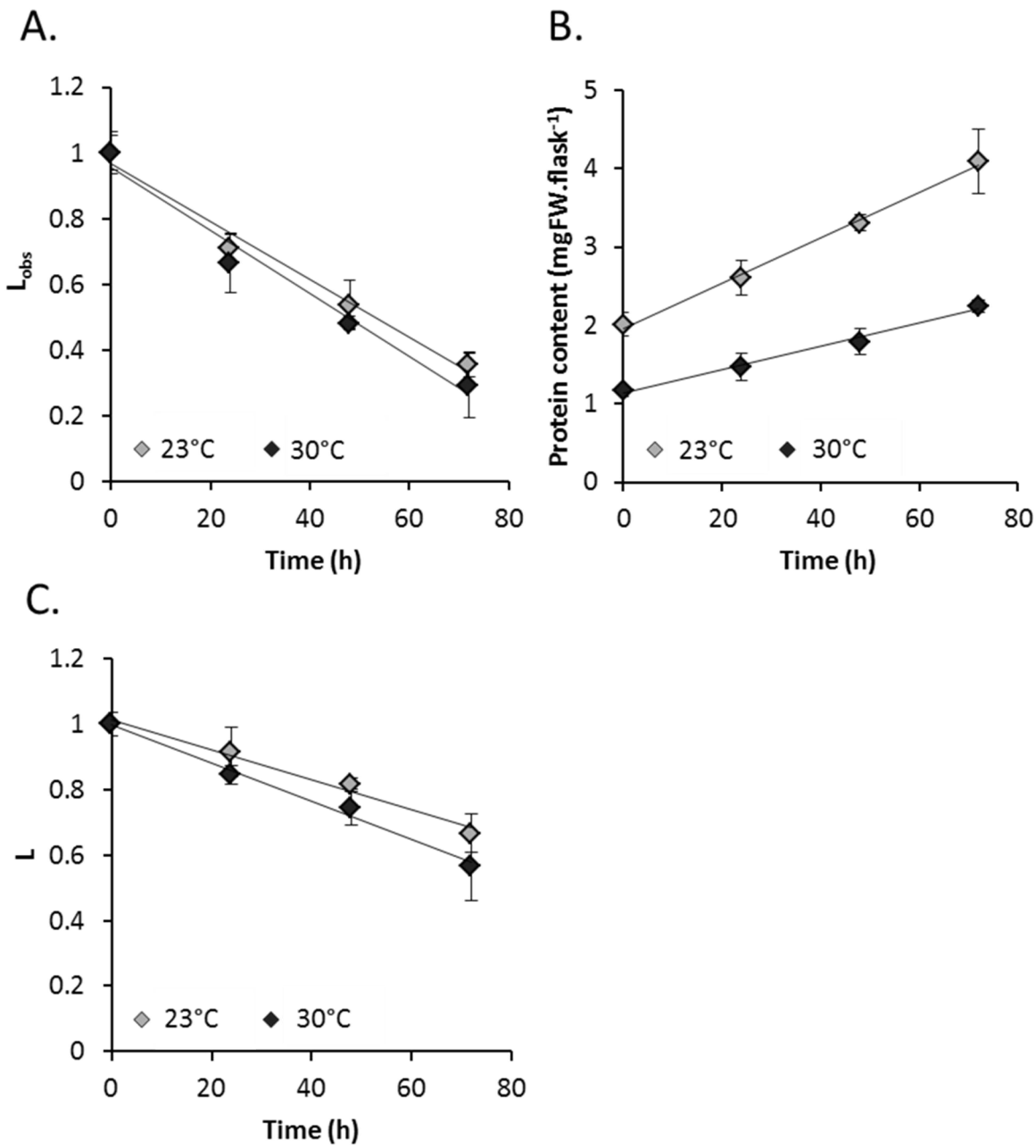


Figure 6.4 Rate of label loss and protein degradation at 23°C and 30°C.

Plants were grown at 23°C or 30°C in media containing 20% (v/v) **D_2O**. At day 14, they were transferred to D_2O-free media and kept at growth temperature until roots were harvested at the time points indicated. Root protein was extracted and labelling of alanine determined by GC-MS. A. Loss of label from alanine. B. Rate of protein accumulation in roots. C. Rate of label loss attributed to protein degradation. L_{obs} = the proportion of ^2H label in protein alanine from experimental data, L = corrected rate of label loss due to protein turnover. Data are the mean (n=6) ± SEM.

Non-growth respiration in response to short-term elevated temperature treatment in *fad2.2* mutants

The data presented above demonstrate that alongside acclimation of non-growth respiration, there is acclimation of ATPase activity while protein turnover rate remains unchanged. Therefore, it can be hypothesised that acclimation of non-growth respiration can be attributed to acclimation of ATP consumption by membrane ATPases. [U-^{14}C]glucose feeding was used to determine carbon incorporation into biomass and CO_2 in 23°C-grown wild-type and *fad2.2* mutant arabidopsis roots during short-term high-temperature treatment. ^{14}C incorporation into biomass was higher at 33°C than 23°C and there were no significant differences in biomass accumulation between wild-type and *fad2.2* mutant roots at 23°C and 33°C (Figure 6.5A). There was a three-fold increase in CO_2 production by wild-type roots at 33°C compared with 23°C. CO_2 production by the *fad2.2* mutant was 2.4-fold higher at 23°C than wild-type, and at 33°C CO_2 production was similar between wild-type and *fad2.2* (Figure 6.5B). Assuming a specific respiratory cost for growth of 0.23 carbons released as CO_2 per carbon entering biomass, non-growth respiration was calculated. Non-growth respiration was similar between wild-type and *fad2.2* at 33°C. However, at 23°C, non-growth respiration was significantly higher in *fad2.2* roots than wild-type (Figure 6.5C).

Discussion

Non-growth respiration acclimates to temperature

Consistent with previous work (Atkin & Tjoelker, 2003), the data presented in this chapter demonstrate that total respiration of excised arabidopsis roots acclimates to sustained changes in temperature; overall root CO_2 production of 30°C-grown roots was 0.94-fold that of 23°C grown roots. This is in comparison with data presented in Chapter 3, which showed that when plants were grown at 23°C and treated at a range of temperatures, overall CO_2 production at 30°C was

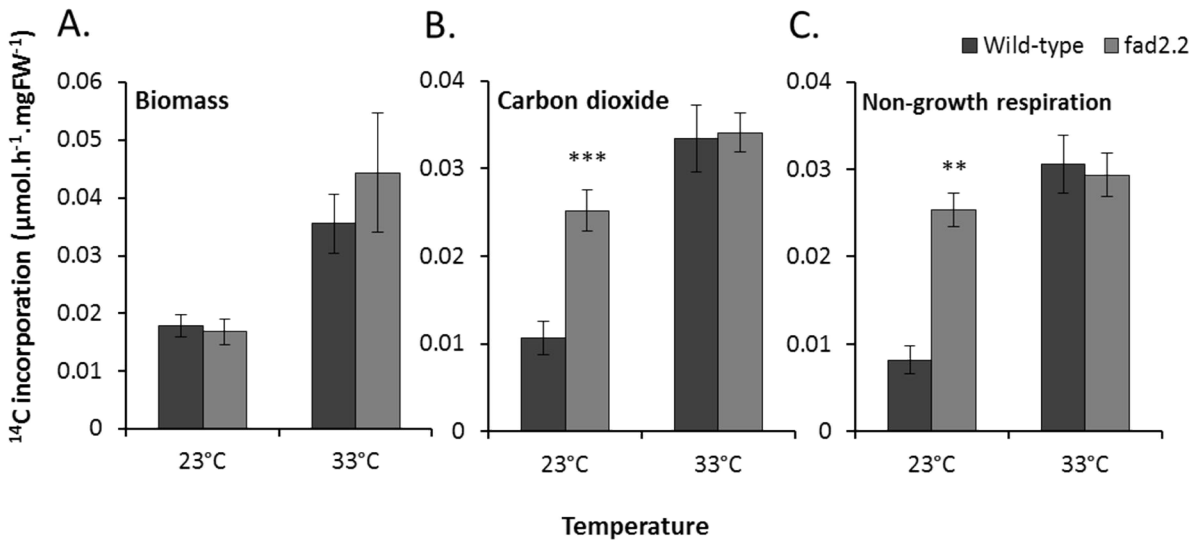


Figure 6.5. ^{14}C incorporation into biomass, CO_2 and non-growth respiration of 23°C-grown wild-type and *fad2.2* arabidopsis plants treated at 23°C and 33°C.

Excised arabidopsis roots were supplied with [U-^{14}**C]**glucose (74 kBq in 5 ml media containing 170 mM glucose, 2.56 mM MES pH 5.7 and 0.22 [w/v] Murashige & Skoog) for 18 hours. A. Label incorporation into biomass. B. Label incorporation into CO_2. C. Non-growth respiration. Data are the mean (n=4) ± SEM. Student's t-test **p=<0.01, ***p=<0.001.

approximately 1.9x higher than CO_2 production at 23°C. Thus, there is complete respiratory homeostasis when plants are grown at 23°C and 30°C. The extremely good acclimation to temperature displayed by arabidopsis roots in these experiments is likely to reflect the fact that the plants were grown, and therefore completely developed, under contrasting temperatures. There is evidence that suggests that the degree of acclimation is lower in tissues that are fully developed before transfer to the new temperature, than tissues that develop at different temperatures. Loveys et al. (2003) compared acclimation of a number of different species to colder temperatures and found that both roots and leaves acclimated to cold temperatures to a greater extent when plants had been developed at the colder conditions than when they were shifted to the new temperature for seven days.

While overall respiration acclimated to the elevated temperature, the rate of ^{14}C incorporation into biomass was higher at 30°C compared with 23°C and showed little acclimation to the

elevated temperature; production of biomass was 1.4x higher at 30°C than at 23°C, this is compared with a 1.5-fold increase with a short-term temperature treatment (Chapter 3). Thus, although the specific costs for growth are lower in roots grown at 30°C, the overall cost for growth is higher at the elevated temperature. It is surprising that carbon accumulation is higher in roots grown at 30°C than at 23°C, given that temperature is often reported as reducing growth rate. Vile et al. (2012) grew arabidopsis accessions at 20°C or 30°C and the dry mass of both shoot and roots was reduced at the high temperature. Additionally, data on protein accumulation at high temperature presented in Figure 6.4B show that there is a lower rate of protein accumulation in plants grown at 30°C. A major difference between the protein accumulation data presented in this chapter and the rate of carbon accumulation in Figure 6.1 is that roots were excised for the [U-^{14}C]feeding experiment. It is possible that root growth was being suppressed while attached to the shoot, but that growth repression was relieved upon removal of the shoot. Restrictions to photosynthesis have been reported to limit plant growth at high temperature (Vile et al., 2012; Wise et al., 2004), however, the seedlings and excised roots used in this study were cultured in exogenous glucose and there are no published accounts of how the presence of photosynthesis affects uptake and metabolism of exogenously supplied glucose. For limitations in photosynthesis to explain the discrepancy in growth results, it would be required that, upon excision, roots would switch from using carbohydrate from the shoot as their primary carbon course source to exogenous glucose, and there is no evidence that this occurs. A possible second mechanism that may restrict growth of roots before excision is the presence of root growth regulation as a consequence of shoot-to-root signalling. Shoot-derived carbohydrate signals have been suggested to initiate root acclimatory responses to phosphorus starvation (Hammond and White, 2011), and it remains a possibility that a similar mechanism might occur upon growth at high temperature. On the other hand, consistent with the results presented here on excised roots, recent work looking at the effect of increasing night-time temperatures on tropical tree seedlings demonstrated that seedlings grown at increased night-time temperatures had a greater

rate of growth. The mechanisms leading to increased growth are unclear, although increased photosynthesis was reported in seedlings treated with high night-time temperature, which may have contributed (Cheesman & Winter, 2013a; Krause et al., 2013).

The rate of non-growth respiration is slightly lower at 30°C than at 23°C. Thus, like total respiration, non-growth respiration of excised arabidopsis roots acclimates to high temperature. Furthermore, given the increase in growth respiration at 30°C, the acclimation of non-growth respiration is sufficient to explain the majority of the acclimation of overall CO_2 production to elevated temperature in this system.

Acclimation of non-growth respiration is accompanied by acclimation of ion leakage and ATPase activity

To explain how non-growth respiration acclimates to elevated temperature, the effect of sustained exposure to elevated temperature on ATP-consuming maintenance processes was studied. The rate of ATP turnover has previously been suggested to control respiratory rate through adenylate control and contribute towards acclimation of respiration to different temperatures (Owen & Tjoelker, 2003; Campbell et al., 2007). Diminished ATP hydrolysis as a consequence of reduced activity of ATP-consuming processes will limit ADP availability and subsequently ATP synthesis. It was shown in Chapter 4 that ATPase activity and protein turnover account for the majority of maintenance ATP consumption, and so the effect of long-term temperature changes on these processes was monitored

The data presented in this chapter show a similar rate of protein turnover between roots grown at 23°C and 30°C. This is similar to results obtained in Chapter 4, which demonstrated no difference in protein turnover with short-term exposure to elevated temperature and suggested that increases in protein turnover were unlikely to lead to the observed increase in non-growth

respiration at elevated temperature. Equally, the consistency of protein turnover rate with long-term temperature treatments means that protein turnover is unable to explain how respiration acclimated to high temperature. Previous studies have shown that protein turnover rate is higher with both short-term (Ferguson et al., 1990) and long-term (Hachiya et al., 2007) elevated temperature treatments, so an unchanging rate of protein degradation across different temperatures presented here is inconsistent with published data.

Assessment of the rate of ion leakage and ATPase activities demonstrated that these factors both acclimate to sustained increases in temperature. Ion leak is dependent on membrane fluidity, and in turn, membrane fluidity is dependent on the saturation of membrane lipids; increased fatty acid saturation results in a more tightly packed and rigid membrane with less fluidity, whereas decreasing lipid saturation increases membrane fluidity. Changes in lipid saturation have been demonstrated in response to changing temperatures; in arabidopsis plants, fatty acid unsaturation was inversely correlated with growth temperature and the proportion of 18:3 fatty acids decreased from 51% after growth at 17°C to 20% at 36°C, whereas 18:2 increased from 10% to 32% (Falcone et al., 2004). Another study showed that 18:3 fatty acids in arabidopsis roots accounted for 46%, 37% and 24% of total fatty acids when plants were grown at 10°C, 20°C and 30°C, respectively (Horiguchi et al., 2000). Therefore, it is likely that the reduction in ion leakage in roots grown at elevated temperature compared with roots treated with short-term elevated temperature is a consequence of alterations in membrane fluidity. Results presented here support a hypothesis that changes in membrane saturation upon sustained changes in growth temperature improves ion leakage rate and consequently ATP consumption for the maintenance of ion gradients, and that this is able to explain acclimation of non-growth respiration at high temperature.

Alterations in membrane fluidity in the *fad2.2* mutant does not lead to reduced non-growth respiration at elevated temperature

To test whether changes in membrane fluidity are sufficient to explain respiratory acclimation, the non-growth respiration of *fad2.2* mutants was determined at 23°C and 33°C. If changes in membrane fluidity contribute to respiratory acclimation, then *fad2.2* mutant plants with increased membrane viscosity may have improved non-growth respiration upon short-term increases in temperature compared to wild-type. Non-growth respiration at 33°C was similar between roots of *fad2.2* and wild-type plants. However, at 23°C, non-growth respiration of *fad2.2* plants was 2.4-fold higher than that of wild-type. There are a number of potential explanations for the results obtained here. Firstly, increased non-growth respiration by the *fad2.2* mutant at 23°C may be occurring as a result of increased fatty acid saturation levels leading to cellular membranes being too rigid at 23°C. At moderate growth temperatures, the membranes of higher plants ordinarily have high levels of polyunsaturated fatty acids in their membranes; trienoic fatty acids (18:3 and 16:3) account for 70% of total fatty acids (Los and Murata 1997). However, the membrane fluidity of the *fad2.2* mutant at 27°C has previously been shown to be similar to that of wild-type arabidopsis at 12°C (Martinière et al., 2011) and it is possible that, while the plants are at a temperature that would not normally be stressful, exposure to 23°C may mimic cold stress in the *fad2.2* plants. Increased rigidity of membranes leads to membrane damage which results in increased electrolyte leakage. Increased electrolyte leakage from tissues exposed to cold treatment has previously been demonstrated in maize (Janda at al., 1999) and cucumber (Wright and Simon, 1973). In *Coffea* genotypes, increased leakage was found upon cold treatment and the most sensitive genotype did not recover on warming, indicating permanent membrane damage (Campos et al., 2003). As discussed in previous chapters, it is likely that the maintenance of ion gradients in the face of increased electrolyte leakage contributes significantly to total ATP consumption and therefore respiratory rate.

Non-growth respiration of *fad2.2* mutant plants at 33°C is similar to *fad2.2* at 23°C and wild-type at 33°C. This is a surprising result because it would be expected that increased saturation of membrane lipids should allow plants to cope better with exposure to high temperature. As discussed previously, there is much evidence suggesting that plants adjust the lipid content of their membranes to cope with high temperature stress. One possibility is that membrane lipids of the *fad2.2* mutant are not optimal for growth at the high temperature: *fad2* mutants have higher levels of 18:1 fatty acids (55.9%) than wild type (6.8%) at 23°C, and decreased 18:2 (6.4% compared with 29.8%) and 18:3 (12.8 compared with 29.1%) fatty acids (Okuley et al., 1994). However, whilst wild-type plants grown at 36°C have a similar 18:3 content to *fad2* mutants at approximately 20%, they have a much higher level of 18:2 fatty acids (32%) and lower level of 18:1 (10%) fatty acids (Falcone et al., 2004), indicating that the *fad2* mutant may have membrane saturation level that is too high for even growth at the higher temperature. Additionally, this result must be taken in the context of the period of growth at 23°C preceding the high-temperature treatment, which is likely to have been stressful for the mutant plants and may have resulted in membrane damage. The plants may have still been recovering from this stress, in which case processes such as membrane repair and protein turnover may have continued into the high-temperature treatment, resulting in a high level of non-growth respiration at 33°C.

Summary

Data presented in this chapter show that respiration acclimates to long-term exposure to elevated temperature, and that overall respiratory acclimation can be accounted for by acclimation of non-growth respiration. There was no evidence that protein turnover was a driver of respiratory acclimation, however, the rate of ion leakage and ATPase activities demonstrated acclimation to high temperature. The response to short-term elevated temperature of non-growth respiration of *fad2.2* mutants was investigated to determine whether increased membrane saturation could

improve non-growth respiration at high temperature. It was shown that *fad2.2* mutants do not have lower rates of non-growth respiration at high temperatures, however, there was the potential for additional stress in the mutant which may explain the high rate of non-growth respiration.

7. Discussion

Summary of results

The first aim of this thesis was to characterise the effect that short-term elevated temperature treatment has on respiratory rate in excised arabidopsis roots, and identify underlying biochemical processes responsible. Increasing temperature lead to an increase in respiratory rate and the majority of the increase in respiration could be attributed to non-growth respiration, associated with changes in ATP production efficiency and consumption for maintenance processes. Construction of ATP budgets under control and elevated temperatures demonstrated that the maintenance of ion gradients is quantitatively the most important ATP-consuming process at high temperature. Additionally, a decrease in P/O ratio of 39% was found at the higher temperature, most likely due to increased basal proton leakage.

The second aim was to explore whether respiratory acclimation occurs with long-term exposure to elevated temperatures and to identify potential biochemical mechanisms. Long-term exposure to high temperature by arabidopsis roots resulted in respiratory acclimation, driven by acclimation of non-growth respiration. Membrane ATPase activity and ion leakage rate were the same or lower in roots acclimated at 30°C and 23°C, suggesting that acclimation of ATP consumption for the maintenance of ion gradients is important for respiratory acclimation.

Key findings

The work presented in this thesis separates the productive role of respiration in providing energy for biomass production from non-growth respiration at high temperatures. Previously, a number of studies have estimated maintenance respiration under different temperature treatments (Van Iersel et al., 2003; Marcelis & Baan Hofman-Eijer, 1995; Szaniawski & Kietkiewicz, 1982), however,

this study is unique in its inclusion of mitochondrial uncoupling as part of the non-growth respiration and in linking increases in respiratory flux under high temperature to individual underlying biochemical processes.

Non-growth respiration is an important component of total respiration

Data presented in this thesis point to the significance of non-growth respiration in the overall respiratory cost of high temperatures. In Chapter 3, it was shown that non-growth respiration has a higher Q_{10} than respiration associated with growth, and consequently can account for the majority of the increase in respiratory rate upon exposure to high temperatures. Equally, it was shown that acclimation of non-growth respiration occurs with longer term exposure to high temperatures, and given the lack of acclimation of growth respiration in this system, respiratory acclimation can be accounted for entirely by acclimation of non-growth respiration. Data on non-growth respiration are in agreement with previous work in which the rate of maintenance respiration was shown to be a large proportion of total respiration. For instance, it was estimated that 80–97% of total respiration was maintenance respiration in mixed grassland (Reekie & Redman, 1987) and maintenance respiration accounted for 48–78% of total respiration in boreal tree species (Lavigne & Ryan, 1997). Additionally, data presented in this thesis corroborate previous work showing increased maintenance under high temperature treatment (Van Iersel et al., 2003; Jones et al., 1978; Szaniawski & Kietkiewicz, 1982). Although it had been suggested that acclimation of maintenance processes might contribute to respiratory acclimation (Atkin & Tjoelker, 2003), this has not previously been directly demonstrated.

Non-growth respiration can be attributed to changes in ATP consumption for the maintenance of ion gradients and P/O ratio

Collectively, the data presented in this thesis suggest that it is likely that increased non-growth respiration at high temperatures involves a combination of mitochondrial uncoupling and ATP cost for the maintenance of ion gradients. A decrease in the P/O ratio has the effect of increasing CO_2 release because to produce the same amount of ATP, more NADH needs to be produced by the TCA cycle as substrate for ATP production by the mtETC. It was argued in Chapter 3 that the majority of CO_2 release is likely to occur as a result of TCA cycle activity. While it is difficult to determine the exact proportion of total CO_2 that is TCA cycle derived, if it is assumed that 100% of CO_2 is released from the TCA cycle and the P/O ratio is reduced by 39%, as is demonstrated in Chapter 5, then this will have the effect of increasing respiration by 1.6-fold. In Chapter 3, respiration was 0.020 µmol CO_2.mg $FW^{-1}18h^{-1}$ at 23°C and 0.041 µmol CO_2.mg $FW^{-1}18h^{-1}$ at 33°C, this change in P/O ratio would explain an increase in respiration at 33°C of 0.032 µmol CO_2.mg $FW^{-1}18h^{-1}$. Thus, while reduction in P/O ratio is likely to have a large impact on respiratory rate at high temperature, even when it is assumed that all CO_2 is released from the TCA cycle, it is not sufficient to explain the increase in respiration at high temperature demonstrated in Chapter 3.

The other factor important in respiratory rate is the rate of ATP consumption. In Chapter 4, an ATP budget was constructed that demonstrated that the maintenance of ion gradients across the tonoplast and plasma membrane consumes proportionally more ATP at 33°C than at 23°C. This suggests that increased ATP consumption for the maintenance of ion gradients was responsible for some of the increase in respiration at high temperature. However, this is contradictory with the data presented in Chapter 5, which showed the rate of ATP turnover to be similar at 23°C and 33°C. The source of this discrepancy is unknown, but may come from experimental error in determining the P/O ratio, as discussed in Chapter 5. This uncertainty makes it difficult to draw firm conclusions on how much of the respiratory increase can be attributed to ATP consumption and production.

Changes in membrane fluidity play a key role in increasing non-growth respiration at high temperature, as well as acclimation to high temperature

Although it is not possible to determine the share of respiratory increase that can be attributed to a change in P/O ratio and increases in ATP consumption for the maintenance of ion gradients, the data in this thesis suggest that the changes in these two processes share a common underlying mechanism of alterations in membrane fluidity at high temperature. Increased fluidity with short-term exposure to temperature is well documented (Carratù et al., 1996; Cossins, 1977; Los & Murata, 2004; Martinière et al., 2011; Sinensky, 1974). It has previously been suggested that membrane fluidity may have an effect on respiration by alleviating adenylate control by increasing mitochondrial proton leakage and increasing ATP consumption to maintain substrate uptake (Atkin & Tjoelker, 2003); however, a direct link between respiratory rate and fluidity of cellular membranes had not been established previously.

Implications for engineering heat tolerance in plants

There is currently much effort to engineer thermal tolerance to high temperatures in crop plants using different approaches; overexpressing heat shock proteins has been shown to improve viability and growth in carrot (Malik et al., 1999) and tomato (Sanmiya et al., 2004). Additionally, heat tolerance has been shown to increase after overexpression of ROS metabolising enzymes, ascorbate peroxidase and superoxide dismutase (Shi et al., 2001; Tang et al., 2006).

Lipids have long been recognised as one of the factors affecting temperature sensitivity in plants, and the data presented in this thesis adds to a body of work that suggests that changing the properties of membranes may be able to improve tolerance to temperature stresses. Most work in this area has looked at cold stress, in particular, the effect of altering the composition of the chloroplast membrane by overexpressing chloroplast-localised FAD proteins. In tobacco (Kodama

et al., 1994; Murata & Dmitry, 1996) reducing the saturation of fatty acids in the chloroplast membrane leads to improved growth at low temperatures, which was shown to be due to sustained rates of photosynthesis (Murata & Dmitry, 1996). Just one study previously has looked at the possibility of altering membrane composition to improve heat tolerance; in tobacco and arabidopsis lacking FAD7 activity, a chloroplast-localised fatty acid desaturase, the level of photosynthetic activity was increased compared with wild-type at temperatures ranging from 25°C to 50°C, subsequently there was an increase in growth rate in the mutants at high temperature (Murakami et al., 2000).

Whilst the work described above focuses on improving plant growth in response to temperature stress by altering chloroplast membranes and improving the rate of photosynthesis, the data presented in this thesis highlight the importance of considering the stability of other biological membranes when thinking about high temperature tolerance. A natural conclusion following on from this might seem to be that one method to improve high temperature tolerance in plants would be to reduce non-growth respiration by adjusting membrane fluidity to allow plants to better cope with high temperatures. However, it is difficult to see why constitutive changes in plant membrane fluidity would be beneficial; acclimation data presented in Chapter 6, as well as previously published data (Falcone et al., 2004; Horiguchi et al., 2000), suggest that plants are able to adjust their membrane fluidity depending the ambient temperature, albeit not fast enough to avoid increases in non-growth respiration over short-term changes in temperature (See Chapter 3). It is perfectly possible to engineer the compositions of plant membranes to investigate whether this improves tolerance to increases in temperature too short-term for acclimation to occur, through differential expression of *FAD* genes. However, a major problem with this approach is the suggestion that alterations in membrane compositions are only able to confer tolerance to high or low temperatures, not both (Iba, 2002). This is illustrated by the low temperature sensitivity of the plants with increased membrane fatty acid saturation, which would, in theory, have greater membrane stability at high temperature; arabidopsis mutants with

reduced levels of polyunsaturated fatty acids died upon 6°C treatment, whereas wild-type plants survived (Miquel et al., 1993), leaving transgenic plants susceptible to greater damage by low temperature stress. This problem has been addressed for improved tolerance to low temperatures in tobacco plants, by expressing *FAD7* under a cold inducible promoter (Khodakovskaya et al., 2006). It is possible that a similar approach could be used to silence FAD genes under high temperature by putting an RNAi construct against *FAD* genes under the control of a heat inducible promoter. Such an approach has been successfully applied for the knockdown of a phytoene desaturase gene using a heat-shock promoter in arabidopsis (Masclaux et al., 2004).

Remaining questions

What is the effect of non-growth respiration on the growth rate of whole plants?

My data shows that biomass accumulation in excised arabidopsis roots increases during short-term increases in temperature, despite the fact that there is an increased rate of non-growth respiration. It has been argued that higher respiration rates as a result of mitochondrial uncoupling or increased ATP costs for maintenance processes will divert substrate from growth processes to maintenance processes and thus reduce growth rate (Amthor, 1984). The work in this thesis appears to challenge this view and demonstrates that growth will continue when enough substrate is available. In contrast to the excised root system used here, in a whole-plant system, the amount of substrate is limited to the amount of carbon fixed by photosynthesis. Photosynthesis, like respiration, is strongly affected by temperature (Berry & Bjorkman, 1980). However, over short-term treatments of minutes to hours, respiratory rate increases more than photosynthetic rate (Campbell et al., 2007; Gifford, 1995), so there remains the potential that substrate supply may be limiting with short-term temperature increases, which may mean that substrate would be preferentially used for non-growth processes, resulting in a lower growth rate.

To test whether substrate is preferentially used for non-growth respiration when substrate is not in abundance, non-growth respiration and growth respiration could either be performed on excised root tissue provided with varying levels of substrate carbohydrate, or in whole plants . The practicalities of determining non-growth respiration in other tissues are discussed below.

Are the conclusions from this study applicable to other plant systems?

There are a number of benefits of using the arabidopsis root system used in this work: firstly the use of a heterotrophic system allows direct measurement of dark respiration without the complication of CO_2 fixation by photosynthesis and CO_2 release by photorespiration. Also, the importance of root respiration to the carbon balance of the whole plant must not be underestimated; it is estimated 8–52% of the CO_2 fixed by photosynthesis is released by root respiration (Atkin 2000). An additional benefit of the use of the arabidopsis root model is the availability of heterotrophic genome-scale metabolic models of arabidopsis (Cheung et al., 2013; Dal'Molin et al., 2010; Poolman et al., 2009; Williams et al., 2010) which allow the calculation of respiratory costs required for biosynthesis, and thus non-growth respiration can be calculated. Additionally, individual costs such as the cost for ion uptake can be split into growth and maintenance components, addressing a major criticism with the growth-maintenance respiration paradigm (Thornley, 2011). Despite the clear advantages of using an arabidopsis root system, to be able to determine if the conclusions about non-growth respiration made here can be used to maximise crop growth under high temperature, similar studies would need to be performed on commercially important species, and an understanding of non-growth respiration in photosynthetic tissues would need to be gained.

The number of plant genome-scale metabolic models is rapidly increasing; since commencing this work, metabolic models of crops such as maize (Saha et al., 2011)) and barley (Grafahrend-Belau et al., 2013) have been published. Additionally, the number of species for which the genome has

been published is growing rapidly. The recent publication of the tomato (Tomato Genome Consortium, 2012) and wheat genomes (International Wheat Genome Sequencing Consortium, 2014) means that there is great potential for the development of metabolic models for more crop species in the near future. With the availability of a greater variety of metabolic models, determination of non-growth respiration, or other studies similar to that performed here, can easily be replicated in agronomically relevant crop species.

To understand how non-growth respiration affects the carbon balance of the whole plant, the effect of temperature on non-growth respiration must be determined in photosynthetic tissues, where dark respiration will interact with processes such as photosynthesis and photorespiration. Direct measurements of dark respiration are not possible in photosynthetic tissues in the light, although attempts have been made to estimate dark respiration based on a number of assumptions (Atkin et al., 1997; Brooks & Farquhar, 1985; Villar et al., 1995). Additionally, the calculation of respiratory costs for growth and non-growth processes is difficult in a system in which a large proportion of the energy required (in the form of ATP and reductant) is supplied by photosynthesis (Raven, 1976). However, many of the recent genome-scale metabolic models include photosynthetic as well as respiratory metabolism, and can be used to calculate respiratory flux in both the light and dark (Cheung et al., 2013; Dal'Molin et al., 2010; Grafahrend-Belau et al., 2013; Poolman et al., 2013; Saha et al., 2011).

What is the effect of abiotic stress combinations on non-growth respiration?

In the field, plants are rarely exposed to a single abiotic stress, but rather experience a combination of stresses. For instance, heat stress has been shown to interact detrimentally with drought, salinity, ozone, pathogen and UV stresses (Mittler, 2006). Plant responses to combined stresses cannot easily be inferred from the responses of the stresses applied individually; different stresses require different responses and combinations of these stresses may involve responses

that are unique to the stress combination. For example, transcriptome data from arabidopsis showed that 454 transcripts were specifically expressed with a combination of heat and drought combination (Rizhsky et al., 2004). Heat and drought is a particularly damaging stress combination, characterised by high respiration rate as a result of high temperature, and low CO_2 fixation due to stomata closing to prevent transpiration (Rizhsky et al., 2002). Consequently, substrate is limited and plant productivity is low (Craufurdf & Peacock, 1993). As discussed previously, it is during substrate limitation that reductions in non-growth respiration are likely to have the biggest impact on growth, and so determination of non-growth respiration and identification of potential biochemical mechanisms under heat and drought stress may help maximise plant growth under these conditions.

Summary

Overall, the data presented in this thesis suggest that increased membrane fluidity is a key driver of non-growth respiration at high temperature and may lead to increased respiration by affecting both ATP consumption and production. Respiratory acclimation may be attributed to changes in membrane fluidity with longer-term exposure to elevated temperature. Future work should focus on determining whether these conclusions are applicable to different plant systems and under heat stress in combination with other commonly occurring stresses such as drought.

Appendix

Table 1: Biomass constraints for FBA: molar flux to output.

The molar flux to each output per glucose consumed was calculated as (proportion of C flux x C atoms in molecule)/ C atoms in glucose.

		23°C		SEM	39°C		SEM
Sugars	**Fructose**	0.06261	±	0.00302	0.0772	±	0.00716
	Glucose	0.06261	±	0.00302	0.0772	±	0.00716
	Sucrose-glucosyl	0.07839	±	0.00378	0.0646	±	0.00599
	Sucrose-fructosyl	0.07839	±	0.00378	0.0646	±	0.00599
Cell wall	**Cellwall C6**	0.25145	±	0.01162	0.15619	±	0.03318
	Cellwall C5	0.06624	±	0.00306	0.04114	±	0.00874
	Starch	0.06697	±	0.00512	0.11887	±	0.01792
Lipids	**Lipid-glycerol**	0.01786	±	0.00115	0.01173	±	0.00152
	Lipid-FA	0.3125	±	0.02015	0.20531	±	0.02665
Organic acids	**Citrate**	0.04367	±	0.00129	0.07068	±	0.00969
	Isocitrate	2.5E-06	±	7.5E-08	4.1E-06	±	5.6E-07
	Malate	0.07636	±	0.00225	0.12356	±	0.01694
	Oxoglutarate	0	±	0	0	±	0
	Succinate	0.00945	±	0.00028	0.01529	±	0.0021
	Urea	0	±	0	0	±	0
	Glycolate	0	±	0	0	±	0
Protein	**Alanine**	0.01876	±	0.00131	0.00969	±	0.0019
	Arginine	0.00596	±	0.00042	0.00308	±	0.0006
	Aspartate	0.0128	±	0.00089	0.00661	±	0.0013
	Cysteine	0.00782	±	0.00055	0.00404	±	0.00079
	Glutamate	0.00042	±	3E-05	0.00022	±	4.3E-05
	Glycine	0.02047	±	0.00143	0.01058	±	0.00207
	Histadine	0.00264	±	0.00018	0.00136	±	0.00027
	Isoleucine	0.00397	±	0.00028	0.00205	±	0.0004
	Leucine	0.01132	±	0.00079	0.00585	±	0.00115
	Lysine	0.01952	±	0.00136	0.01008	±	0.00198

	Methionine	0.00469	±	0.00033	0.00242	±	0.00048
	Phenylalanine	0.00657	±	0.00046	0.00339	±	0.00067
	Proline	0.01933	±	0.00135	0.00999	±	0.00196
	Serine	0.02278	±	0.00159	0.01177	±	0.00231
	Threonine	0.0073	±	0.00051	0.00377	±	0.00074
	Tryptophan	0.00537	±	0.00037	0.00278	±	0.00054
	Tyrosine	0.00705	±	0.00049	0.00364	±	0.00071
	Valine	0.01024	±	0.00071	0.00529	±	0.00104
	GABA	0	±	0	0	±	0
Amino acids	**Alanine**	0.03837	±	0.00072	0.03458	±	0.01236
	Arginine	0	±	0	0	±	0
	Aspargine	0.0029	±	5.5E-05	0.00261	±	0.00093
	Cysteine	0	±	0	0	±	0
	Glutamate	0.11063	±	0.00209	0.0997	±	0.03564
	Glycine	0.00222	±	4.2E-05	0.002	±	0.00071
	Histidine	0	±	0	0	±	0
	Isoleucine	0	±	0	0	±	0
	Leucine	0.00016	±	2.9E-06	0.00014	±	5E-05
	Lysine	0.04005	±	0.00076	0.03609	±	0.0129
	Methionine	0	±	0	0	±	0
	Phenylalanine	0.00025	±	4.7E-06	0.00022	±	8E-05
	Proline	0.00254	±	4.8E-05	0.00229	±	0.00082
	Serine	0.02019	±	0.00038	0.01819	±	0.0065
	Threonine	0	±	0	0	±	0
	Tryptophan	0	±	0	0	±	0
	Tyrosine	3.8E-05	±	7.1E-07	3.4E-05	±	1.2E-05
	Valine	0.00061	±	1.2E-05	0.00055	±	0.0002
	GABA	0.00478	±	9E-05	0.00431	±	0.00154

References

Achard, P., Renou, J.P., Berthomé, R., Harberd, N.P. and Genschik, P. (2008). Plant DELLAs restrain growth and promote survival of adversity by reducing the levels of reactive oxygen species. *Curr. Biol*. 18: 656–60.

Ahn, S.-J., Im, Y.-J., Chung, G.-C. and Cho, B.-H. (2000). Sensitivity of plasma membrane H^+-ATPase of cucumber root system in response to low root temperature. *Plant Cell Rep*. 19: 831–835.

Alonso, A.P., Dale, V.L. and Shachar-Hill, Y. (2010). Understanding fatty acid synthesis in developing maize embryos using metabolic flux analysis. *Metab. Eng*. 12: 488–97.

Alonso, A.P., Goffman, F.D., Ohlrogge, J.B. and Shachar-Hill, Y. (2007). Carbon conversion efficiency and central metabolic fluxes in developing sunflower (*Helianthus annuus* L.) embryos. *Plant J*. 52: 296–308.

Alonso, A.P., Val, D.L. and Shachar-Hill, Y. (2011). Central metabolic fluxes in the endosperm of developing maize seeds and their implications for metabolic engineering. *Metab. Eng*. 13: 96–107.

Amirsadeghi, S., Robson, C., McDonald, A.E. and Vanlerberghe, G.C. (2006). Changes in plant mitochondrial electron transport alter cellular levels of reactive oxygen species and susceptibility to cell death signaling molecules. *Plant Cell Physiol*. 47: 1509–19.

Amthor, J. (2000). The McCree–de Wit–Penning de Vries–Thornley respiration paradigms: 30 years later. *Ann. Bot*. 86: 1–20.

Amthor, J.S. (1984). The role of maintenance respiration in plant growth. *Plant Cell Environ*. 7: 561–569.

ap Rees, T and Beevers, H. (1960) Pathways of glucose dissimilation in carrot slices. *Plant Physiol*. 35: 830–838.

Apel, K. and Hirt, H. (2004). Reactive oxygen species: metabolism, oxidative stress, and signal transduction. *Annu. Rev. Plant Biol*. 55: 373–99.

Armstrong, A.F., Badger, M.R., Day, D., Barthet, M.M., Smith, P.M.C., Millar, A.H., Whelan, J.I.M. and Atkin, O.K. (2008). Dynamic changes in the mitochondrial electron transport chain underpinning cold acclimation of leaf respiration. *Plant Cell Environ*. 31: 1156–1169.

Atkin, O.K., Westbeek, M. H. M., Cambridge, M., Lambers, H. and Pons, T. L. (1997). Leaf respiration in light and darkness. *Plant Physiol.* 113: 961–965.

Atkin, O.K. and Tjoelker, M.G. (2003). Thermal acclimation and the dynamic response of plant respiration to temperature. *Trends Plant Sci*. 8: 343–51.

Atkin, O.K., Edwards, E.J., and Loveys, B.R. (2000). Response of root respiration to changes in temperature and its relevance to global warming. *New Phytol*. 147: 141–154.

Averill, R.H., Bailey-Serres, J. and Kruger, N.J. (1998). Co-operation between cytosolic and plastidic oxidative pentose phosphate pathways revealed by genotypes of maize. *Plant J*. 14: 449–457.

Bidwell, R. H. S., Barr, R. A. and Steward, F.C. (1964) Protein synthesis and turnover in cultured plant tissue: sources of carbon for synthesis and the fate of protein breakdown products. *Nature* 233: 267–373.

Bouma, J., Janssen, J.A., Kock, M.J. De, Leeuwen, Van, P. H. and Lambers, H. (1994). Respiratory energy requirements and rate of protein turnover in vivo determined by the use of an inhibitor of protein synthesis and a probe to assess its effect. *Physiol. Plant*. 92: 585–594.

Brand MD (2000) Uncoupling to survive? The role of mitochondrial inefficiency in ageing. *Exp. Geront*. 35; 811–820.

Brand, M.D. (1990). The proton leak across the mitochondrial inner membrane. *Biochim. Biophys. Acta* 1018: 128–33.

Brand, M.D. and Nicholls, D.G. (2011). Assessing mitochondrial dysfunction in cells. *Biochem. J.* 435: 297–312.

Brand, M.D., Harper, M.E. and Taylor, H.C. (1993). Control of the effective P/O ratio of oxidative phosphorylation in liver mitochondria and hepatocytes. *Biochem. J*. 291: 739–48.

Brand, M.D., Pakay, J.L., Ocloo, A., Kokoszka, J., Wallace, D.C., Brookes, P.S. and Cornwall, E.J. (2005). The basal proton conductance of mitochondria depends on adenine nucleotide translocase content. *Biochem. J.* 392: 353–62.

Brandalise, M., Maia, I.G., Borecký, J., Vercesi, A.E. and Arruda, P. (2003). Overexpression of plant uncoupling mitochondrial protein in transgenic tobacco increases tolerance to oxidative stress. *J. Bioenerg. Biomembr.* 35: 203–9.

Brooks, A. and Farquhar, G. D. (1985). Effect of temperature on the CO_2/O_2 specificity of ribulose-1,5-biphosphate carboxylase/oxygenase and the rate of respiration in the light. *Planta* 165, 397–406.

Burgos, A., Szymanski, J., Seiwert, B., Degenkolbe, T., Hannah, M. a, Giavalisco, P. and Willmitzer, L. (2011). Analysis of short-term changes in the *Arabidopsis thaliana* glycerolipidome in response to temperature and light. *Plant J*. 66: 656–68.

Calegario, F.F., Cosso, R.G., Fagian, M.M., Almeida, F.V., Jardim, W.F., Jezek, P., Arruda, P. and Vercesi, A.E. (2003). Stimulation of potato tuber respiration by cold stress is associated with an increased capacity of both plant uncoupling mitochondrial protein (PUMP) and alternative oxidase. *J. Bioenerg. Biomembr*. 35: 211–20.

Campbell, C., Atkinson, L., Zaragoza-Castells, J., Lundmark, M., Atkin, O. and Hurry, V. (2007). Acclimation of photosynthesis and respiration is asynchronous in response to changes in temperature regardless of plant functional group. *New Phytol*. 176: 375–89.

Campos, P.S., Quartin, V., Ramalho, J.C. and Nunes, M.A. (2003). Electrolyte leakage and lipid degradation account for cold sensitivity in leaves of *Coffea sp*. plants*. J. Plant Physiol*. 160: 283–92.

Carratù, L., Franceschelli, S., Pardini, C.L., Kobayashi, G.S., Horvath, I., Vigh, L. and Maresca, B. (1996). Membrane lipid perturbation modifies the set point of the temperature of heat shock response in yeast. *Proc. Natl. Acad. Sci. U. S. A*. 93: 3870–5.

Cheesman, A.W. and Winter, K. (2013a). Elevated night-time temperatures increase growth in seedlings of two tropical pioneer tree species. *New Phytol*. 197: 1185–92.

Cheesman, A.W. and Winter, K. (2013b). Growth response and acclimation of CO_2 exchange characteristics to elevated temperatures in tropical tree seedlings. *J. Exp. Bot*. 64: 3817–28.

Cheung, C.Y.M., Williams, T.C.R., Poolman, M.G., Fell, D.A., Ratcliffe, R.G. and Sweetlove, L.J. (2013). A method for accounting for maintenance costs in flux balance analysis improves the prediction of plant cell metabolic phenotypes under stress conditions. *Plant J.* 75: 1050–61.

Chifflet, S., Torriglia, a, Chiesa, R. and Tolosa, S. (1988). A method for the determination of inorganic phosphate in the presence of labile organic phosphate and high concentrations of protein: application to lens ATPases. *Anal. Biochem*. 168: 1–4.

Christensen A.H., Sharrock R.A. and Quail P.H. (1992) Maize polyubiquitin genes: structure, thermal perturbation of expression and transcript splicing, and promoter activity following transfer to protoplasts by electroporation. *Plant Mol. Biol*. 18: 675–689.

Clifton, R., Millar, a H. and Whelan, J. (2006). Alternative oxidases in Arabidopsis: a comparative analysis of differential expression in the gene family provides new insights into function of non-phosphorylating bypasses. *Biochim. Biophys. Acta* 1757: 730–741.

Considine, M.J., Goodman, M., Echtay, K.S., Laloi, M., Whelan, J., Brand, M.D. and Sweetlove, L.J. (2003). Superoxide stimulates a proton leak in potato mitochondria that is related to the activity of uncoupling protein. *J. Biol. Chem*. 278: 22298–302.

Cooke, R.J., Grego, S., Roberts, K. and Davies, D. D. (1980). The mechanism of deuterium oxide-induced protein degradation in *Lemna minor*. *Planta* 148: 374–380.

Cossins, A.R., Christiansen, J. and Prosser, C.L. (1978) Adaptation of biological membranes to temperature. The lack of homeoviscous adaptation in the sarcoplasmic reticulum. *Biochim. Biophys. Acta* 511: 442–454.

Cottingham, I.R. and Moore, L. (1984). Partial purification and properties of the external NADH dehydrogenase from cuckoo-pint (*Arum maculatum*) mitochondria. *Biochem. J*. 224: 171–9.

Covey-Crump, E.M., Attwood. R.G. and Atkin, O.K. (2002). Regulation of root respiration in two species of *Plantago* that differ in relative growth rate: the effect of short- and long-term changes in temperature. *Plant Cell Environ.* 25: 1501–1513.

Covey-Crump, E.M., Bykova, N.V., Affourtit, C., Hoefnagel, M.H.N., Gardeström, P. and Atkin, O.K. (2007). Temperature-dependent changes in respiration rates and redox poise of the ubiquinone pool in protoplasts and isolated mitochondria of potato leaves. *Physiol. Plant*. 129: 175–184.

Craufurdf, B.P.Q. and Peacock, J.M. (1993). Effect of heat and drought stress on sorghum (*Sorghum bicolor*). II Grain yield. *Expl. Agric*. 29: 77–86.

Criddle, R.S., Breidenbach, R.W., Rank, D.R., Hopkin, M.S. and Hansen L.D. (1990). Simultaneous calorimetric and respirometric measurements on plant tissues. *Thermochim. Acta* 172: 213–221.

Criddle, R.S., Smith, B.N. and Hansen, L.D. (1997). A respiration based description of plant growth rate responses to temperature. *Planta* 1: 441–445.

Dal'Molin, C. G. D. O., Quek, L.-E., Palfreyman, R. W., Brumbley, S. M. and Nielsen, L. K. (2010). C4GEM, a genome-scale metabolic model to study C4 plant metabolism. *Plant Physiol*. 154: 1871–85.

Davies, J.M., Hunt, I, and Sanders, D. (1994). Vacuolar H^+-pumping ATPase variable transport coupling ratio controlled by pH. *Proc. Natl. Acad. Sci. U. S. A*. 91: 8547–51.

Dawis, S.M., Walseth, T.F., Deeg, M., Heyman, R., Graeff, R.M. and Goldberg, N.D. (1989). Adenosine triphosphate utilization rates and metabolic pool sizes in intact cells measured by transfer of ^{18}O from water. *Biophys. J*. 55: 79–99.

Day, D.A., Moore, A.L., Dry, I.B., Wiskich, J.T. and Azcon-Bieto, J. (1988). Regulation of nonphosphorylating electron transport pathways in soybean cotyledon mitochondria and its implications for fat metabolism. *Plant Physiol*. 86: 1199–204.

De Visser, R., Spitters, C.J., T. and Bouma, TJ, 1992. Energy costs of protein turnover: theoretical calculation and experimental estimation from regression of respiration on protein concentration of full-grown leaves. *In* Molecular, Biochemical and Physiological Aspects of Plant Respiration (H. Lambers and L.H.W. van der Plas, eds.) 493–508. SPB Academic Publishing, The Hague.

Drose, S. and Altendorf, K. (1997). Bafilomycins and concanamycins as inhibitors of V-ATPases and P-ATPases. *J. Exp. Biol.* 8: 1–8.

Du, C.-X., Fan, H.-F., Guo, S.-R., Tezuka, T. and Li, J. (2010). Proteomic analysis of cucumber seedling roots subjected to salt stress. *Phytochemistry* 71: 1450–9.

Dyer, T.A. and Osborne, D.J. (1971). Leaf nucleic acids. *J. Exp. Bot.* 22: 552–560.

Echtay, K.S., Winkler, E., Frischmuth, K., and Klingenberg, M. (2001). Uncoupling proteins 2 and 3 are highly active H^+ transporters and highly nucleotide sensitive when activated by coenzyme Q (ubiquinone). *Proc. Natl. Acad. Sci. U. S. A.* 98: 1416–21.

Elhafez, D., Murcha, M.W., Clifton, R., Soole, K.L., Day, D. and Whelan, J. (2006). Characterization of mitochondrial alternative NAD(P)H dehydrogenases in Arabidopsis: intraorganelle location and expression. *Plant Cell Physiol*. 47: 43–54.

Falcone, D.L., Ogas, J.P. and Somerville, C.R. (2004). Regulation of membrane fatty acid composition by temperature in mutants of Arabidopsis with alterations in membrane lipid composition. *BMC Plant Biol*. 4: 17.

Ferguson, D.L., Guikema, J. and Paulsen, G.M. (1990). Ubiquitin pool modulation and protein degradation in wheat roots during high temperature stress. *Plant Physiol*. 92: 740–6.

Frantz, J.M. and Bugbee, B. (2005). Acclimation of plant populations to shade : photosynthesis , respiration , and carbon use efficiency. *J. Amer. Soc. Hort. Sci.* 130: 918–927.

Fredlund, K.M., Rasmusson, A.G. and Møller, I.M. (1991). Oxidation of external NAD(P)H by purified mitochondria from fresh and aged red beetroots (*Beta vulgaris* L.). *Plant Physiol.* 97: 99–103.

Freeman, D., Bartlett, S., Radda, G. and Ross, B. (1983). Energetics of sodium transport in the kidney. Saturation transfer ^{31}P-NMR. *Biochim. Biophys. Acta* 762: 325–336.

Geisler, D., Broselid, C., Hederstedt, L. and Rasmusson, A.G. (2007). Ca^{2+}-binding and Ca^{2+}-independent respiratory NADH and NADPH dehydrogenases of *Arabidopsis thaliana*. *J. Biol. Chem.* 282: 28455–64.

Genschik, P., Parmentier Y., Durr A., Merbach J., Criqui M., Jamet, E. and Fleck J. (1992). Ubiquitin genes are differentially regulated in protoplast-derived cultures of *Nicotiana sylvestris* and in response to various stress. *Plant. Mol. Biol*. 20: 897–910.

Gifford, R.M. (2003). Plant respiration in productivity models: conceptualisation, representation and issues for global terrestrial carbon-cycle research. *Funct. Plant Biol*. 30: 171–186.

Gill, S.S. and Tuteja, N. (2010). Reactive oxygen species and antioxidant machinery in abiotic stress tolerance in crop plants. *Plant Physiol. Biochem*. 48: 909–30.

Giraud, E., Ho, L.H.M., Clifton, R., Carroll, A., Estavillo, G., Tan, Y.-F., Howell, K. a, Ivanova, A., Pogson, B.J., Millar, A.H. and Whelan, J. (2008). The absence of ALTERNATIVE OXIDASE1a in Arabidopsis results in acute sensitivity to combined light and drought stress. *Plant Physiol*. 147: 595–610.

Gonzalez-Meler, M., Ribas-Carbo, M., Giles, L. and Siedow, J. (1999). The effect of growth and measurement temperature on the activity of the alternative respiratory pathway. *Plant Physiol*. 120: 765–72.

Gruhler, A., Schulze, W.X., Matthiesen, R., Mann, M. and Jensen, O.N. (2005). Stable isotope labeling of Arabidopsis thaliana cells and quantitative proteomics by mass spectrometry. *Mol. Cell. Proteomics* 4: 1697–709.

Guy, R.D., Berry, J.A., Fogel, M.L. and Hoering, T.C. (1989). Differential fractionation of oxygen isotopes by cyanide-resistant and cyanide-sensitive respiration in plants. *Planta* 177: 483–491.

Guy, R.D. and Vanlerberghe, G.C. (2005). Partitioning of respiratory electrons in the dark in leaves of transgenic tobacco with modified levels of alternative oxidase. *Physiol. Plant*. 125: 171–180.

Hachiya, T., Terashima, I. and Noguchi, K. (2007). Increase in respiratory cost at high growth temperature is attributed to high protein turnover cost in *Petunia x hybrida* petals. *Plant Cell Environ.* 30: 1269–83.

Hammond, J.P. and White, P.J. (2011). Sugar signaling in root responses to low phosphorus availability. *Plant Physiol.* 156: 1033–1040.

Hansen, L.D., Thomas, N.R. and Arnholdt-Schmitt, B. (2009). Temperature responses of substrate carbon conversion efficiencies and growth rates of plant tissues. *Physiol. Plant*. 137: 446–58.

Harrison, P.W. and Kruger, N.J. (2008). Validation of the design of feeding experiments involving [^{14}C]substrates used to monitor metabolic flux in higher plants. *Phytochemistry* 69: 2920–7.

Hatzfeld, W.-D. and Stitt, M. (1990). A study of the rate of recycling of triose phosphates in heterotrophic *Chenopodium rubrum* cells, potato tubers, and maize endosperm. *Planta* 180: 198–204.

Hill, S.A. and ap Rees, T. (1994). Fluxes of carbohydrate metabolism in ripening bananas. *Planta* 44: 52–60.

Hinkle, P.C. (2005). P/O ratios of mitochondrial oxidative phosphorylation. *Biochim. Biophys. Acta* 1706: 1–11.

Hoefnagel, M., Rich, P.R., Zhang, Q. and Wiskich, J.T. (1997). Substrate kinetics of the plant mitochondrial alternative oxidase and the effects of pyruvate. *Plant Physiol*. 115: 1145–1153.

Horiguchi, G., Fuse, T., Kawakami, N., Kodama, H. and Iba, K. (2000). Temperature-dependent translational regulation of the ER omega-3 fatty acid desaturase gene in wheat root tips. *Plant J.* 24: 805–13.

Hourton-Cabassa, C., Matos, A.R., Arrabaça, J., Demandre, C., Zachowski, A. and Moreau, F. (2009). Genetically modified *Arabidopsis thaliana* cells reveal the involvement of the mitochondrial fatty acid composition in membrane basal and uncoupling protein-mediated proton leaks. *Plant Cell Physiol*. 50: 2084–91.

Huffaker, R.C. and Peterson, L.W. (1974). Protein turnover in plants and possible means of its regulation. *Annu. Rev. Plant Physiol*. 25: 363–392.

Humphrey, T.J. and Davies, D.D. (1975). A new method for the measurement of protein turnover. *Biochem. J*. 148: 119–27.

Humphrey, T.J. and Davies, D.D. (1976). A sensitive method for measuring protein turnover based on the measurement of 2-^{3}H-labelled amino acids in protein. *Biochem. J*. 156: 561–8.

Iersel, M.W. Van, Bail, L.H. and Tagetes, L. (2003). Short-term temperature change affects the carbon exchange characteristics and growth of four bedding plant species. *J. Amer. Soc. Hort. Sci.* 128: 100–106.

International Wheat Genome Sequencing Consortium (2014). A chromosome-based draft sequence of the hexaploid bread wheat (*Triticum aestivum*) genome. *Science* 345: 288–299.

IPCC, 2013: *Climate Change 2013: The Physical Science Basis. Contribution of Working Group I to the Fifth Assessment Report of the Intergovernmental Panel on Climate Change* [Stocker, T.F., D. Qin, G.-K. Plattner, M. Tignor, S.K. Allen, J. Boschung, A. Nauels, Y. Xia, V. Bex and P.M. Midgley (eds.)]. Cambridge University Press, Cambridge, United Kingdom and New York, NY, USA, pp 1535.

Jacobs, M. and Taiz, L. (1980). Vanadate inhibition of auxin-enhanced H secretion and elongation in pea epicotyls and oat coleoptiles. *Proc. Natl. Acad. Sci. U. S. A*. 77: 7242–6.

Janda T,, Szalai G., Tari I. and Paldi E. (1999) Hydroponic treatment with salicylic acid decreases the effects of chilling injury in maize (*Zea mays L.*) plants. *Planta* 208: 175–180.

Janicka-Russak, M., Kabała, K., Wdowikowska, A. and Kłobus, G. (2013). Modification of plasma membrane proton pumps in cucumber roots as an adaptation mechanism to salt stress. *J. Plant Physiol.* 170: 915–22.

Johansson, F.I., Michalecka, A.M., Møller, I.M. and Rasmusson, A.G. (2001). Oxidation and reduction of pyridine nucleotides in alamethicin-permeabilised plant mitochondria. *Biochem. J*. 15: 193–202.

Jones, M.B., Leafe, E.L., Stiles, W. and Collett, B. (1978). Pattern of respiration of a perennial ryegrass crop in the field. *Ann. Bot.* 42: 693–703.

Kane, P.M. (1995). Disassembly and reassembly of the yeast vacuolar H^+-ATPase *in vivo*. *J. Biol. Chem.* 270: 17025–17032.

Kawaga, T., Lord, J.M. and Beevers, H. (1973). The origin and turnover of organelle membranes in castor. *Plant Physiol.* 51: 61–65.

Kawasaki, S., Borchert, C., Deyholos, M., Wang, H., Brazille, S., Kawai, K., Galbraith, D. and Bohnert, H.J. (2001). Gene expression profiles during the initial phase of salt stress in rice. *Plant Cell* 13: 889–905.

Kettner, C., Bertl, A., Obermeyer, G., Slayman, C. and Bihler, H. (2003). Electrophysiological analysis of the yeast V-type proton pump: variable coupling ratio and proton shunt. *Biophys. J*. 85: 3730–8.

Khodakovskaya, M., McAvoy, R., Peters, J., Wu, H. and Li, Y. Enhanced cold tolerance in transgenic tobacco expressing a chloroplast omega-3-fatty acid desaturase gene under the control of a cold-inducible promoter. *Planta* 233: 1090–1100.

Kingsley-Hickman, P.B., Sako, E.Y., Mohanakrishnan, P., Robitaille, P.M., From, H., Foker, J.E. and Uğurbil, K. (1987). ^{31}P NMR studies of ATP synthesis and hydrolysis kinetics in the intact myocardium. *Biochemistry* 26: 7501–10.

Kodama H., Hamada T., Horiguchi G., Nishimura M. and Iba K. (1994) Genetic enhancement of cold tolerance by expression of a gene for chloroplast ω-3 fatty acid desaturase in transgenic tobacco. *Plant Physiol.* 105: 601-605.

Koeppe, D.E. and Miller, R.J. (1972). Oxidation of reduced nicotinamide adenine dinucleotide phosphate by isolated corn mitochondria. *Plant Physiol.* 49: 353–357.

Krause, G.H., Cheesman, A.W., Winter, K., Krause, B. and Virgo, A. (2013). Thermal tolerance, net CO_2 exchange and growth of a tropical tree species, *Ficus insipida*, cultivated at elevated daytime and nighttime temperatures. *J. Plant Physiol.* 170: 822–7.

Kruger, N.J., Le Lay, P. and Ratcliffe, R.G. (2007). Vacuolar compartmentation complicates the steady-state analysis of glucose metabolism and forces reappraisal of sucrose cycling in plants. *Phytochemistry* 68: 2189–96.

Kruse, J., Hopmans, P. and Adams, M. (2008). Temperature responses are a window to the physiology of dark respiration: differences between CO_2 release and O_2 reduction shed light on energy conservation. *Plant Cell Environ.* 31: 901–14.

Kurimoto, K., Millar, A.H., Lambers, H., Day, D. and Noguchi, K. (2004). Maintenance of growth rate at low temperature in rice and wheat cultivars with a high degree of respiratory homeostasis is associated with a high efficiency of respiratory ATP production. *Plant Cell Physiol*. 45: 1015–22.

Laloi, M., Klein, M., Riesmeier, J.W. and Muller-Rober, B. (1997). A plant cold-induced uncoupling protein. *Nature* 389: 135–136.

Lavigne, M. B. and Ryan M. G. (1997). Growth and maintenance respiration rates of aspen, black spruce and jack pine stems at northern and southern BOREAS sites. *Tree Physiol.* 17: 543–551.

Li, L., Nelson, C.J., Solheim, C., Whelan, J. and Millar, A.H. (2012). Determining degradation and synthesis rates of arabidopsis proteins using the kinetics of progressive ^{15}N labeling of two-dimensional gel-separated protein spots. *Mol. Cell. Proteomics* 11: M111.010025.

Lonien, J. and Schwender, J. (2009). Analysis of metabolic flux phenotypes for two Arabidopsis mutants with severe impairment in seed storage lipid synthesis. *Plant Physiol.* 151: 1617–34.

Los, D. and Murata, N. (2004). Membrane fluidity and its roles in the perception of environmental signals. *Biochim. Biophys. Acta* 1666: 142–57.

Loveys, B.R., Atkinson, L.J., Sherlock, D.J., Roberts, R.L., Fitter, H., and Atkin, O.K. (2003). Thermal acclimation of leaf and root respiration: an investigation comparing inherently fast- and slow-growing plant species. *Global Change Biol*. 9: 895–910.

Low, R. and Rausch, T. (1996). In suspension-cultured *Daucus carota* cells salt stress stimulates H^+ -transport but not ATP hydrolysis of the V-ATPase. *J. Exp. Bot.* 47: 1725–1732.

Lyons, J.M. and Raison, J.K. (1970). Oxidative activity of mitochondria isolated from plant tissues sensitive and resistant to chilling injury. *Plant Physiol*. 45: 386–9.

Macfarlane, C., Hansen, L.D., Florez-Sarasa, I. and Ribas-Carbo, M. (2009). Plant mitochondria electron partitioning is independent of short-term temperature changes. *Plant Cell Environ*. 32: 585–91.

Maia I.G., Benedetti C.E., Leite A., Turcinelli S.R., Vercesi A.E. and Arruda P. (1998). AtPUMP: an Arabidopsis gene encoding a plant uncoupling mitochondrial protein. *FEBS Lett.* 3: 403–406.

Malik, M. K., Slovin, J. P., Hwang, C. H. and Zimmerman, J. L. (1999). Modified expression of a carrot small heat shock protein gene, Hsp17.7, results in increased or decreased thermotolerance. *Plant J*. 20: 89–99.

Marcelis, L.F.M. and Baan Hofman-Eijer, L.R. (1995). Growth and maintenance respiratory costs of cucumber fruits as affected by temperature, and ontogeny and size of the fruits. *Physiol. Plant*. 93: 484–492.

Martinière, A., Shvedunova, M., Thomson, A.J.W., Evans, N.H., Penfield, S., Runions, J. and McWatters, H.G. (2011). Homeostasis of plasma membrane viscosity in fluctuating temperatures. *New Phytol*. 192: 328–37.

Martinoia E., Heck, U. and Wiemken A. (1981) Vacuoles as storage compartments for nitrate in barley leaves. *Nature* 289: 292–294.

Masakapalli, S.K., Le Lay, P., Huddleston, J.E., Pollock, N.L., Kruger, N.J. and Ratcliffe, R.G. (2010). Subcellular flux analysis of central metabolism in a heterotrophic Arabidopsis cell suspension using steady-state stable isotope labeling. *Plant Physiol*. 152: 602–19.

Matic S, Geisler, D., Møller, I.M., Widell, S. and Rasmusson, A.G. (2005). Alamethicin permeabilizes plasma membrane and mitochondria but not tonoplast in tobacco (*Nicotiana tabacum* L. cv Bright Yellow) suspension cells. *Biochem. J*. 389: 695–704.

Maxclaux, F., Charpenteau, M., Takahashi, T., Pont-Lezica, R. and Galaud, J. (2004). Gene silencing using a heat-inducible RNAi system in Arabidopsis. *Biochem. Biophys. Res. Comm*: 321, 364–369.

Maxwell, D.P., Wang, Y. and McIntosh, L. (1999). The alternative oxidase lowers mitochondrial reactive oxygen production in plant cells. *Proc. Natl. Acad. Sci. U. S. A*. 96: 8271–6.

McCarlie, V.W., Hansen, L.D., Smith, B.N., Monsen, S.B. and Ellingson, D.J. (2003). Anabolic rates measured by calorespirometry for eleven subpopulation of *Bromus tectorum* match temperature profiles. *Russ. J. Plant Physiol.* 50: 183–191.

McDonald, A.E., Sieger, S.M. and Vanlerberghe, G.C. (2002). Methods and approaches to study plant mitochondrial alternative oxidase. *Physiol. Plant*. 116: 135–143.

McNulty, A.M.Y.K., Departtnent, W.R.C., and Wilson, J.T. (1987). The relationship between respiration and temperature in leaves of the arctic plant *Saxifraga cernua*. *Plant Cell Environ*. 10: 319–325.

Melo, A.M.P., Robert, T.H. and Møller, I.M. (1996). Evidence for the presence of two rotenone-insensitive NAD(P)H dehydrogenases on the inner surface of the inner membrane of potato tuber mitochondria. *Biochim. Biophys. Acta* 1276: 133–139.

Michalecka, A.M., Svensson, Å.S., Johansson, F.I., Agius, S.C., Johanson, U., Brennicke, A., Binder, S. and Rasmusson, A.G. (2003). Arabidopsis genes encoding mitochondrial type II NAD(P)H dehydrogenases have different evolutionary origin and show distinct responses to light. *Plant Physiol*. 133: 642–652.

Millar, A., Atkin, O., Ian R., Henry, B., Farquhar, G. and Day, D.A. (1998). Analysis of respiratory chain regulation in roots of soybean seedlings. *Plant Physiol.* 117: 1083–93.

Millenaar, F.F. and Lambers, H. (2003). The alternative oxidase: *in vivo* regulation and function. *Plant Biol.* 5: 2–15.

Miller, A.J. and Smith, S.J. (1996). Nitrate transport and compartmentation in cereal root cells. *J. Exp. Bot.* 47: 843–854.

Miquel, M., James, D., Dooner, H. and Browse, J. (1993). Arabidopsis requires polyunsaturated lipids for low-temperature survival. *Proc. Natl. Acad. Sci. U. S. A*. 90: 6208–12.

Mizuno, N., Sugie, A., Kobayashi, F. and Takumi, S. (2008). Mitochondrial alternative pathway is associated with development of freezing tolerance in common wheat. *J. Plant Physiol.* 165: 462–7.

Møller I.M. and Lin W. (1986) Membrane bound NAD(P)H dehydrogenases in higher plant cells. *Annu. Rev. Plant Physiol.* 37: 309-334.

Møller, I.M. (2001). Plant mitochondria and oxidative stress: Electron transport , NADPH turnover, and metabolism of reactive oxygen species. *Annu. Rev. Plant Physiol. Plant Mol. Biol*. 42: 561–591.

Møller, I.M., Bérczi, A., Van Der Plas, L.H.W. and Lambers, H. (1988). Measurement of the activity and capacity of the alternative pathway in intact plant tissues : Identification of problems and possible solutions. *Physiol. Plant*. 72: 642–649.

Møller, I.M., Chow, W.-S., Palmer, J.M. and Barber, J. (1981). 9-Aminoacridine as a fluorescent probe of the electrical diffuse layer associated with the membranes of plant mitochondria. *Biochem. J.* 193: 37–46.

Møller, I.M., Jensen, P.E. and Hansson, A. (2007). Oxidative modifications to cellular components in plants. *Ann. Rev. Plant Biol.* 58: 459–481.

Müller, M., Siems, W., Buttgereit, F., Dumdey, R. and Rapoport, S.M. (1986). Quantification of ATP-producing and consuming processes of Ehrlich ascites tumour cells. *Eur. J. Biochem*. 161: 701–5.

Müller, M.L. and Taiz, L. (2002). Regulation of the lemon-fruit V-ATPase by variable stoichiometry and organic acids. *J. Membr. Biol*. 185: 209–20.

Murakami, Y., Tsuyama, M., Kobayashi, Y., Kodama, H. and Iba, K. (2000) Trienoic fatty acids and plant tolerance of high temperature. *Science* 287: 467–479.

Nelson C.J., Li L., Jacoby R.P. and Millar A.H. (2013). Degradation rate of mitochondrial proteins in *Arabidopsis thaliana* cells*. J. of Proteome Res.* 12: 3449–3459.

Nelson, C.J., Li, L. and Millar, A.H. (2014). Quantitative analysis of protein turnover in plants. *Proteomics* 14: 579–92.

Nemutlu, E., Zhang, S., Gupta, A., Juranic, N.O., Macura, S.I., Terzic, A., Jahangir, A. and Dzeja, P. (2012). Dynamic phosphometabolomic profiling of human tissues and transgenic models by ^{18}O-assisted ^{31}P NMR and mass spectrometry. *Physiol. Genomics* 44: 386–402.

Nicholls, D.G. and Bernson, V. (1977). The inter-relationships between respiratory rates, proton electrochemical gradients*. Eur. J. Biochem*. 612: 601–612.

Nobes, D., Brown, C., Olive, N. and Brand, D. (1990). Non-ohmic proton conductance of the mitochondrial in hepatocytes. *J. Biol. Chem*. 265: 12903-12909.

Nogales, A., Muñoz-Sanhueza, L., Hansen, L.D. and Arnholdt-Schmitt, B. (2013). Calorespirometry as a tool for studying temperature response in carrot (*Daucus carota* L.). *Eng. Life Sci*. 13: 541–548.

Nogueira, F.T.S., Sassaki, F.T. and Maia, I.G. (2011). *Arabidopsis thaliana* uncoupling proteins (AtUCPs): insights into gene expression during development and stress response and epigenetic regulation. *J. Bioenerg. Biomembr*. 43: 71–9.

O'Quin, J.B., Bourassa, L., Zhang, D., Shockey, J.M., Gidda, S.K., Fosnot, S., Chapman, K.D., Mullen, R.T. and Dyer, J.M. (2010). Temperature-sensitive post-translational regulation of plant omega-3 fatty-acid desaturases is mediated by the endoplasmic reticulum-associated degradation pathway. *J. Biol. Chem.* 285: 21781–96.

Oaks, A. and Bidwell, R.H.S. (1970) Compartmentation of intermediary metabolites. *Ann. Rev. Plant. Physiol.* 21, 43–66.

Ohlrogge, J. and Browse, J. (1995). Lipid biosynthesis. *Plant Cell* 7: 957–970.

Okuley, J., Lightner, J., Feldmann, K., Yadav, N., Lark, E., and Browse, J. (1994). Arabidopsis FAD2 gene encodes the enzyme that is essential for polyunsaturated lipid synthesis. *Plant Cell* 6: 147–158.

Oshima, T. and Tamiya, N. (1961). Mechanism of transamination action. *Biochem J*. 78, 116–119.

Palmgren, M.G., Larsson, C. and Sommarin, M. (1990). Proteolytic activation of the plant plasma membrane H^+-ATPase by removal of a terminal segment. *J. Biol. Chem*. 265: 13423–6.

Palmieri, L., Picault, N., Arrigoni, R., Besin, E., Palmieri, F. and Hodges, M. (2008). Molecular identification of three Arabidopsis thaliana mitochondrial dicarboxylate carrier isoforms: organ distribution, bacterial expression, reconstitution into liposomes and functional characterization. *Biochem. J*. 410: 621–9.

Pasqualini, S., Paolocci, F., Borgogni, A., Morettini, R. and Ederli, L. (2007). The overexpression of an alternative oxidase gene triggers ozone sensitivity in tobacco plants. *Plant Cell Environ*. 30: 1545–56.

Penning de Vries, F.W., Brunsting, H. and van Laar, H.H. (1974). Products, requirements and efficiency of biosynthesis: a quantitative approach. *J. Theor. Biol*. 45: 339–77.

Penning de Vries, F.W.T. (1975). The cost of maintenance processes in plant cells. *Ann. Bot*. 39: 77–92.

Poder, D. and Penot, M. (1992). The effect of vanadate on phosphate transport in aged potato tuber tissue (*Solarium tuberosum*). *J. Exp. Bot.* 43: 189–193.

Pomeroy, M.K. and Andrews, C.J. (1975). Effect of temperature on respiration of mitochondria and shoot segments from cold hardened and non-hardened wheat and rye seedlings. *Plant Physiol.* 56: 703–6.

Poolman, M. G., Kundu, S., Shaw, R., & Fell, D.A.. (2013). Responses to light intensity in a genome-scale model of rice metabolism. *Plant Physiol.*, 162: 1060–72.

Poorter, H., Van der Werf, A., Atkin, O.K. and Lambers, H. (1991). Respiratory energy requirements of roots vary with the potential growth rate of a plant species. *Physiol. Plant*. 83: 469–475.

Portillo, F. (2000). Regulation of plasma membrane H^+-ATPase in fungi and plants. *Biochim. Biophys. Acta* 1469: 31–42.

Purvis, A.C. (2001). Reduction of superoxide production by mitochondria oxidising NADH in the presence of organic acids. *J. Plant Physiol*. 158: 159–165

Quigg, A. and Beardall, J. (2003). Protein turnover in relation to maintenance metabolism at low photon flux in two marine microalgae. *Plant Cell Environ.* 25: 693–703.

Rachmilevitch, S., Lambers, H. and Huang, B. (2008). Short-term and long-term root respiratory acclimation to elevated temperatures associated with root thermotolerance for two Agrostis grass species. *J. Exp. Bot*. 59: 3803–9.

Raven, J.A. (1975). The quantitative role of 'dark' respiratory processes in heterotrophic and photolithotrophic plant growth. *Ann. Bot*. 95: 641–648

Rea, P.A., Kim, Y., Sarafian, V., Poole, R.J., Davies, J.M. and Sanders, D. (1992). Vacuolar H^+-translocating pyrophosphatases: a new category of ion translocase. *Trends Biochem. Sci.* 17: 348–53.

Regenberg, B., Villalba, J.M., Lanfermeijer, F.C. and Palmgren, M.G. (1995). C-terminal deletion analysis of plant plasma membrane H^+-ATPase: yeast as a model system for solute transport across the plant plasma membrane. *Plant Cell* 7: 1655–66.

Rizhsky, L., Liang, H., Shuman, J., Shulaev, V., Davletova, S. and Mittler, R. (2004). When defense pathways collide . The response of arabidopsis to a combination of drought and heat stress. *Plant Physiol.* 134: 1683–1696.

Roberts, J.K., Wemmer, D. and Jardetzky, O. (1984). Measurement of mitochondrial ATPase activity in maize root tips by saturation transfer p nuclear magnetic resonance. *Plant Physiol*. 74: 632–9.

Robinson, D.G., Albrecht, S. and Moriysu, Y. (2004). The V-ATPase inhibitors concanamycin A and bafilomycin A lead to Golgi swelling in tobacco BY-2 cells. *Protoplasma* 224: 255–60.

Robson, M.J. and Parsons, A.J. (1981). Respiratory efflux of carbon dioxide from mature and meristematic tissue of uniculm barley during eighty hours of continuous darkness. *Ann. Bot*. 48: 727–731.

Rontein, D., Dieuaide-Noubhani, M., Dufourc, E.J., Raymond, P. and Rolin, D. (2002). The metabolic architecture of plant cells. Stability of central metabolism and flexibility of anabolic pathways during the growth cycle of tomato cells*. J. Biol. Chem*. 277: 43948–60.

Saha, R., Suthers, P.F. and Maranas, C.D. (2011). Zea mays iRS1563: a comprehensive genome-scale metabolic reconstruction of maize metabolism. PloS One, 6: e21784.

Sanmiya, K., Suzuki, K., Egawa, Shono, M. (2004). Mitochondrial small heat-shock protein enhances thermotolerance in tobacco plants. *FEBS Lett*. 557: 265–268

Scheibe, R., Backhausen, J.E., Emmerlich, V. and Holtgrefe, S. (2005). Strategies to maintain redox homeostasis during photosynthesis under changing conditions*. J. Exp. Bot*. 56: 1481–9.

Scheurwater, I., Cornelissen, C., Dictus, F., Welschen, R. and Lambers, H. (1998). Why do fast- and slow-growing grass species differ so little in their rate of root respiration, considering the large differences in rate of growth and ion uptake? *Plant Cell Environ*. 21: 995–1005.

Scheurwater, I., Dünnebacke, M., Eising, R., and Lambers, H. (2000). Respiratory costs and rate of protein turnover in the roots of a fast-growing (*Dactylis glomerata* L.) and a slow-growing (*Festuca ovina* L.) grass species. *J. Exp. Bot.* 51: 1089–97.

Schneider, W., Siems, W. and Grune, T. (1990). Balancing of energy-consuming processes of rat hepatocytes. *Cell Biochem. Funct*. 8: 227–32.

Schwarzländer, M., Logan, D.C., Johnston, I.G., Jones, N.S., Meyer, A.J., Fricker, M.D. and Sweetlove, L.J. (2012). Pulsing of membrane potential in individual mitochondria: a stress-induced mechanism to regulate respiratory bioenergetics in Arabidopsis. *Plant Cell* 24: 1188–201.

Schwender, J., Goffman, F., Ohlrogge, J.B. and Shachar-Hill, Y. (2004). Rubisco without the Calvin cycle improves the carbon efficiency of developing green seeds. *Nature* 432: 779–782.

Schwender, J., Ohlrogge, J.B. and Shachar-Hill, Y. (2003). A flux model of glycolysis and the oxidative pentosephosphate pathway in developing Brassica napus embryos. *J. Biol. Chem*. 278: 29442–53.

Schwender, J., Shachar-Hill, Y., and Ohlrogge, J.B. (2006). Mitochondrial metabolism in developing embryos of *Brassica napus. J. Biol. Chem*. 281: 34040–7.

Searle, S.Y., Thomas, S., Griffin, K.L., Horton, T., Kornfeld, A., Yakir, D., Hurry, V. and Turnbull, M.H. (2011). Leaf respiration and alternative oxidase in field-grown alpine grasses respond to natural changes in temperature and light. *New Phytol*. 189: 1027–39.

Shi, W. M., Muramoto, Y. Ueda, A. and Takabe, T. (2001) Cloning of peroxisomal ascorbate peroxidase gene from barley and enhanced thermotolerance by overexpressing in *Arabidopsis thaliana*. *Gene* 273: 23–27.

Sieger, S.M., Kristensen, B.K., Robson, C., Amirsadeghi, S., Eng, E.W.Y., Abdel-Mesih, A., Møller, I.M. and Vanlerberghe, G.C. (2005). The role of alternative oxidase in modulating carbon use efficiency and growth during macronutrient stress in tobacco cells. *J. Exp. Bot*. 56: 1499–515.

Sinensky, M. (1974). Homeoviscous adaptation–a homeostatic process that regulates the viscosity of membrane lipids in *Escherichia coli*. *Proc. Natl. Acad. Sci. U. S. A*. 71: 522–5.

Smith, A.M.O., Ratcliffe, R.G. and Sweetlove, L.J. (2004). Activation and function of mitochondrial uncoupling protein in plants. *J. Biol. Chem*. 279: 51944–52.

Smith, B.N., Walker, J.L., Stone, R.L., Jones, A.R. and Hansen, L.D. (2001). Temperature-dependent respiration-growth relations in ancestral maize cultivars. *USDA For. Serv. Proc.:* 276–279.

Solomon, P.S. and Oliver, R.P. (2001). The nitrogen content of the tomato leaf apoplast increases during infection by *Cladosporium fulvum*. *Planta* 213, 241–249.

Steer, M.W. (1988). Plasma membrane turnover in plant cells. *J. Exp. Bot.* 39: 987–996.

Stevens, T.H. and Forgac, M. (1997). Structure, function and regulation of the vacuolar H^+-ATPase. *Annu. Rev. Cell Dev. Biol*. 13: 779–808.

Stuart, J., Brindle, K.M., Harper, J. and Brand, M.D. (1999). Mitochondrial proton leak and the uncoupling proteins. *J. Bioenerg. Biomembr*. 31: 517–25.

Sun, C.W. and Callis, J. (1997). Independent modulation of *Arabidopsis thaliana* polyubiquitin mRNAs in different organs and in response to environmental changes. *Plant J*. 11: 1017–27.

Svensson, A.S. and Rasmusson, A.G. (2001). Light-dependent gene expression for proteins in the respiratory chain of potato leaves. *Plant J*. 28: 73–82.

Sweetlove, L.J. Taylor, N.L. and Leaver C.J. (2007). Isolation of intact functional mitochondria from the model plant *arabidopsis thaliana. Methods Mol. Biol.* 372: 125–136

Sweetlove, L.J., Williams, T.C.R., Cheung, C.Y.M. and Ratcliffe, R.G. (2013). Modelling metabolic CO_2 evolution--a fresh perspective on respiration. *Plant Cell Environ*. 36: 1631–40.

Szaniawski, R.K. and Kietkiewicz, M. (1982). Maintenance and growth respiration in shoots and roots of sunflower plants grown at different root temperatures. *Physiol. Plant*. 54: 500–504.

Tang, L., Kwon S.Y., Kim, S.H., Kim, J.S., Cho, K.Y., Sung, C.K., Kwak, S.S. and Lee, H.S. (2006) Enhanced tolerance of transgenic potato plants expressing both superoxide dismutase and ascorbate peroxidase in chloroplasts against oxidative stress and high temperature. *Plant Cell Rep.* 25: 1380–6.

Thornley, J.H.M. (2011). Plant growth and respiration re-visited: maintenance respiration defined - it is an emergent property of, not a separate process within, the system - and why the respiration : photosynthesis ratio is conservative. *Ann. Bot*. 108: 1365–80.

Thygerson, T., Harris, J.M., Smith, B.N., Hansen, L.D., Pendleton, R.L. and Booth, D.T. (2002). Metabolic response to temperature for six populations of winterfat (*Eurotia lanata*). *Thermochim. Acta* 394: 211–217.

Tjoelker, M.G., Oleksyn, J. and Reich, P.B. (1999). Acclimation of respiration to temperature and CO2 in seedlings of boreal tree species in relation to plant size and relative growth rate. *Global Change Biol*. 5: 679–691.

Tjoelker, M.G., Oleksyn, J. and Reich, P.B. (2001). Modelling respiration of vegetation: evidence for a general temperature-dependent Q_{10}. *Global Change Biol*. 7: 223–230.

Tomato Genome Consortium (2012). The tomato genome sequence provides insights into fleshy fruit evolution. *Nature* 485: 635–641.

Tsiantis, M.S., Bartholomew, D.M. and Smith, J.A.C. (1996). Salt regulation of transcript levels for the c subunit of a leaf vacuolar H(+)-ATPase in the halophyte *Mesembryanthemum crystallinum*. *Plant J*. 9: 729–36.

Umbach, A.L., Wiskich, J.T. and Siedow, J.N. (1994). Regulation of alternative oxidase kinetics by pyruvate and intermolecular disulfide bond redox status in soybean seedling mitochondria. *FEBS Lett.* 348: 181–4.

Umbach, A.L. and Siedow, J.N. (1993). Covalent and noncovalent dimers of the cyanide-resistant alternative oxidase protein in higher plant mitochondria and their relationship to enzyme activity. *Plant Physiol*. 103: 845–854.

Umbach, A.L., Fiorani, F. and Siedow, J.N. (2005). Characterization of transformed Arabidopsis with altered alternative oxidase levels and analysis of effects on reactive oxygen species in tissue. *Plant Physiol*. 139: 1806–1820.

Uphaus, R.A. and Blake, M.I. (1975). Deuterium isotope effects in *Nicotiana tabacum*. *Can. J. Bot.*53: 2128–2133.

Van Iersel, M.W. (2003). Carbon use efficiency depends on growth respiration , maintenance respiration , and relative growth rate. *Plant Cell Environ*. 26: 1441–1449.

Vanlerberghe, G.C. (2013). Alternative oxidase: a mitochondrial respiratory pathway to maintain metabolic and signaling homeostasis during abiotic and biotic stress in plants*. Int. J. Mol. Sci*. 14: 6805–47.

Vanlerberghe, G.C. and Mcintosh, L. (1992). Lower growth temperature increases alternative pathway capacity and alternative oxidase protein in tobacco. *Plant Physiol.* 100: 115–119.

Vercesi, A.E., Borecký, J., Maia, I.D.G., Arruda, P., Cuccovia, I.M. and Chaimovich, H. (2006). Plant uncoupling mitochondrial proteins. *Annu. Rev. Plant Biol*. 57: 383–404.

Vidal, G., Ribas-Carbo, M., Garmier, M., Dubertret, G., Rasmusson, A.G., Mathieu, C., Foyer, C.H. and De Paepe, R. (2007). Lack of respiratory chain complex I impairs alternative oxidase engagement and modulates redox signaling during elicitor-induced cell death in tobacco. *Plant Cell* 19: 640–55.

Vijayraghaven V. and Soole K. (2010) Effect of short- and long-term phosphate stress on the non-phosphorylating pathway of mitochondrial electron transport in *Arabidopsis thaliana*. *Funct. Plant Biol.* 37: 455–466.

Vile, D., Pervent, M., Belluau, M., Vasseur, F., Bresson, J., Muller, B., Granier, C. and Simonneau, T. (2012). Arabidopsis growth under prolonged high temperature and water deficit: independent or interactive effects? *Plant Cell Environ*. 35: 702–18.

Villar, R., Held, A., & Merino, J. (1995). Dark leaf respiration in light and darkness of an evergreen and a deciduous plant species. *Plant Physiol.* 107: 421–427.

Penning de Vries, F.W.T. (1975). The cost of maintenance processes in plant cells. *Ann. Bot.* 1: 77–92.

Wahl, S.A., Dauner, M. and Wiechert, W. (2004). New tools for mass isotopomer data evaluation in (^{13})C flux analysis: mass isotope correction, data consistency checking, and precursor relationships. *Biotechnol. Bioeng*. 85: 259–68.

Wang, M.-C., Peng, Z.-Y., Li, C.-L., Li, F., Liu, C. and Xia, G.-M. (2008). Proteomic analysis on a high salt tolerance introgression strain of *Triticum aestivum/Thinopyrum ponticum. Proteomics* 8: 1470–89.

Williams, T.C.R., Poolman, M.G., Howden, A.J.M., Schwarzlander, M., Fell, D. a, Ratcliffe, R.G. and Sweetlove, L.J. (2010). A genome-scale metabolic model accurately predicts fluxes in central carbon metabolism under stress conditions. *Plant Physiol*. 154: 311–23.

Wilson, D. (1982). Response to selection for dark respiration rate of mature leaves in *Lolium perenne* and its effects on growth of young plants and simulated swards. *Ann. Bot*. 49: 303–312.

Wilson, D. and Jones, J.G. (1982). Effect of selection for dark respiration rate of mature leaves on crop yields of *Lolium perenne cv* . S23. *Ann. Bot.* 313–320.

Wilson, R.H. and Hanson, J.B. (1969). The effect of respiratory inhibitors on NADH , succinate and malate oxidation in corn mitochondria. *Plant Physiol.* 44: 1335–1341.

Wink, M. (1993). The plant vacuole: a multifunctional compartment. *J. Exp. Bot*. 44: 231–246.

Wise, R.R., Olson, a. J., Schrader, S.M. and Sharkey, T.D. (2004). Electron transport is the functional limitation of photosynthesis in field-grown Pima cotton plants at high temperature. *Plant Cell Environ*. 27: 717–724.

Wiskich, J.T. snf Dry, J.B. (1985). The tricarboxylic acid cycle in plant mitochondria: its operation and regulation. *In* Encyclopaedia of Plant Physiology. Higher Plant Cell Respiration (Douce, R. and Day, D.A. eds.) 18: 281–313. Springer-Verlag, Berlin and New York.

Wright, M. and Simon, E.W. (1973). Chilling injury in cucumber leaves. *J. Exp. Bot*. 24: 400–411.

Yang, X.-Y., Chen, W.-P., Rendahl, A.K., Hegeman, A.D., Gray, W.M. and Cohen, J.D. (2010). Measuring the turnover rates of Arabidopsis proteins using deuterium oxide: an auxin signaling case study. *Plant J*. 63: 680–95.

Yoshida, S. and Tagawa, F. (1979). Alteration of the respiratory function in chill-sensitive callus due to low temperature stress: Involvement of the alternate pathway. *Plant Cell Physiol.* 20: 1243–1250.

Zagdanska, B. (1995). Respiratory energy demand for protein turnover and ion transport in wheat leaves upon water deficit. *Physiol. Plant*. 95: 428–436.

Zeleznikar, R.J. and Goldberg, N.D. (1991). Kinetics and compartmentation of energy metabolism in intact skeletal muscle determined from ^{18}O labeling of metabolite phosphoryls. *J. Biol. Chem*. 266: 15110–9.

Zeleznikar, R.J., Heyman, R., Graeff, R.M., Walseth, T.F., Dawis, S.M., Butz, E. and Goldberg, N.D. (1990). Evidence for compartmentalized adenylate kinase catalysis serving a high energy phosphoryl transfer function in rat skeletal muscle. *J. Biol. Chem*. 265: 300–11.

Zerihun, A., McKenzie, B.A. and Morton, J.D. (1998). Photosynthate costs associated with the utilization of different nitrogen – forms : influence on the carbon balance of plants and shoot – root biomass partitioning. *New Phytol*. 138: 1–11.

Zhang, J.-H., Liu, Y.-P., Pan, Q.-H., Zhan, J.-C., Wang, X.-Q. and Huang, W.-D. (2006). Changes in membrane-associated H^+-ATPase activities and amounts in young grape plants during the cross adaptation to temperature stresses. *Plant Sci*. 170: 768–777.

Zörb, C., Schmitt, S., Neeb, A., Karl, S., Linder, M. and Schubert, S. (2004). The biochemical reaction of maize (*Zea mays* L.) to salt stress is characterized by a mitigation of symptoms and not by a specific adaptation. *Plant Sci*. 167: 91–100.